Metabolomics approaches to decipher the antibacterial mechanisms of yerba mate (*Ilex paraguariensis)* against *Staphylococcus aureus* and *Salmonella enterica* serovar Typhimurium

A Dissertation Presented for the
Doctor of Philosophy
Degree
The University of Tennessee, Knoxville

Caroline Sue Rempe
August 2016

ACKNOWLEDGEMENTS

I am very grateful for everyone who has helped me during my journey as a graduate student, starting with the support and encouragement of Dr. Harry Richards and Dr. Cynthia Peterson who brought me to the University of Tennessee through the SCALE-IT fellowship program. The interdisciplinary SCALE-IT program encouraged me to learn computational skills, presented me with valuable networking opportunities, and allowed me to develop collaborative projects with my peers. I also want to thank Dr. Albrecht von Arnim for his continued support and for the many opportunities I've had as a GST student, especially the chances to teach Perl, genetics, and a KIDSU summer camp and the opportunity to participate in the GST recruitment process. I would like to thank my advisor Dr. C. Neal Stewart for his constant support and encouragement and my committee members, Dr. Timothy Tschaplinski, Dr. Alison Buchan, and Dr. Cynthia Peterson, for their support and helpful suggestions. I additionally want to express my gratitude to Dr. Kellie Burris for fostering my microbiology skills, listening to all my ideas and problems and advising me in the directions to take my work. My gratitude also goes to Dr. Scott Lenaghan for his patient guidance and helpful discussions about my experimental successes, failures, and interpretations. I am also grateful to Dr. Timothy Tschaplinski and Nancy Engle for their willingness to work with me to learn how to run and analyze GC-MS experiments on their equipment. I would also like to thank Dr. Hayriye Bozkurt for helpful suggestions and encouragement, Dr. P. M. Davidson for the generous use of his BSL-2 lab space, and Dr. Arnold Saxton for his quick responses to my statistics questions. Additional thanks go to Dr. Shawn Campagna and his group, particularly Dr. Hector Castro Gonzalez and Eric Tague, for extracting my samples and running LC-MS analyses. Finally, I want to thank all the other individuals in my lab, GST, SCALE-IT, my family, and my friends for their continued support and encouragement.

ABSTRACT

The increasing prevalence of drug-resistant pathogens is an urgent problem that requires novel methods of bacterial control. Plant extracts inhibit bacterial pathogens and could contain antibacterial compounds with novel mechanisms of action. Yerba mate, a common South American beverage made from *Ilex paraguariensis*, has antibiotic activity against a broad range of bacterial pathogens. In this work, an attempt was first made to characterize the antibacterial source of an aqueous yerba mate extract by generating a series of extract fractions, collecting GC-MS and antibacterial activity profiles, and then ranking the hundreds of compounds by their presence in fractions with high antibacterial activity. Quinic acid, quercetin, and 5-hydroxy pipecolic acid were highly ranked, suggesting an association between the antibacterial activity of yerba mate against methicillin-resistant *Staphylococcus aureus* (MRSA). Next, metabolites that accumulated in the supernatants of *Salmonella* Typhimurium and *Lactobacillus casei* cultures were surveyed for decreases in phenolic compounds that might signify metabolism of bioactive yerba mate components. No decreases in phenolic compounds were observed. The hypothesis that phenolic compounds might chelate iron as a mechanism of antibacterial activity was also tested; exogenous iron sulfate stimulated the partial recovery of *S*. Typhimurium to the inhibitory effect of yerba mate in a milk system. Finally, an assessment of potential antibacterial mechanisms of action was undertaken by surveying the metabolites produced by *Salmonella* Typhimurium in the presence of yerba mate extract and conducting assays to assess cell membrane integrity and catalase activity. No effect on the cell membrane was observed while catalase activity was reduced in the presence of yerba mate extract. Metabolomics revealed significant differences in central carbon metabolism, the cell wall precursor UDP-N-acetylglucosamine, the regulatory metabolites alpha-ketoglutarate and acetylphosphate, the

energy metabolite NAD^+, and a match to yohimbine, which has known antibacterial activity. Future work can move closer to understanding the antibacterial value of yerba mate extract and its constituents by testing specific mechanistic hypotheses based on metabolic alterations, further examining 5-hydroxy pipecolic acid and yohimbine for antibacterial activity and mechanism, and annotating currently unknown compounds that could have antibacterial activity or be additional key metabolites pointing to specific mechanisms of action.

TABLE OF CONTENTS

CHAPTER I Introduction 1
Emergence of antibiotics 1
Antibacterial resistance overview 2
Plants as sources of novel antibacterial compounds 4
Scope of dissertation 6
References 7
Appendix 9
Figures 9
CHAPTER II Systems biology approaches to unraveling antibacterial mechanisms of plant phenolic compounds 10
Summary 11
Introduction 11
Membrane disruption by phenolic compounds 13
Non-membrane mechanisms of action 16
Key functional characteristics 18
Synergistic antibacterial activity 20
Systems biology methods 21
Conclusion 25
References 27
Appendix 32
Figures 32
Tables 33
CHAPTER III Computational ranking of yerba mate small molecules based on their predicted contribution to antibacterial activity against methicillin-resistant *Staphylococcus aureus* 34
Abstract 35
Introduction 36
Materials and methods 37
Yerba mate extractions 37
Antimicrobial susceptibility tests 38
GC-MS sample preparation and instrument parameters 40
Data analysis 41
Results 45
Discussion 49
Conclusion 53
Acknowledgements 53
References 55
Appendix 58
Figures 58
Tables 61
Supporting Information 64
CHAPTER IV Metabolites accumulated during *Salmonella enterica* serovar Typhimurium and *Lactobacillus casei* yerba mate treatment and the rescuing effect of exogenous iron sulfate on *S.* Typhimurium 71
Abstract 72

Introduction 73
Materials and methods 75
Yerba mate aqueous extraction 75
Phenolic content determination 75
Bacterial culture maintenance 76
Bacterial growth experiments 76
Metabolomics 77
Data analysis 78
Iron assays 79
Results 81
Extract and phenolic content 81
Bacterial growth with yerba mate extract 81
Metabolomics 82
Iron binding assays 82
Bacterial growth with iron supplementation 83
Discussion 83
Conclusion 87
Acknowledgements 87
References 88
Appendix 91
Figures 91
Tables 94
Supporting information 95
CHAPTER V Metabolic analysis of the mechanisms of action of yerba mate extract on *Salmonella enterica* serovar Typhimurium 97
Abstract 98
Introduction 99
Results 101
Discussion 103
Influx from tea extract 107
General stress conditions 107
Antibiotic specific stressors 108
Conclusion 113
Materials and methods 114
Yerba mate aqueous extraction 114
Bacterial culture maintenance 115
Bacterial growth experiments 115
Crystal violet membrane integrity assay: 116
Catalase activity assay 117
Metabolomics 117
Data analysis 118
Metabolomics data analysis 118
Acknowledgements 120
References 121
Appendix 127
Figures 127

Tables 132
Supporting information 139
CHAPTER VI Conclusion 145
VITA 147

LIST OF TABLES

Table 1. Known antibacterial mechanisms of action of phenolic compounds. (attachment) 33
Table 2. Top 20 unique retention times ranked by antimicrobial significance against MRSA using random forests. 61
Table 3. Rank biased overlap comparison of lists. 62
Table 4. Top ten results for each attribute ranking method. (attachment) 63
Table 5. Classification accuracy of a single major mz peak for each of the 3 identified compounds of interest. 63
Table 6. Predicted functional groups from Golm 63
Table 7. *L. casei* metabolites found to be significantly different between treatments with 'control_no_bacteria' = milk+tea, 'control_no_tea' = milk+bacteria, and 'tea' = milk+tea+bacteria. Extracted ion intensity values normalized to a gallic acid internal standard are listed with data ranges in parentheses. (attached) 94
Table 8. *S.* Typhimurium metabolites found to be significantly different between treatments with 'control_no_bacteria= milk+tea, 'control_no_tea ' = milk+bacteria, and 'tea' = milk+tea+bacteria. Extracted ion intensity values normalized to a gallic acid internal standard are listed with data ranges in parentheses. (attached) 94
Table 9. Significant differences between $control_{no_tea}$ and tea at 0 min 132
Table 10. Significant differences between $control_{no_tea}$ and tea at 40 min 133
Table 11. Significant differences between $control_{no_tea}$ and tea at 240 min 135
Table 12. Significant differences between $control_{no_bacteria}$ and tea at 0 min 136
Table 13. Significant differences between $control_{no_bacteria}$ and tea at 40 min 137
Table 14. Significant differences between $control_{no\ bacteria}$ and tea at 240 min 138

Table S 1. Final parameters implemented with XCMS for feature detection and retention time correction of mass spectral data. 65
Table S 2. Ranking values of top 10 attributes for each ranking method. (attachment) 66
Table S 3. Antimicrobial activity assays of aqueous yerba mate acetonitrile fractions. 66
Table S 4. Antimicrobial activity assays of aqueous yerba mate methanol fractions. 67
Table S 5. Summary of compounds identified as potential antibacterials from GC-MS data and MIC concentrations against methicillin-sensitive *Staphylococcus aureus* (SA) and methicillin-resistant *S. aureus* (MRSA) from literature. 68
Table S 6. Accuracies of classification methods shown in confusion matrices. 68
Table S 7. Predicted functional groups listed for the top 10 compounds with retention time (RT), retention index (RI) and name if known. 69
Table S 10. Peak-picking parameters for metabolomics data analysis with Maven software. These parameters were used for both targeted and untargeted analyses but targeted analyses were limited to identifiable compounds. 143
Table S 11. Pure catalase tested for activity in the presence of yerba mate extract ($control_{no\ bacteria}$). Pure catalase (5 U) in buffer was compared to pure catalase (5 U) with incubated yerba mate extract ($control_{no\ bacteria}$). No significant difference was observed between catalase in buffer and catalase treated with incubated yerba mate extract sampled at different times. 144
Table S 12. Complete list of all metabolites found with LC-MS. (attachment) 144
Table S 13. List of all identified metabolites found with LC-MS. (attachment) 144

LIST OF FIGURES

Figure 1. Bacterial mechanisms of resistance to antimicrobials. Inability of antimicrobial to cross cell barrier (decreased penetration), active membrane pump to shuttle out toxic compounds from within the cell (efflux pump), enzymatic degradation of antimicrobials (modification or inactivation of enzymes), and modification of the target site (prevents binding) (adapted from Abreu et al., 2012)..... 9
Figure 2. Antibacterial mechanisms of action summarized for A. common antibiotic classes and B. plant phenolic compounds (adapted from Helander et al. 1997, Brown et al. 2015, Kohanski et al. 2010). PBP: penicillin binding protein. Effects of exogenous magnesium were not tested on a Gram-positive organism, only a Gram-negative organism..... 32
Figure 3. Overlay of initial yerba mate extract fraction chromatograms. A) The black chromatogram corresponds to a yerba mate extract fraction that demonstrated antibacterial activity against methicillin-resistant *Staphylococcus aureus* (MRSA); the red chromatogram corresponds to a yerba mate fraction that had no antibacterial activity against MRSA. B) Retention times of identified compounds and quantification in sorbitol equivalents were reported. 58
Figure 4. Growth of methicillin-sensitive (SA) and methicillin-resistant *Staphylococcus aureus* (MRSA) in the presence of single or multiple pure compounds at proportions approximated from GC-MS quantification. Growth with compounds alone or together was compared to the positive growth control (no chemical added) to determine inhibitory activity. Statistically significant differences greater (*) or less (**) than control are marked by asterisks. Concentrations follow the GC-MS quantification values in Figure 3, but in µg/ml. Growth of A. SA 27708, B. MRSA 33591, and C. MRSA 33593 are reported at 24 h. 59
Figure 5. Growth of methicillin-sensitive (SA) and methicillin-resistant *Staphylococcus aureus* MRSA) in the presence of pure compounds. At concentrations of 10 µg/ml (chemical_1), 20 µg/ml (chemical_2) and 100 µg/ml (chemical_3), growth with compounds was compared to the positive growth control (no chemical added) to determine inhibitory activity. Statistically significant differences greater (*) or less (**) than control are marked by asterisks. Growth of A. SA 113, B. SA 27708, C. MRSA 33591, and D. MRSA 33593 are reported at 48 h. SA113 had a significant block by treatment interaction, so no conclusions can be drawn from it. 60
Figure 6. Growth trends (log CFU/ml) of A. *S. Typhimurium*, B. *L. acidophilus*, C. *L. casei*, and D. *L. bulgaricus* in UHT skim milk at different concentrations of yerba mate extract. Error bars represent ± 1 standard deviation (triplicate experiment)..... 91
Figure 7. Plots show competition assays of ferrozine; A. Fe^{2+} ($FeSO_4$) and C. Fe^{3+} ($FeCl_3$) were tested and controls without ferrozine were also tested with B. Fe^{2+} and D. Fe^{3+}. Experiments were done at least in duplicate. Error bars represent standard deviation..... 92
Figure 8. Growth of *S*. Typhimurium in 3 concentrations of iron ($FeSO_4$) and 2 concentrations of yerba mate extract ("tea") is plotted over time. Error bars show standard deviation for 3 replicates with the exception of the 10 h time point, which only had 2 replicates. 93
Figure 9. Growth of *S*. Typhimurium with A. ca. 6 log CFU/ml starting culture and 0 to 20 mg/ml yerba mate extract (n=3) or with B. ca. 9 log CFU/ml starting culture and 0 to 80 mg/ml yerba mate extract (n=3 for 0.5 and 1 h and n=7 for all other time points). Error bars show standard deviation. Statistically significant differences are marked by an asterisk for B only (RBD repeated measures ANOVA)..... 127

Figure 10. *S*. Typhimurium bioassays under control$_{no\ tea}$, tea, and control$_{no\ bacteria}$ treatments to test A. catalase activity with a simple foam assay and B. membrane integrity based on the uptake of crystal violet dye. Error bars show standard deviation. Statistically significant differences between control$_{no\ tea}$ and tea in A or between control$_{no\ bacteria}$ and tea in B are marked by an asterisk (RBD repeated measures ANOVA). n=4 for both A and B. 128
Figure 11. TCA cycle with plots displaying abundance of identifiable metabolites in three yerba mate extract treatments (control$_{no\ tea}$, tea, control$_{no\ bacteria}$) and at three timepoints (0, 40, 240 min). Asterisks mark significant differences between one control treatment at a single time point and the tea treatment at the corresponding time point. The citrate plot shows pooled results for citrate/isocitrate and the succinate plot shows pooled results for succinate/methylmalonate since these metabolite groups are indistinquishable with the methods used..... 129
Figure 12. Glycolysis pathways with plots displaying abundance of identifiable metabolites in three yerba mate extract treatments (control$_{no\ tea}$, tea, control$_{no\ bacteria}$) and at three timepoints (0, 40, 240 min). Asterisks mark significant differences between one control treatment at a single time point and the tea treatment at the corresponding time point. 130
Figure 13. Metabolites that are included in the discussion but not in the TCA cycle or glycolysis pathways. Plots display abundance of identifiable metabolites in three yerba mate extract treatments (control$_{no\ tea}$, tea, control$_{no\ bacteria}$) and at three timepoints (0, 40, 240 min). Asterisks mark significant differences between one control treatment at a single time point and the tea treatment at the corresponding time point. 131

Figure S 1. Heatmaps showing feature detection and retention time correction of GC-MS data. A and B correspond to methicillin-resistant *Staphylococcus aureus* (MRSA) and C and D correspond to methicillin-sensitive *S. aureus* (SA). Blue and red dots are from samples obtained at different times that are in need of retention time correction. The A and C heatmaps display data points before retention time correction and the B and D heatmaps display data points after retention time correction. The complete overlap of blue over red would show perfect retention time correction. 64
Figure S 2. UV- vis spectra of yerba mate (32 mg/ml or 64 mg/ml equivalents) with iron at varying concentrations. 95
Figure S 3. Saturation assays are plotted for A. Fe^{2+} ($FeSO_4$) and B. Fe^{3+} ($FeCl_3$); absorbance was monitored at 380 nm. No ferrozine was added for this assay. Experiments were done at least in duplicate; error bars represent standard deviation. 96
Figure S 4. Optical density at 600 nm of S. Typhimurium under 3 treatment types (control$_{no\ tea}$, tea, control$_{no\ bacteria}$). There were no significant differences between control$_{no\ tea}$ and tea treatments. Error bars represent standard deviation. n=4 139
Figure S 5. Pentose phosphate pathway with plots displaying abundance of identifiable metabolites in three yerba mate extract treatments (control$_{no\ tea}$, tea, control$_{no\ bacteria}$) and at three timepoints (0, 40, 240 min). Asterisks mark significant differences between one control treatment at a single time point and the tea treatment at the corresponding time point. Error bars represent 95% confidence intervals. 140
Figure S 6. Valine, leucine, and isoleucine biosynthesis pathway with plots displaying abundance of identifiable metabolites in three yerba mate extract treatments (control$_{no\ tea}$, tea, control$_{no\ bacteria}$) and at three timepoints (0, 40, 240 min). Asterisks mark significant differences

between one control treatment at a single time point and the tea treatment at the corresponding time point. Error bars represent 95% confidence intervals. 141
Figure S 7. Additional metabolites with significant differences between treatments; plots display abundance of identifiable metabolites in three yerba mate extract treatments ($control_{no\ tea}$, tea, $control_{no\ bacteria}$) and at three timepoints (0, 40, 240 min). Asterisks mark significant differences between one control treatment at a single time point and the tea treatment at the corresponding time point. Error bars represent 95% confidence intervals. 142

LIST OF ATTACHMENTS

Table 1. Known antibacterial mechanisms of action of plant phenolic compounds. (attachment)……..……Table_1_review_summary.pdf
Table 7. *L. casei* metabolites found to be significantly different between treatments with ‘control_no_bacteria= milk+tea, ‘control_no_tea ’ = milk+bacteria, and ‘tea’ = milk+tea+bacteria. Extracted ion intensity values normalized to a gallic acid internal standard are listed with data ranges in parentheses. (attached)……..Table7_p_ranks_Lcasei_sig.xls
Table 8. *S.* Typhimurium metabolites found to be significantly different between treatments with ‘control_no_bacteria= milk+tea, ‘control_no_tea ’ = milk+bacteria, and ‘tea’ = milk+tea+bacteria. Extracted ion intensity values normalized to a gallic acid internal standard are listed with data ranges in parentheses. (attached)……..Table8_p_ranks_STyphim_sig.xls
Table S 2. Ranking values of top 10 attributes for each ranking method. (attachment)……...……Table4_top10results.pdf
Table S 12. Complete list of all metabolites found with LC-MS. (attachment)……..TableS12_all-untargeted.xls
Table S 13. List of all identified metabolites found with LC-MS. (attachment)……..TableS13_all-targeted.xls

CHAPTER I
INTRODUCTION

Emergence of antibiotics

The germ theory of disease proposed by Louis Pasteur and Robert Koch changed popular approaches to medicine in the late 1800s and encouraged "chemotherapy" treatments with antiseptic chemicals. However, internal bacterial infections remained a major problem, particularly as fatal secondary infections of influenza victims in the 1918 pandemic (reviewed by Brundage & Shanks, 2008). A solution came serendipitously to Alexander Fleming, who observed that a contaminating mold (*Penicillium notatum*) prevented the growth of bacteria on an unattended agar plate (Fleming, 1929). Despite a delay of more than a decade in gaining recognition and mass production, the mold-produced penicillin stimulated the golden age of antibiotics in the 1950s, during which many novel compounds with new mechanisms of action were discovered and put to use in combating human and animal bacterial disease. Unfortunately, the beginnings of a new threat presented itself as strains of penicillin-resistant staphylococci were noted, and were associated with "adaptation" (Abraham et al., 1941) to penicillin. Since then, selection pressure for bacterial pathogens with resistance mechanisms have led to rising populations of pathogens with resistance to many common antibiotics; there are thus fewer and fewer treatment options remaining for infections of these bacteria (reviewed by Levy & Marshall, 2004). The urgency of this problem is highlighted by a study published less than a month ago that reported on a strain of *E. coli* with resistance to colistin, a "last resort" antibacterial, that was found in the U.S. for the first time (McGann et al., 2016). The ever-increasing presence of multi-drug resistant bacteria has pushed the search for new compounds and new mechanisms of action, but the search strategies of the 1950s, which focused on bacterial and fungal-derived compounds and their synthetic derivatives (reviewed by Lewis, 2013), seem

to be unfruitful in finding new antibacterial drugs. This has promoted a recent trend of searching other domains of life, including plants, for novel antibacterial compounds.

Antibacterial resistance overview

Antibacterial resistance exists through alterations in antibacterial-targeted cell structures, the modification or metabolism of the antibacterial, reduced permeability of the cell, and active efflux pumps that remove antibacterial compounds from the cell (Figure 1). Common antibacterial classes have distinct mechanisms of action that result in distinct resistance mechanisms. Beta-lactams act on the cell wall by binding penicillin-binding proteins, so resistance mechanisms include mutant penicillin binding proteins and beta-lactamase enzymes that degrade beta-lactam antibacterials. Macrolides, tetracyclines, aminoglycosides, and oxazolidinones all act on the ribosome (reviewed by Walsh et al., 2003) but in different binding locations, resulting in resistance mechanisms based on binding site mutations, modification of the antibacterial, and efflux by efflux pumps (reviewed by Wilson, 2014). Fluoroquinolones target DNA gyrase, so DNA gyrase mutants, altered cell permeability, and efflux pumps are mechanisms of fluoroquinolone resistance. Membrane permeability changes and efflux pumps can specifically exclude or remove certain chemical classes, or they can act non-specifically to prevent multiple classes of chemicals from entering the cells or to actively export them (reviewed by Kumar & Schweizer, 2005).

This dissertation focuses on two globally relevant bacterial pathogens: methicillin-resistant *Staphylococcus aureus* (MRSA), which has been implicated in thousands of deaths annually in the U.S. (CDC, 2013), and *Salmonella enterica* serovar Typhimurium, which was implicated in 30 deaths and thousands of infections in the U.S. in 2014 (CDC, 2015).

The most obvious approach to combat growing antibacterial resistance is to find new antibacterial compounds, but traditional search strategies of screening for inhibitory activity tend to rediscover the same compounds and directed high-throughput screens have had limited success; screening strategies have been limited by proper target selection and limited chemical diversity (reviewed by Silver, 2011). Natural products, though, could be a viable source of diverse chemical structures that are capable of inhibiting pathogenic bacteria by novel mechanisms, as this dissertation will explore.

There are alternative, cooperative strategies to discover novel compounds that are also being considered. With the increasingly limited effectiveness of existing antibacterial compounds, social and cultural strategies to carefully regulate antibacterial use have been proposed. These strategies include better tracking of the spread of resistance to guide control methods, halting the prophylactic use of sub-therapeutic concentrations of antibacterials in domestic animals and plants, isolating hospitalized individuals with multi-drug resistant (MDR) infections, and working with healthcare providers to differentiate viral from bacterial infections (reviewed by Levy & Marshall, 2004). Since the development of resistance will remain an issue even with novel antibacterials that have novel mechanisms of action, social strategies will likely be necessary to maintain effective antibacterial treatments.

Additional strategies to combat antibacterial resistance by interfering with virulence factors (i.e. toxins, quorum sensing) are also an active area of investigation and show promise for inhibiting disease-causing traits of bacterial pathogens without selecting for resistance in the population (reviewed by Bhardwaj, Vinothkumar, & Rajpara, 2013; Hauser, Mecsas, & Moir, 2016). The monoclonal antibody raxibacumab was approved by the FDA in 2012 for binding anthrax toxin in anthrax infections and three other monoclonal antibody inhibitors are currently

undergoing clinical trials (shigamab, bexlotoxumab, MEDI4893) (reviewed by Hauser et al., 2016). Phage therapy and microbiome modulation are also potential strategies to fight bacterial pathogens that may redirect selective pressures so that alternating treatment strategies can be applied (reviewed by Hauser et al., 2016).

Plants as sources of novel antibacterial compounds

Although alternatives to traditional antibacterial drugs are in development, they are not at a stage where they can be applied as regular treatment options for major MDR pathogens, so the continued search for novel compounds in natural products with diverse structures and novel mechanisms of action is still a valuable route of exploration. An extensive review of the antimicrobial use of plants by humans has suggested that phytochemicals in particular will be important in the discovery of novel therapeutics (Cowan, 1999). More recent studies have validated the potential for specific phytochemicals to effectively inhibit pathogenic bacteria with known antimicrobial resistance both alone and in synergy with other compounds; in one example a compound blocked the non-specific resistance mechanism of efflux pumps and another compound exerted a toxic effect (Tegos, Stermitz, Lomovskaya, & Lewis, 2002). Many whole plant extracts have also been observed to have antibacterial activity against bacterial pathogens, but only a subset of these studies have actually delved into the mechanistic questions that must be addressed in order to understand the circumstances under which a botanical can effectively inhibit bacterial pathogens.

This work focused on an initial characterization of the antibacterial activity of an aqueous extract of yerba mate. Yerba mate is a beverage prepared from the heat-processed leaves of *Ilex paraguarienses* and has a long history of human use in South American culture. It has been found to have antibacterial activity against *Staphylococcus aureus*, methicillin-resistant

Staphylococcus aureus (MRSA), *Salmonella*, *Listeria*, and pathogenic *Escherichia coli* (Burris, Davidson, Stewart, & Harte, 2011; Burris, Higginbotham, & Stewart, 2015; El-Sonbaty & Araby, 2014; Girolometto, Avancini, Carvalho, & Wiest, 2009; Gonzalez-gil et al., 2014; Martin et al., 2013; Rempe et al., 2015). As an extract that is "generally recognized as safe" (GRAS) by the U.S. Food and Drug Administration (FDA) for human consumption (electronic Code of Federal Regulations, subpart A, 182.20), it could be a useful antibacterial additive to foods and might contain bioactive components with novel antibacterial mechanisms. Yerba mate is known to contain a diverse array of phytochemicals, including polyphenolics, xanthine alkaloids (the stimulants caffeine, theobromine, and theophylline), and saponins (Heck & De Mejia, 2007). Phytochemical classes with known antibacterial activity include phenolics, terpenoids, alkaloids, lectins, polypeptides, and polyacetylenes (Cowan, 1999). Phenolic compounds are abundant in yerba mate and include the antibacterial compounds quercetin, kaempferol, caffeoylquinic acids, and feruloylquinic acids (Heck & De Mejia, 2007). Although these compounds should contribute to the antibacterial activity of yerba mate, no previous attempts have been made to determine whether one of these phenolics or another compound was the major contributor to antibacterial activity. Furthermore, while mechanisms of quercetin and kaempferol alone have been assayed, no previous attempts have been made to survey the mechanisms of action of the whole extract. This dissertation reviews the known mechanisms of action of plant phenolic compounds, reports an initial effort to identify the constituents of yerba mate contributing to antibacterial activity against MRSA, and investigates the major mechanisms of action enacted by the whole extract against *S*. Typhimurium.

Scope of dissertation

This dissertation is organized into 6 chapters. This introduction provides a short history of antibacterial development, mechanisms of antibacterial resistance and strategies to overcome antibacterial resistance, and an overview of plants as a source of antibacterial compounds with a focus on yerba mate. Chapter 2 discusses the known mechanisms of action of phenolic compounds and the role of systems biology methods in discovering novel mechanisms of action. Chapters 3-5 encompass the breadth of the research; Chapters 3 is a published peer-reviewed article, Chapter 4 is unpublished, and Chapter 5 will be submitted for peer-reviewed publication. Chapter 3 investigated the yerba mate compounds that contributed to antibacterial activity against methicillin-resistant *Staphylococcus aureus* based on the computational comparison of yerba mate fractions with differing antibacterial activities. Chapter 4 evaluated the accumulated metabolites of *Salmonella Typhimurium* and *Lactobacillus casei* grown in the presence of yerba mate in a milk system. Chapter 5 assessed the metabolic pathways of *Salmonella* Typhimurium at time points selected to glean information into the mechanisms of action of yerba mate extract. Finally, conclusions and future research directions are discussed in Chapter 6.

References

Abraham, E.P. et al., 1941. Futher observations on penicillin. *The Lancet*, 238(6155), pp.177–189.

Bhardwaj, A.K., Vinothkumar, K. & Rajpara, N., 2013. Bacterial quorum sensing inhibitors: attractive alternatives for control of infectious pathogens showing multiple drug resistance. *Recent patents on anti-infective drug discovery*, 8(1), pp.68–83.

Brundage, J.F. & Shanks, G.D., 2008. Deaths from bacterial pneumonia during 1918-19 influenza pandemic. *Emerging Infectious Diseases*, 14(8), pp.1193–1199.

Burris, K.P. et al., 2011. Antimicrobial activity of yerba mate (*Ilex paraguariensis*) aqueous extracts against *Escherichia coli* O157:H7 and *Staphylococcus aureus*. *Journal of food science*, 76(6), pp.M456–62.

Burris, K.P., Higginbotham, K.L. & Stewart, C.N., 2015. Aqueous extracts of yerba mate as bactericidal agents against methicillin-resistant *Staphylococcus aureus* in a microbiological medium and ground beef mixtures. *Food Control*, 50, pp.748–753.

CDC, 2013. Antibiotic resistance threats in the United States, 2013. *U. S. Department of Health and Human Services: Centers for Disease Control and Prevention*, pp.1–114.

CDC, 2015. National Antimicrobial Resistance Monitoring System for Enteric Bacteria (NARMS): Human Isolates Final Report, 2013.

Cowan, M.M., 1999. Plant products as antimicrobial agents. *Clinical microbiology reviews*, 12(4), pp.564–82.

El-Sonbaty, S.M. & Araby, E., 2014. Microbial regulation and protective effects of yerba mate (*Ilex paraguariensis*) in gamma-irradiated mice intestine ScienceDirect. *Journal of Radiation Research and Applied Sciences*, 7(2), pp.64–73.

Fleming, A., 1929. On the antibacterial action of cultures of a penicillium, with special reference to their use in the isolation of *B. influenzae*. *British Journal of Experimental Pathology*, 10(3), pp.226–236.

Girolometto, G. et al., 2009. Antibacterial activity of yerba mate (*Ilex paraguariensis* A.St.-Hil.) extracts. *Revista Brasileira de Plantas Medicinais*, 11(1), pp.49–55.

Gonzalez-gil, F. et al., 2014. Yerba mate enhances probiotic bacteria growth in vitro but as a feed additive does not reduce *Salmonella* Enteritidis colonization *in vivo*. *Poultry Science*, 93, pp.434–440.

Hauser, A.R., Mecsas, J. & Moir, D.T., 2016. Beyond antibiotics: new therapeutic approaches for bacterial infections. *Clinical infectious diseases: an official publication of the Infectious Diseases Society of America*, 63, pp.89–95.

Heck, C.I. & De Mejia, E.G., 2007. Yerba mate tea (*Ilex paraguariensis*): A comprehensive review on chemistry, health implications, and technological considerations. *Journal of Food Science*, 72(9), pp.138–151.

Kumar, A. & Schweizer, H.P., 2005. Bacterial resistance to antibiotics: Active efflux and reduced uptake. *Advanced Drug Delivery Reviews*, 57(10), pp.1486–1513.

Levy, S.B. & Marshall, B., 2004. Antibacterial resistance worldwide: causes, challenges and responses. *Nat.Med.*, 10(1078-8956 (Print)), pp.S122–S129.

Lewis, K., 2013. Platforms for antibiotic discovery. *Nature reviews. Drug discovery*, 12(5), pp.371–87.

Martin, J.G.P. et al., 2013. Antimicrobial activity of yerba mate (*Ilex Paraguariensis* St. Hil.) against food pathogens. *Revista Argentina de Microbiologia*, 45(2), pp.93–98.

McGann, P. et al., 2016. *Escherichia coli* harboring mcr-1 and blaCTX-M on a novel IncF plasmid: first report of mcr-1 in the USA. *Antimicrobial Agents and Chemotherapy*, 60(7), pp.4420–1.

Rempe, C.S. et al., 2015. Computational ranking of yerba mate small molecules based on their predicted contribution to antibacterial activity against methicillin-resistant *Staphylococcus aureus*. *Plos One*, 10(5), p.e0123925.

Silver, L.L., 2011. Challenges of antibacterial discovery. *Clinical microbiology reviews*, 24(1), pp.71–109.

Tegos, G. et al., 2002. Multidrug pump inhibitors uncover remarkable activity of plant antimicrobials. *Antimicrobial Agents and Chemotherapy*, 46(10), pp.3133–3141.

Walsh, S.E. et al., 2003. Activity and mechanism of action of selected biocidal agents on Gram -positive and -negative bacteria. *Journal of Applied Microbiology*, 94, pp.240–247.

Wilson, D.N., 2014. Ribosome-targeting antibiotics and mechanisms of bacterial resistance. *Nature reviews. Microbiology*, 12(1), pp.35–48.

Appendix

Figures

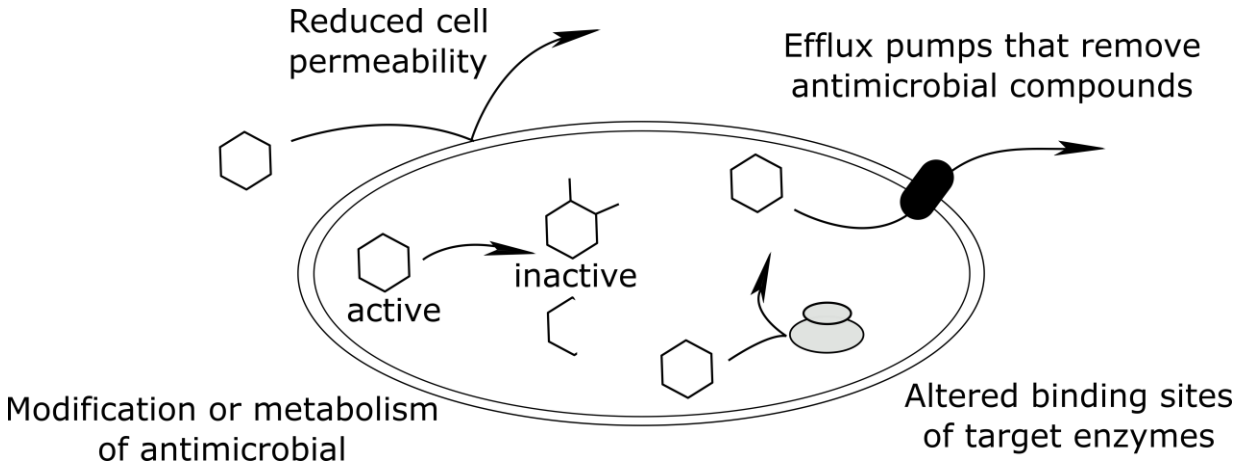

Figure 1. Bacterial mechanisms of resistance to antimicrobials. Inability of antimicrobial to cross cell barrier (decreased penetration), active membrane pump to shuttle out toxic compounds from within the cell (efflux pump), enzymatic degradation of antimicrobials (modification or inactivation of enzymes), and modification of the target site (prevents binding) (adapted from Abreu et al., 2012).

CHAPTER II
SYSTEMS BIOLOGY APPROACHES TO UNRAVELING ANTIBACTERIAL MECHANISMS OF PLANT PHENOLIC COMPOUNDS

A version of this chapter will be submitted to the *Journal of Applied Microbiology* for peer-reviewed publication by Caroline S. Rempe, Kellie P. Burris, Scott C. Lenaghan, and C. Neal Stewart, Jr.:

CS Rempe, SC Lenaghan, KP Burris, and CN Stewart, Jr. contributed to the conception, writing, and revising of this review article.

Summary

Drug resistance of bacterial pathogens is a growing problem that can be addressed through the discovery of compounds with novel mechanisms of antibacterial activity. Plants offer a plethora of compounds that have demonstrated broad antibacterial activity. While plant phenolic compounds may provide novel mechanisms of action, only known mechanisms of action have been evaluated. With systems biology approaches, antibacterial mechanisms can be assessed without the bias of target-directed bioassays to enable the discovery of novel mechanism(s) of action against drug resistant microorganisms.

Key words: phenolic, antibacterial, mechanisms of action, systems biology

Introduction

Each group of multi-drug resistant bacteria has been directly linked to thousands of deaths annually across the globe, with resistant *Shigella* species and *Mycobacterium tuberculosis* each causing more than one million deaths annually (WHO, 2014). In the United States (U.S.), drug resistant bacteria are the primary cause of more than 23,000 deaths and 2 million serious infections each year, of which resistant *Clostridium difficile*, *Enterobacteriaceae* species, and *Neisseria gonorrhoeae* are considered “urgent threats” (CDC, 2013). These numbers will continue to rise as multi-drug resistant bacteria become more prevalent; the recent

documentation of colistin-resistant *Escherichia coli* in the U.S. suggests that even "last resort" antibiotics with major side effects are likely to lose their effectiveness (McGann et al., 2016). Phenolic compounds found in plants can combat multi-drug resistant bacteria (reviewed by Abreu, McBain, & Simões, 2012), but their mechanisms of action must be thoroughly characterized before they can be rationally used as antibacterial treatments. Several common mechanisms of action have been verified to contribute to the antibacterial activity of phenolic compounds, but very few attempts have been made to seek novel mechanisms of action.

The general structural categories of plant-derived phenolics, as categorized by Cowan (1999), include simple phenolics, phenolic acids, quinones, flavonoids/flavones/flavonols, coumarins, and tannins. Although phenolics are classified as compounds with a hydroxylated aromatic ring, Cowan categorized flavones as "phenolic structures containing one carbonyl group" (Cowan, 1999), which prompted the inclusion of flavones in this work. A useful review of phytochemical classes and their general antibacterial modes of action has already been compiled (Borges, Saavedra, & Simões, 2015), as has as a detailed review of flavonoid mechanisms of action, including cytoplasmic membrane damage, topoisomerase inhibition, NADH-cytochrome c reductase inhibition, and ATP synthase inhibition (Cushnie & Lamb, 2011). More recent flavonoid reviews have focused on mechanisms of action involving cell membranes (Tsuchiya, 2015; Verstraeten, Fraga, & Oteiza, 2015). The mechanisms of action of phenolic compounds were additionally reviewed with an emphasis on structural features correlated to specific mechanisms (Gyawali & Ibrahim, 2014).

Most methods to determine antibacterial mechanisms are target-directed assays that directly test single proteins or other cellular targets *in vitro*. These target-directed methods are required to fully understand mechanisms of action, but they have no chance of identifying novel

targets since activity assays only assess whether or not the pre-selected target was inhibited. An expansion to undirected systems biology approaches that survey all targets within the detection range for a given technology will allow for the identification of novel mechanisms of action that can combat multi-drug resistant bacterial pathogens. Target-directed assays are very informative since established bioassay protocols against a single target can definitively assign binding and inhibitory activity of compounds with enzymes known to be essential to cell survival. However, target-directed assays also limit the scope of mechanisms that can be identified, which is undesirable when existing antibacterial mechanisms of action threaten to become obsolete with the rise of resistant bacteria. This is where undirected approaches like systems biology have value, in the broad, unbiased survey of possible mechanisms that can be used to formulate new hypotheses for novel target-directed assays.

In this review, we aim to assess the current state of mechanistic investigations of plant phenolic antibacterial compounds and survey systems biology approaches that have successfully contributed to determining antibacterial mechanisms.

Membrane disruption by phenolic compounds

Membrane disruption, in both Gram-positive and Gram-negative bacteria, contributes to the antibacterial activity of most plant phenolics that have been mechanistically assessed (Table 1). Many of the membrane integrity analyses cited in Table 1 combined several common, simple methods to monitor the influx of hydrophobic dyes or antibiotics, the efflux of intracellular constituents, and microscopic observation. While these membrane permeability analyses provided valuable information about membrane disruption, they gave little, if any, direction to the specific major mechanisms of action of a compound. Furthermore, they generally left an open question as to whether the compound altered membrane stability by interfering with

intracellular processes or by direct interaction with membrane components. Other more unique assays have also been conducted, for example, in the quantification of cell surface hydrophobicity the tendency of a hydrophilic water drop to spread or bead when in contact with a bacterial lawn was measured (Borges, Ferreira, Saavedra, & Simões, 2013). This assay more specifically characterized the effect of gallic and ferulic acids, which were observed to increase surface hydrophilicity of Gram-negative bacteria and hydrophobicity of Gram-positive bacteria (Borges et al., 2013). Nevertheless, this measure of surface hydrophobicity could also be attributed to either direct interaction with the membrane or an interaction with intracellular components that impact cell wall chemistry.

Once a membrane effect is known to exist, specific binding assays or model membrane insertion assays (T. Wu, He, et al., 2013) can confidently test direct interactions between specific components. Model membranes have already been used to test the direct interaction of epicatechin gallate and epigallocatechin gallate with membranes (Hashimoto, Kumazawa, Nanjo, Hara, & Nakayama, 1999; Kumazawa et al. 2004). However, the extensive diversity in bacterial membrane composition (Sohlenkamp & Geiger, 2016) would likely require specific assays with each organism of interest. Another unique assay that may be useful in assessing direct membrane binding is the addition of exogenous magnesium to a basic membrane integrity assay. This assessment revealed a dependence on magnesium akin to an ethylenediaminetetraacetic acid (EDTA) control for the membrane-disrupting activity of gallic acid (Nohynek et al., 2006). Since magnesium ions are known to stabilize Gram-negative bacterial membranes, this simple assay might easily test direct membrane interactions involving magnesium, though other integral cell functions involving magnesium should also be considered.

A particularly in-depth study was conducted for epigallocatechin gallate's mechanism of action against methicillin-resistant *Staphylococcus aureus* (MRSA) and its contribution to renewed beta-lactam susceptibility. The study assessed purified cell wall components, phosphorus content, the effects of exogenous peptidoglycan on activity, adherence to glass, penicillin binding protein abundance, Triton-X-100 autolysis, bacteriolytic enzymes, free lipoteichoic acid, and lysostaphin's pentaglycine cleavage activity. Each of these methods focused on addressing a particular hypothesis of epigallocatechin gallate's mechanism of action, which is an ideal, albeit time-consuming, approach for a mechanistic assessment. Nevertheless, the specific mechanism of action remained unknown despite the new knowledge of epigallocatechin gallate's observed cell adherence, accumulated autolysins, increased lipoteichoic acid release, lack of effect on penicillin binding proteins, and reduced effect on Triton-X autolysis and lysostaphin lysis (Stapleton, Shah, Ehlert, Hara, & Taylor, 2007). Another method that has given mechanistic insight, but not a specific mechanism of action, was the use of high resolution gas chromatography (HRGC) lipid profiling to identify specific lipids altered by the presence of eugenol, carvacrol, or thymol in both Gram-negative and Gram-positive bacteria (Di Pasqua et al., 2007). All three tested phenolics were observed to increase major fatty acids (palmitic, oleic, cis-10 heptadecenoic acids) in Gram-negative bacteria while Gram-positive *S. aureus* lipid profiles changed across several fatty acids. *S. aureus* treatment with thymol, though, resulted in a clear increase in saturated fatty acids and decrease in unsaturated fatty acids, which could be due to a desaturase response to cell leakage (Di Pasqua et al., 2007). While this type of untargeted assessment requires interpretation, it gives a greater depth of information than most of the basic membrane disruption assays. When iterations of logically planned assays are performed, as in the epigallocatechin example discussed before the HRGC study, a good depth of

information is also obtained. However, conducting iterations of assays is time and labor intensive while HRGC can gather information on many potential targets simultaneously. Although no liquid chromatography-mass spectrometry (LC-MS) lipidomics experiment to deduce the mechanisms of action of a phenolic was encountered in the literature, a basic LC-MS experiment can measure an even larger range of metabolites than HRGC and more confidently identify them; this technology can profile the relative abundance of thousands of lipids simultaneously and is easily automated (Wenk, 2005). More untargeted approaches capable of profiling thousands of compounds in a single experiment will be useful in the rapid generation of mechanistic hypotheses that can subsequently be tested with a relevant subset of targeted assays.

Non-membrane mechanisms of action

Assessments for non-membrane mechanisms of action can also be categorized into target-directed assays for known mechanisms of action and undirected experiments that take a systems-wide approach to exploring mechanisms of action. Among the plant phenolics tested in Table 1, targeted assays have discovered DNA gyrase inhibitory activity for 10 phenolic compounds (Ohemeng, Schwender, Fu, & Barrett, 1993; T. Wu, Zang, He, Pan, & Xu, 2013), type III secretion inhibition for 9 compounds (Tsou et al., 2016), inhibition of helicase activity for 5 phenolic compounds (Xu et al., 2001), multi-drug efflux pump inhibitors for 3 compounds (Bag & Chattopadhyay, 2014; Fiamegos et al., 2011; E. C. J. Smith et al., 2007), dehydratase inhibition for 3 compounds (Zhang et al., 2008), protein kinase inhibition for 2 compounds (Shakya et al., 2011), and single phenolic compounds among which one inhibited urease activity (Moon et al., 2013), one bound iron (Chung, Lu, & Chou, 1998), one inhibited succinate dehydrogenase and malate dehydrogenase (Yao et al., 2012), one intercalated into DNA (Lou et al., 2012), one induced DNA fragmentation, an ROS response, and suppressed FtsZ expression

(Hwang & Lim, 2015), and one bound to the FtsZ protein and inhibited FtsZ assembly (Rai, Singh, Roy, & Panda, 2008). Many of these results clearly come from a single study picking a mechanism of action and screening several phenolic compounds for activity. This approach generates valuable information and more such screens are needed to assess phenolic antibacterial mechanisms. Nevertheless, the major mechanism(s) of a compound could easily be overlooked with a screening approach if multiple mechanisms exist. This problem seems likely when looking at one of the most-studied phenolics, quercetin, and its diverse list of mechanisms (cell membrane disruption, DNA intercalation, DNA gyrase inhibition, type III secretion inactivation, dehydratase inhibition (HpFabZ), and protein kinase inhibition; Table 1).

A general methodological approach to these targeted assessments was to verify antibacterial activity, purify the target enzyme, and characterize its phenolic-bound and unbound structures using spectrophotometric techniques. As an example, after gathering antibacterial activity data and purifying the FtsZ enzyme, curcumin was observed to inhibit the FtsZ protofilament assembly by monitoring assembly kinetics with light scattering, to bind to purified FtsZ based on an increase in bound-curcumin fluorescence at 495 nm, and was noted to alter the secondary structure of FtsZ based on a circular dichroism analysis (Rai et al., 2008). In some studies, however, only inhibitory activity was determined and structural binding characteristics were not assessed (Bag & Chattopadhyay, 2014; Ohemeng et al., 1993; E. C. J. Smith et al., 2007). The most specific interaction details were found by the 2 studies that obtained crystal structures of quercetin or apigenin bound to the enzymes they inhibited (Shakya et al., 2011; Zhang et al., 2008). One of these studies moved to the next step in mechanistic understanding by introducing a single amino acid mutation to the enzyme in order to verify the importance of a key binding interaction (Zhang et al., 2008). Unfortunately, the conserved tyrosine that was

mutated did not alter binding, so the specific, necessary interaction points between quercetin or apigenen and FabZ still need to be validated (Zhang et al., 2008). There were also 2 studies in which detailed structure mechanisms were determined with molecular docking, but not further validated through single amino acid mutation or crystal structures (Fiamegos et al., 2011; Plaper et al., 2003). Detailed structural characterizations of phenolic binding mechanisms are a valuable contribution to the field that can facilitate successful computational prioritizations of potentially active compounds and predictions of compound activities to guide both natural product testing and rational antibacterial design.

Only one study in Table 1 that is not membrane-specific can be called untargeted: the proteomics assessment of thymol antibacterial activity against *Salmonella* Thompson (Di Pasqua, Mamone, Ferranti, Ercolini, & Mauriello, 2010). This study found altered abundances of citric acid cycle enzymes, ATP synthesis enzymes, stress-related chaperone proteins, cell envelope proteins, and an absence of the antioxidant protein thioredoxin 1 in treated cells. Although a specific mechanism of action was not identified here, valuable information was produced that verified the cell membrane disruption observed in other thymol-treated Gram-negative bacteria and added several additional possible protein targets. Additional assays to test different portions of the impacted pathways, thioredoxin, and relevant regulatory proteins are still needed, of course, but it is now clear that membrane disruption alone was not the sole mechanism of action of thymol against *S.* Thompson and that intracellular proteins, including thioredoxin, may be important targets (Di Pasqua et al., 2010).

Key functional characteristics

Mechanisms characterized to the level of atomic interaction points are rare in the examples of Table 1, but give the most specific mechanistic information. Crystal structures of quercetin and

apigenin bound to FabZ showed that quercetin and apigenen, which differ only in 2 hydroxyl groups, similarly bind between amino acid groups to block substrates from passing through a tunnel to reach the active site (Zhang et al., 2008). Hydrophobic interactions likely sandwich the phenolic ring between a tyrosine and proline in one binding site and between a phenylalanine and an isoleucine in a second binding site. In the crystal structure of quercetin-bound resistance kinases, hydrogen bonds between hydroxyl groups and nearby amino acids appeared to be the primary interactions (Shakya et al., 2011). Based on several flavonoids tested, the absence of a particular carbonyl group was necessary for binding and the hydroxyl position was important (Shakya et al., 2011). A molecular docking study of quercetin and DNA gyrase proposed that quercetin has one mechanism by which it binds DNA, stabilizes the DNA-gyrase complex, and induces DNA cleavage in addition to a second mechanism by which it inhibits DNA supercoiling by competitively binding to the ATP binding site of the DNA gyrase B subunit (Plaper et al., 2003). Another molecular docking study surveyed the localization of caffeoylquinic acids to an efflux pump and determined that caffeoyquinic acids tended to bind in a position that blocked the efflux pump (Fiamegos et al., 2011).

Similar trends in functional groups that contribute to bioactivity are seen in many structure activity relationship studies. Electron distribution, as impacted by the number and location of hydroxyl groups and double bonds, has been the major factor associated with antibacterial activity of flavonoids (reviewed by Gyawali & Ibrahim, 2014; Shapiro & Guggenheim, 1998; Wu, Zang, et al., 2013; Wu, He, et al., 2013). Electron localization and other structural features also impact molecular hydrophobicity, which impacts the types of membrane interactions that are possible.

Other studies have found hydroxyl counts and positions to be important for bioactivity extending beyond flavonoids and into the broader category of phenolics. A quantitative structure activity relationship (QSAR) analysis with more than 100 phenolics and related compounds used MIC values against the oral bacteria *Porphyomonas gingivalis*, *Selenomonas artemidis*, and *Streptococcus sobrinus* and found that a hydroxyl group attached to an aromatic ring was required for low MICs (Shapiro & Guggenheim, 1998). Exceptions to the general trend of key hydroxyl placement have been observed through isomers that had different antibacterial activities, suggesting that chirality is also an important factor (Friedman, Henika, & Mandrell, 2002; reviewed by Gyawali & Ibrahim, 2014). Interestingly, the number of hydroxyl groups has also been correlated with antioxidant activity (reviewed by Balasundram, Sundram, & Samman, 2006; Rice-Evans, Miller, & Paganga, 1996). However, any relationship between antioxidant activity and antibacterial activity is not fully understood.

Synergistic antibacterial activity

If specific mechanisms of action are known, phenolic compounds can be rationally combined with other antibacterial compounds to synergistically combat multi-drug resistant bacteria. Synergistic effects have already been observed for many phenolic compounds when combined with antibiotics currently in use (reviewed by Aiyegoro & Okoh, 2009; Amin, Khurram, Khattak, & Khan, 2015; Hemaiswarya & Doble, 2010; essential oil components reviewed by Langeveld, Veldhuizen, & Burt, 2014; Lim et al., 2016; Oh & Jeon, 2015). Many synergistic effects have been attributed to membrane-disrupting compounds, including phenolics, that allow intracellular toxins faster/easier access to their targets (Amin et al., 2015; Hemaiswarya & Doble, 2010; Oh & Jeon, 2015). Additionally, strains that use efflux pumps to remove toxins can be attacked by blocking the efflux pumps with one compound and applying an intracellular toxin as

a second compound for synergistic killing (Oh & Jeon, 2015; reviewed by Prasch & Bucar, 2015; Tegos & Stermitz, 2002). The down-regulation of efflux pump proteins has also been observed (Oh & Jeon, 2015). Synergistic effects between other modes of action may also exist and could improve the functionality of existing antibacterial compounds, especially in combating drug resistance mechanisms.

Systems biology methods

Phenolic compounds from natural sources have been assessed for antibacterial mechanisms related to membranes and specific protein and/or pathway targets (Table 1; Figure 2). However, most of these assays are limited to target-directed tests of known antibacterial mechanisms and do not facilitate the discovery of novel mechanisms of action or multiple mechanisms of action. An undirected systems biology approach could reveal the major known and/or unknown mechanism(s) of action (Vincent, Ehmann, Mills, Perros, & Barrett, 2016). In particular, -omics approaches could reveal unknown mechanisms quickly, with less effort than other systems biology approaches.

Non-omics systems biology approaches include affinity chromatography, which requires immobilizing the antibacterial compound in a column, eluting it with any bound proteins, and then characterizing the bound protein (reviewed Wong, Cheng, He, & Chen, 2008); phage display of translated peptides, which requires several rounds of “biopanning” to remove phage-displayed peptides that were not bound by the tested antibacterial compound (reviewed Wong et al., 2008); and the high-throughput but still time intensive methods of screening for novel targets followed by screening for inhibitors of targets (reviewed by Harvey, Edrada-Ebel, & Quinn, 2015; Miesel, Greene, & Black, 2003; Payne, Gwynn, Holmes, & Pompliano, 2007). Also included are time-intensive chemical-chemical interaction approaches that screen the effects of a

compound of unknown mechanism in combination with each compound of a diverse set of antibiotics with known mechanisms (Farha & Brown, 2010). A recent review discussed another major method, the time-consuming construction and screening of genetic mutants for antibacterial resistance (Farha & Brown, 2016). This method has had success, but also has the potential to simply reveal mechanisms of resistance that are distinct from mechanisms of antibacterial action.

Metabolomics is capable of using µl volumes of extracted samples to gain information on potentially thousands of metabolites that define antibacterial mechanisms in 30 min per sample for some system platforms (Lu et al., 2010). The major limitations of -omics approaches are the ranges of detection for different technologies and the availability of annotated information for a given organism. In the metabolomics example, high resolution LC-MS systems can give a good representation of major bacterial metabolic pathways, but lipids, high molecular-weight compounds, and volatile compounds generally require separate runs on different instrument platforms (reviewed by Aretz & Meierhofer, 2016; Dettmer, Aronov, & Hammock, 2007). On the annotation aspect, bacterial pathogens have long been a focal point of bacterial research, so they are relatively well studied and have readily accessible, consistently annotated data in a recent database dedicated to pathogens (Wattam et al., 2014), though annotated genomes and metabolomes in general are still far from comprehensive (Aretz & Meierhofer, 2016; Médigue & Moszer, 2007). Thus, -omics analyses should be a viable option for determining antibacterial mechanisms of uncharacterized compounds. Metabolomics has already proven useful for determining mechanisms of action that impact specific metabolic functions. The mechanisms of action of a thymidine kinase inhibitor (AZ1), a 1-deoxy D-xylulose 5-phosphate (DXR) pathway inhibitor (fosmidomycin), and a lipid A synthesis inhibitor (CHIR-090) were readily identified

with *E. coli* metabolomics data by data analysts blinded to the antibiotics used (Vincent et al., 2016). However, in the analysis of other compounds, the metabolomics data showed non-specific upregulation of many metabolites for a peptidoglycan cross-linking inhibitor, a DNA ligase inhibitor, and an enoyl-acyl carrier protein inhibitor. Furthermore, no discernible metabolic differences were observed between a control and an antibiotic treatment that uncoupled the proton gradient of the electron transport chain. Measurement limitations in observing peptidoglycan molecules (too large) and mono-, di-, and tri-phosphates (differing ionizabilities) were possible reasons for the lack of relevant information from the peptidoglycan inhibitor and oxidative phosphorylation inhibitor (Vincent et al., 2016). Belenky et al. (2015) were also able to differentiate antibacterial compound treatments based on the affected *E. coli* metabolome after 60 and 90 min of treatment, but not after 30 min. It was not specified whether the known cellular targets of ampicillin, kanamycin, and norfloxacin could be determined from their respective metabolomes, but the ROS hypothesis of cell death was supported based on similarly high levels of a metabolic marker for DNA/RNA oxidation across all antibiotic treatments (Belenky, Ye, Porter, Cohen, et al., 2015). Another metabolomic study successfully used the exometabolome of *S. aureus* to determine the previously unknown antibacterial mechanism of action of triphenylbismuthdichloride (TPBC). By comparing the exometabolome of TPBC-treated *S. aureus* to the exometabolomes of kanamycin, ciprofloxacin, trimethoprim, and fluoropyruvate it was observed that only TPBC and fluoropyruvate continuously accumulated pyruvate. Thus, the pyruvate dehydrogenase inhibition activity of TPBC was hypothesized and then verified by an enzyme activity assay with cell lysate (Birkenstock et al., 2012). Another study used a similar comparison methodology to hypothesize the mechanism of the non-phenolic plant natural product dihydrocucurbitacin F-25-O-acetate. The metabolic profile of *S. aureus* treated with

dihydrocucurbitacin F-25-O-acetate clustered with the metabolic profile of *S. aureus* treated with vancomycin, a known inhibitor of peptidoglycan synthesis (Biao-Yi, Yu, & Zeng-Liang, 2008).

A scheme to classify compounds into known mechanisms of action was also recently used with NMR metabolomics, where a partial least squares discriminant analysis of the metabolic "fingerprints" of *E. coli* treated with one of 9 antibiotics of known mechanism gave 91% accuracy with intracellular data and 30% accuracy with extracellular data (Hoerr et al., 2016). Another systems biology approach similarly classified phenotypes based on the Raman spectra of dried *E. coli* cells to distinguish antibacterial mechanisms of action; 15 antibacterial compounds representing protein synthesis inhibitors, cell wall synthesis inhibitors, DNA synthesis inhibitors, and RNA synthesis inhibitors were differentiable with 83.6% accuracy by mechanistic class. Ampicillin was always incorrectly classified with the final model based on a linear discriminant analysis of principle components, but overlap between the mechanism groups could explain this and other misclassification tendencies (Athamneh, Alajlouni, Wallace, Seleem, & Sengera, 2014). Classification schemes like these can only classify data into known mechanisms of action. However, unknown mechanisms of action should not group into known mechanistic classes and could thus be singled out for further characterization.

Transcriptomic studies have tended to highlight pathways impacted by an antibacterial compound without identifying a specific mechanism of action (Yu et al. 2012, Bionda et al. 2013, Elnakady et al. 2016), although transcriptional profiling of bacterial mutants revealed expression trends that were used to predict phenylalanyl-tRNA synthetase inhibition and bacterial acetyl coenzyme A carboxylase inhibition as the primary mechanisms of action of two novel antibacterial compounds (C Freiberg, Fischer, & Brunner, 2005). A 2004 review cites transcriptomic and proteomic studies that used transcriptomics or proteomics to assess

antibacterial mechanisms, some of which were successful in identifying mechanisms of action (Christoph Freiberg, Brötz-Oesterhelt, & Labischinski, 2004). More recently, proteomics showed its usefulness in mechanistic assessments by providing evidence for a second mechanism of action of the atypical tetracycline chelocardin, which inhibits peptidyl transferase at low concentrations and causes membrane depolarization at high concentrations in *B. subtilis* (Stepanek, Lukežič, Teichert, Petković, & Bandow, 2016).

Structural systems pharmacology has also made strides in identifying antibacterial mechanisms through combining multiple -omics approaches. A recent study was able to use an *E. coli* K12 genome scale metabolic model integrated with protein structures to correctly predict the antibacterial mechanisms of fosfomycin, and sulfathiazole. This model was also able to predict additional mechanisms of action for (1-hydroxyheptane-1,1-diyl)bis(phosphonic acid) and cholesteryl oleate and predict potential inhibitors of a protein target (tryptophan synthase beta subunit) with no previously known inhibitors. However, many false positives were also observed, which could be attributed to the static protein structures used to evaluate ligand binding (Chang, Xie, Bourne, & Palsson, 2013).

Systems biology approaches in assessments of phenolic antibacterial mechanisms of action are relatively rare: Nakayama et al. (2015) used proteomics to identify a set of membrane proteins that epicatechin gallate may inhibit in *Bacillus subtilis* (Nakayama et al., 2015) while Di Pasqua et al. (2007) used HRGC to evaluate membrane effects of thymol, carvacrol, and eugenol and Di Pasqua et al. (2010) used proteomics to identify proteins and pathways altered by thymol.

Conclusion

The mechanisms of action of most naturally derived phenolic compounds are not well characterized. Of the compounds reviewed here, mechanistic assessments have found specific

antibacterial targets, including DNA, DNA gyrase, multi-drug efflux pumps, FabZ, protein kinases, helicase, and FtsZ. The identification of these antibacterial targets through target-directed methods enables the rational use of phenolic compounds against bacterial pathogens susceptible to these known mechanisms of action. However, target-directed approaches have no opportunity to discover novel mechanisms of action, which is a necessary step to combat multi-drug resistant bacteria. A systems-biology approach to investigating the antibacterial mechanisms of phenolic compounds is not yet common in determining phenolic antibacterial mechanisms of action, but will likely push the field forward by speeding up mechanistic determinations and removing the bias of testing for currently known mechanisms.

References

Abreu, A.C., McBain, A.J., Simões, M., 2012. Plants as sources of new antimicrobials and resistance-modifying agents. Nat. Prod. Rep. 29, 1007–21.

Aiyegoro, O.A., Okoh, A.I., 2009. Use of bioactive plant products in combination with standard antibiotics: implications in antimicrobial chemotherapy. J. Med. Plants Res. 3, 1147–1152.

Amin, M.U., Khurram, M., Khattak, B., Khan, J., 2015. Antibiotic additive and synergistic action of rutin, morin and quercetin against methicillin resistant *Staphylococcus aureus*. BMC Complement. Altern. Med. 15, 59.

Aretz, I., Meierhofer, D., 2016. Advantages and pitfalls of mass spectrometry based metabolome profiling in systems biology. Int. J. Mol. Sci. 17, 632.

Athamneh, A.I.M., Alajlouni, R.A., Wallace, R.S., Seleem, M.N., Sengera, R.S., 2014. Phenotypic profiling of antibiotic response signatures in *Escherichia coli* using Raman spectroscopy. Antimicrob. Agents Chemother. 58, 1302–1314.

Bag, A., Chattopadhyay, R.R., 2014. Efflux-pump inhibitory activity of a gallotannin from *Terminalia chebula* fruit against multidrug-resistant uropathogenic *Escherichia coli*. Nat. Prod. Res. 28, 37–41.

Balasundram, N., Sundram, K., Samman, S., 2006. Phenolic compounds in plants and agri-industrial by-products: antioxidant activity, occurrence, and potential uses. Food Chem. 99, 191–203.

Belenky, P., Ye, J.D., Porter, C.B.M., Cohen, N.R., Lobritz, M.A., Ferrante, T., Jain, S., Korry, B.J., Schwarz, E.G., Walker, G.C., Collins, J.J., 2015. Bactericidal antibiotics induce toxic metabolic perturbations that lead to cellular damage. Cell Rep. 13, 968–980.

Biao-Yi, Z., Yu, Y., Zeng-Liang, Y., 2008. Investigation of antimicrobial model of *Hemsleya pengxianensis* W.J. Chang and its main active component by metabolomics technique. J. Ethnopharmacol. 116, 89–95.

Birkenstock, T., Liebeke, M., Winstel, V., Krismer, B., Gekeler, C., Niemiec, M.J., Bisswanger, H., Lalk, M., Peschel, A., 2012. Exometabolome analysis identifies pyruvate dehydrogenase as a target for the antibiotic triphenylbismuthdichloride in multiresistant bacterial pathogens. J. Biol. Chem. 287, 2887–2895.

Borges, A., Ferreira, C., Saavedra, M.J., Simões, M., 2013. Antibacterial activity and mode of action of ferulic and gallic acids against pathogenic bacteria. Microb. Drug Resist. 19, 256–265.

Borges, A., Saavedra, M.J., Simões, M., 2015. Insights on antimicrobial resistance, biofilms and the use of phytochemicals as new antimicrobial agents. Curr. Med. Chem. 22, 2590–2614.

CDC, 2013. Antibiotic resistance threats in the United States, 2013. U. S. Dep. Heal. Hum. Serv. Centers Dis. Control Prev. 1–114.

Chang, R.L., Xie, L., Bourne, P.E., Palsson, B.O., 2013. Antibacterial mechanisms identified through structural systems pharmacology. BMC Syst. Biol. 7, 102.

Chung, K.T., Lu, Z., Chou, M.W., 1998. Mechanism of inhibition of tannic acid and related

compounds on the growth of intestinal bacteria. Food Chem. Toxicol. 36, 1053–1060.

Cowan, M.M., 1999. Plant products as antimicrobial agents. Clin. Microbiol. Rev. 12, 564–82.

Cushnie, T.P.T., Lamb, A.J., 2011. Recent advances in understanding the antibacterial properties of flavonoids. Int. J. Antimicrob. Agents 38, 99–107.

Dettmer, K., Aronov, P.A., Hammock, B., 2007. Mass spectrometry-based metabolomics. Mass Spectrom. Rev. 26, 51–78.

Di Pasqua, R., Betts, G., Hoskins, N., Edwards, M., Ercolini, D., Mauriello, G., 2007. Membrane toxicity of antimicrobial compounds from essential oils. J. Agric. Food Chem. 55, 4863–4870.

Di Pasqua, R., Mamone, G., Ferranti, P., Ercolini, D., Mauriello, G., 2010. Changes in the proteome of *Salmonella enterica* serovar Thompson as stress adaptation to sublethal concentrations of thymol. Proteomics 10, 1040–1049.

Farha, M.A., Brown, E.D., 2010. Chemical probes of *Escherichia coli* uncovered through chemical-chemical interaction profiling with compounds of known biological activity. Chem. Biol. 17, 852–862.

Farha, M.A., Brown, E.D., 2016. Strategies for target identification of antimicrobial natural products. Nat. Prod. Rep. 33, 668–680.

Fiamegos, Y.C., Kastritis, P.L., Exarchou, V., Han, H., Bonvin, A.M.J.J., Vervoort, J., Lewis, K., Hamblin, M.R., Tegos, G.P., 2011. Antimicrobial and efflux pump inhibitory activity of caffeoylquinic acids from *Artemisia absinthium* against Gram-positive pathogenic bacteria. PLoS One 6, 1–12.

Freiberg, C., Brötz-Oesterhelt, H., Labischinski, H., 2004. The impact of transcriptome and proteome analyses on antibiotic drug discovery. Curr. Opin. Microbiol. 7, 451–459.

Freiberg, C., Fischer, H.P., Brunner, N.A., 2005. Discovering the mechanism of action of novel antibacterial agents through transcriptional profiling of conditional mutants discovering the mechanism of action of novel antibacterial agents through transcriptional profiling of conditional mutants 49, 749–759.

Friedman, M., Henika, P.R., Mandrell, R.E., 2002. Bactericidal activities of plant essential oils and some of their isolated constituents against *Campylobacter jejuni*, *Escherichia coli*, *Listeria monocytogenes*, and *Salmonella enterica*. J. Food Prot. 65, 1545–1560.

Gyawali, R., Ibrahim, S. a., 2014. Natural products as antimicrobial agents. Food Control 46, 412–429.

Harvey, A.L., Edrada-Ebel, R., Quinn, R.J., 2015. The re-emergence of natural products for drug discovery in the genomics era. Nat. Rev. Drug Discov. 14, 111–129.

Hashimoto, T., Kumazawa, S., Nanjo, F., Hara, Y., Nakayama, T., 1999. Interaction of tea catechins with lipid bilayers investigated with liposome systems. Biosci. Biotechnol. Biochem.

Hemaiswarya, S., Doble, M., 2010. Synergistic interaction of phenylpropanoids with antibiotics against bacteria. J. Med. Microbiol. 59, 1469–1476.

Hoerr, V., Duggan, G.E., Zbytnuik, L., Poon, K.K.H., Große, C., Neugebauer, U., Methling, K.,

Löffler, B., Vogel, H.J., 2016. Characterization and prediction of the mechanism of action of antibiotics through NMR metabolomics. BMC Microbiol. 16, 82.

Hwang, D., Lim, Y.-H., 2015. Resveratrol antibacterial activity against *Escherichia coli* is mediated by Z-ring formation inhibition via suppression of FtsZ expression. Sci. Rep. 5, 1–10.

Kumazawa, S., Kajiya, K., Naito, A., Saito, H., Tuzi, S., Tanio, M., Suzuki, M., Nanjo, F., Suzuki, E., Nakayama, T., 2004. Direct evidence of interaction of a green tea polyphenol, epigallocatechin gallate, with lipid bilayers by solid-state nuclear magnetic resonance. Biosci. Biotechnol. Biochem. 68, 1743–7.

Langeveld, W.T., Veldhuizen, E.J.A., Burt, S.A., 2014. Synergy between essential oil components and antibiotics: a review. Crit. Rev. Microbiol. 40, 76–94.

Lim, A., Subhan, N., Jazayeri, J.A., John, G., Vanniasinkam, T., Obied, H.K., 2016. Plant phenols as antibiotic boosters: *in vitro* interaction of olive leaf phenols with ampicillin. Phyther. Res. 30, 503–509.

Lou, Z., Wang, H., Rao, S., Sun, J., Ma, C., Li, J., 2012. *p*-Coumaric acid kills bacteria through dual damage mechanisms. Food Control 25, 550–554.

Lu, W., Clasquin, M.F., Melamud, E., Amador-Noguez, D., Amy, A., Rabinowitz, J.D., 2010. Metabolome analysis via reversed-phase ion-pairing liquid chromatography coupled to a stand alone orbitrap mass spectrometer. Anal. Chem. 82, 3212–3221.

McGann, P., Snesrud, E., Maybank, R., Corey, B., Ong, A.C., Clifford, R., Hinkle, M., Whitman, T., Lesho, E., Schaecher, K.E., 2016. *Escherichia coli* harboring mcr-1 and blaCTX-M on a novel IncF plasmid: first report of mcr-1 in the USA. Antimicrob. Agents Chemother. 60, 4420–1.

Médigue, C., Moszer, I., 2007. Annotation, comparison and databases for hundreds of bacterial genomes. Res. Microbiol. 158, 724–736.

Miesel, L., Greene, J., Black, T.A., 2003. Genetic strategies for antibacterial drug discovery. Nat. Rev. Genet. 4, 442–456.

Moon, S.H., Lee, J.H., Kim, K.T., Park, Y.S., Nah, S.Y., Ahn, D.U., Paik, H.D., 2013. Antimicrobial effect of 7-O-butylnaringenin, a novel flavonoid, and various natural flavonoids against *Helicobacter pylori* strains. Int. J. Environ. Res. Public Health 10, 5459–5469.

Nakayama, M., Shimatani, K., Ozawa, T., Shigemune, N., Tomiyama, D., Yui, K., Katsuki, M., Ikeda, K., Nonaka, A., Miyamoto, T., 2015. Mechanism for the antibacterial action of epigallocatechin gallate (EGCg) on *Bacillus subtilis*. Biosci. Biotechnol. Biochem. 79, 845–854.

Nohynek, L.J., Alakomi, H., Kähkönen, M.P., Heinonen, M., Ilkka, M., Puupponen-pimiä, R.H., Helander, I.M., 2006. Berry phenolics : antimicrobial properties and mechanisms of action against severe human pathogens. Nutr. Cancer 54, 18–32.

Oh, E., Jeon, B., 2015. Synergistic anti-*Campylobacter jejuni* activity of fluoroquinolone and macrolide antibiotics with phenolic compounds. Front. Microbiol. 6, 1–9.

Ohemeng, K.A., Schwender, C.F., Fu, K.P., Barrett, J.F., 1993. DNA gyrase inhibitory and antibacterial activity of some flavones. Bioorg. Med. Chem. Lett. 3, 225–230.

Payne, D.J., Gwynn, M.N., Holmes, D.J., Pompliano, D.L., 2007. Drugs for bad bugs: confronting the challenges of antibacterial discovery. Nat. Rev. Drug Discov. 6, 29–40.

Plaper, A., Golob, M., Hafner, I., Oblak, M., Šolmajer, T., Jerala, R., 2003. Characterization of quercetin binding site on DNA gyrase. Biochem. Biophys. Res. Commun. 306, 530–536.

Prasch, S., Bucar, F., 2015. Plant derived inhibitors of bacterial efflux pumps: an update. Phytochem. Rev. 14, 961–974.

Rai, D., Singh, J.K., Roy, N., Panda, D., 2008. Curcumin inhibits FtsZ assembly: an attractive mechanism for its antibacterial activity. Biochem. J. 410, 147–155.

Rice-Evans, C. a., Miller, N.J., Paganga, G., 1996. Structure-antioxidant activity relationships of flavonoids and phenolic acids. Free Radic. Biol. Med. 20, 933–956.

Shakya, T., Stogios, P.J., Waglechner, N., Evdokimova, E., Ejim, L., Blanchard, J.E., McArthur, A.G., Savchenko, A., Wright, G.D., 2011. A small molecule discrimination map of the antibiotic resistance kinome. Chem. Biol. 18, 1591–1601.

Shapiro, S., Guggenheim, B., 1998. Inhibition of oral bacteria by phenolic compounds. Part 1. QSAR analysis using molecular connectivity. Quant. Struct. Relationships 17, 327–337.

Smith, E.C.J., Kaatz, G.W., Seo, S.M., Wareham, N., Williamson, E.M., Gibbons, S., 2007. The phenolic diterpene totarol inhibits multidrug efflux pump activity in *Staphylococcus aureus*. Antimicrob. Agents Chemother. 51, 4480–3.

Sohlenkamp, C., Geiger, O., 2016. Bacterial membrane lipids: Diversity in structures and pathways. FEMS Microbiol. Rev. 40, 133–159.

Stapleton, P.D., Shah, S., Ehlert, K., Hara, Y., Taylor, P.W., 2007. The β-lactam-resistance modifier (-)-epicatechin gallate alters the architecture of the cell wall of *Staphylococcus aureus*. Microbiology 153, 2093–2103.

Stepanek, J.J., Lukežič, T., Teichert, I., Petković, H., Bandow, J.E., 2016. Dual mechanism of action of the atypical tetracycline chelocardin. Biochim. Biophys. Acta 1864, 645–654.

Tegos, G., Stermitz, F., 2002. Multidrug pump inhibitors uncover remarkable activity of plant antimicrobials. Antimicrob. Agents Chemother. 46, 3133–3141.

Tsou, L.K., Lara-Tejero, M., Rosefigura, J., Zhang, Z.J., Wang, Y.C., Yount, J.S., Lefebre, M., Dossa, P.D., Kato, J., Guan, F., Lam, W., Cheng, Y.C., Galán, J.E., Hang, H.C., 2016. Antibacterial flavonoids from medicinal plants covalently inactivate type III protein secretion substrates. J. Am. Chem. Soc. 138, 2209–2218.

Tsuchiya, H., 2015. Membrane interactions of phytochemicals as their molecular mechanism applicable to the discovery of drug leads from plants. Molecules 20, 18923–18966.

Verstraeten, S. V., Fraga, C.G., Oteiza, P.I., 2015. Interactions of flavan-3-ols and procyanidins with membranes: mechanisms and the physiological relevance. Food Funct. 6, 32–40.

Vincent, I.M., Ehmann, D.E., Mills, S., Perros, M., Barrett, M.P., 2016. Untargeted metabolomics to ascertain antibiotic modes of action. Antimicrob. Agents Chemother. 60, 2281–91.

Wattam, A.R., Abraham, D., Dalay, O., Disz, T.L., Driscoll, T., Gabbard, J.L., Gillespie, J.J., Gough, R., Hix, D., Kenyon, R., MacHi, D., Mao, C., Nordberg, E.K., Olson, R., Overbeek, R., Pusch, G.D., Shukla, M., Schulman, J., Stevens, R.L., Sullivan, D.E., Vonstein, V., Warren, A., Will, R., Wilson, M.J.C., Yoo, H.S., Zhang, C., Zhang, Y., Sobral, B.W., 2014. PATRIC, the bacterial bioinformatics database and analysis resource. Nucleic Acids Res. 42, 581–591.

Wenk, M.R., 2005. The emerging field of lipidomics. Nat Rev Drug Discov 4, 594–610.

WHO, 2014. Antimicrobial resistance. Bull. World Health Organ. 61, 383–94.

Wong, C.C., Cheng, K.W., He, Q.Y., Chen, F., 2008. Unraveling the molecular targets of natural products: insights from genomic and proteomic analyses. Proteomics - Clin. Appl. 2, 338–354.

Wu, T., He, M., Zang, X., Zhou, Y., Qiu, T., Pan, S., Xu, X., 2013a. A structure-activity relationship study of flavonoids as inhibitors of *E. coli* by membrane interaction effect. Biochim. Biophys. Acta 1828, 2751–6.

Wu, T., Zang, X., He, M., Pan, S., Xu, X., 2013b. Structure-activity relationship of flavonoids on their anti- *Escherichia coli* activity and inhibition of DNA gyrase. J. Agric. Food Chem. 61, 8185–8190.

Xu, H., Ziegelin, G., Schröder, W., Frank, J., Ayora, S., Alonso, J.C., Lanka, E., Saenger, W., 2001. Flavones inhibit the hexameric replicative helicase RepA. Nucleic Acids Res. 29, 5058–5066.

Yao, X., Zhu, X., Pan, S., Fang, Y., Jiang, F., Phillips, G.O., Xu, X., 2012. Antimicrobial activity of nobiletin and tangeretin against *Pseudomonas*. Food Chem. 132, 1883–1890.

Zhang, L., Kong, Y., Wu, D., Zhang, H., Wu, J., Chen, J., Ding, J., Hu, L., Jiang, H., Shen, X., 2008. Three flavonoids targeting the β-hydroxyacyl-acyl carrier protein dehydratase from *Helicobacter pylori*: crystal structure characterization with enzymatic inhibition assay. Protein Sci. 17, 1971–1978.

Appendix

Figures

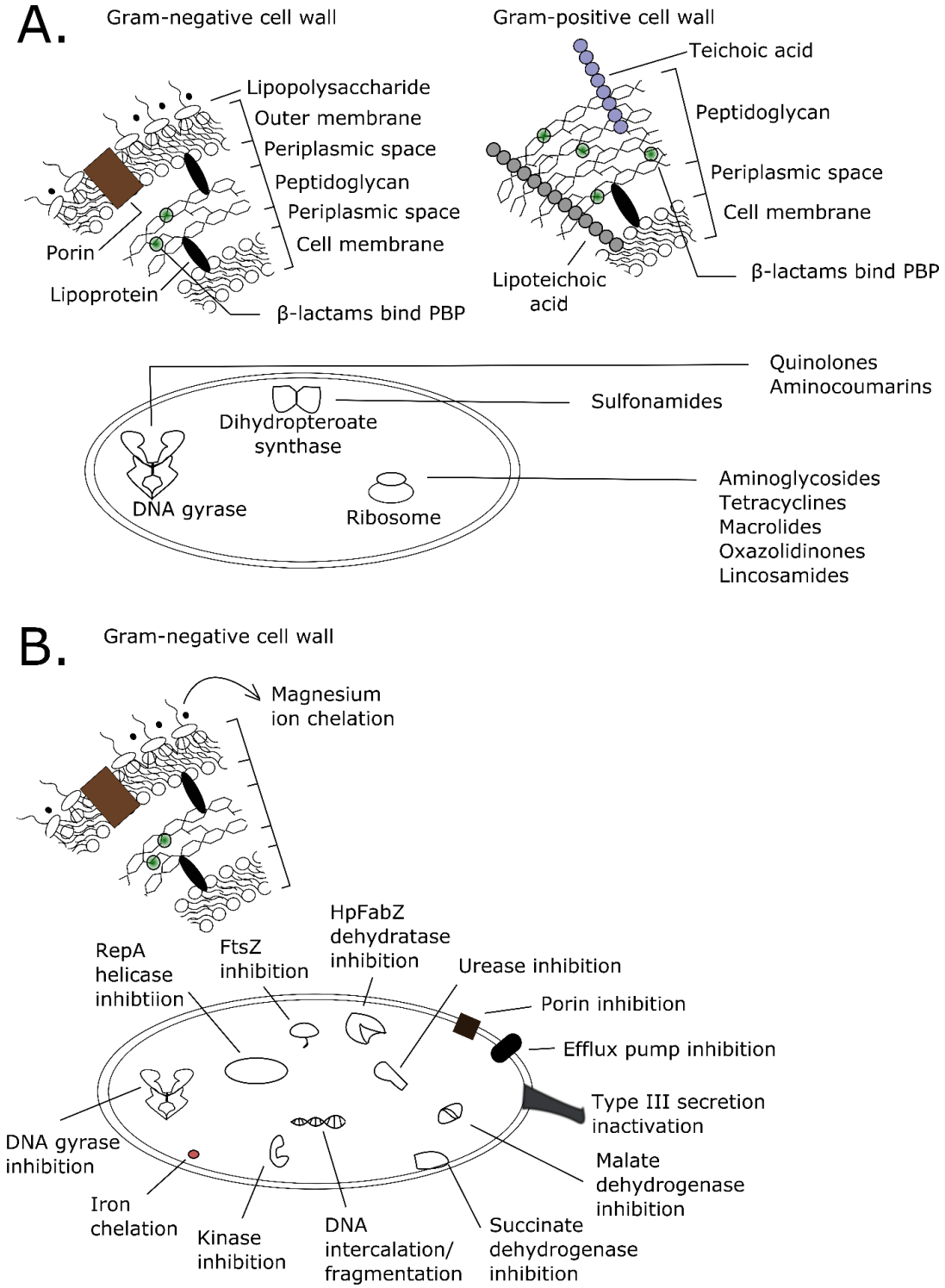

Figure 2. Antibacterial mechanisms of action summarized for A. common antibiotic classes and B. plant phenolic compounds (adapted from Helander et al. 1997, Brown et al. 2015,

Figure 2 legend continued

Kohanski et al. 2010). PBP: penicillin binding protein. Effects of exogenous magnesium were not tested on a Gram-positive organism, only a Gram-negative organism.

Tables

Table 1. Known antibacterial mechanisms of action of phenolic compounds. (attachment)

CHAPTER III
COMPUTATIONAL RANKING OF YERBA MATE SMALL MOLECULES BASED ON THEIR PREDICTED CONTRIBUTION TO ANTIBACTERIAL ACTIVITY AGAINST METHICILLIN-RESISTANT *STAPHYLOCOCCUS AUREUS*

A version of this chapter was originally published by Caroline S. Rempe, Kellie P. Burris, Hannah L. Woo, Benjamin Goodrich, Denise Koessler Gosnell, Timothy J. Tschaplinski, and C. Neal Stewart, Jr.:

CS Rempe, KP Burris, HL Woo, B Goodrich, DK Gosnell, TJ Tschaplinski, CN Stewart. (2015) Computational ranking of yerba mate small molecules based on their predicted contribution to antibacterial activity against methicillin-resistant *Staphylococcus aureus*. PLOS ONE 10(5): e0123925. doi:10.1371/journal.pone.0123925

This project was driven by CS Rempe, who worked with the coauthors to gain funding from an internal IRE research grant through the former NSF IGERT program SCALE-IT. CS Rempe, KP Burris, HL Woo, B Goodrich, DK Gosnell, TJ Tschaplinski, and CN Stewart conceived and designed the experiments, CS Rempe, KP Burris, HL Woo, B Goodrich, and DK Gosnell performed the experiments and analyzed the data. TJ Tschaplinski and CN Stewart contributed reagents, materials, and analysis tools. All authors contributed to the writing and revising of the paper.

Abstract

The aqueous extract of yerba mate, a South American tea beverage made from *Ilex paraguariensis* leaves, has demonstrated bactericidal and inhibitory activity against bacterial pathogens, including methicillin-resistant *Staphylococcus aureus* (MRSA). The gas chromatography-mass spectrometry (GC-MS) analysis of two unique fractions of yerba mate aqueous extract revealed 8 identifiable small molecules in those fractions with antimicrobial activity. For a more comprehensive analysis, a data analysis pipeline was assembled to prioritize

compounds for antimicrobial testing against both MRSA and methicillin-sensitive *S. aureus* using forty-two unique fractions of the tea extract that were generated in duplicate, assayed for activity, and analyzed with GC-MS. As validation of our automated analysis, we checked our predicted active compounds for activity in literature references and used authentic standards to test for antimicrobial activity. 3,4-dihydroxybenzaldehyde showed the most antibacterial activity against MRSA at low concentrations in our bioassays. In addition, quinic acid and quercetin were identified using random forests analysis and 5-hydroxy pipecolic acid was identified using linear discriminant analysis. We also generated a ranked list of unidentified compounds that may contribute to the antimicrobial activity of yerba mate against MRSA. Here we utilized GC-MS data to implement an automated analysis that resulted in a ranked list of compounds that likely contribute to the antimicrobial activity of aqueous yerba mate extract against MRSA.

Introduction

Antibiotic resistance is a significant problem for human and animal health since the development and production of novel antimicrobials has lagged behind the evolution of bacteria for multi-drug resistance. Methicillin-resistant *Staphylococcus aureus* (MRSA) is a pathogenic biotype of global concern because of its resistance to multiple antibiotics (World Health Organization, 2014). Bioactive plant compounds are a potential source for novel antimicrobial formulations; however, the isolation and identification of a novel antimicrobial component among hundreds of compounds can be costly and time-consuming. Therefore, a prioritization of compounds based on bioactivity is a useful first step of an efficient antimicrobial discovery process.

Recent reports have shown that an aqueous extract of yerba mate tea, from the plant *Ilex paraguariensis*, is bactericidal and inhibitory to the growth of bacterial pathogens (Burris et al., 2011; Burris, Davidson, Stewart, Zivanovic, & Harte, 2012), including MRSA (Burris et al.,

2015) and could contain one or more novel antimicrobial compounds. Although many compound classes could contribute to antimicrobial activity, this study focused on compounds, like phenolics, that are readily detected with gas chromatography-mass spectrometry (GC-MS) when derivitized with trimethylsilyl (TMS) groups. Small phenolic molecules are known to be prevalent in yerba mate (Heck & de Mejia, 2007) and have antimicrobial activity against many pathogens, including MRSA (reviewed in Cowan, 1999; Saleem et al., 2010), and so serve as a reasonable initial focus in the search for yerba mate antimicrobial constituents. Phenolics previously observed in extracts of yerba mate tea include caffeic acid, caffeoylquinates, caffeoylshikimates, dicaffeoylquinates, feruloylquinates, kaempferol, quercetin, and rutin, which have been observed to have beneficial properties ranging from antioxidant to antitumor activities (reviewed in Heck and de Mejia, 2007). Recently, MRSA-antimicrobial activity of yerba mate was characterized (Burris et al., 2015; Martin et al., 2013). In addition, Martin et al. 2013 identified chlorogenic acid and caffeic acid in the yerba mate extracts to be active against bacterial food pathogens, however, these compounds were not tested against MRSA.

The purpose of our study was to isolate and identify the compounds contributing to yerba mate's antimicrobial activity against MRSA. This study expanded on previous assessments by both identifying compounds with antimicrobial activity against MRSA using a unique assembly of existing methods and testing authentic standards.

Materials and methods

Yerba mate extractions

Dried leaves of a single commercial brand of yerba mate tea (Taragui; Argentina; 100% leaves; *I. paraguariensis*) were purchased from a local international supermarket. Extracts were obtained using previous methods (Burris et al., 2012) with modifications. Commercial tea leaves were

finely ground to a particle size of less than 300 µm using a commercial food blender (Oster, Boca Raton, Fla., USA). Sterile deionized water was added to ground leaves at a ratio of 3.6 ml to 1 g ground tissue, was allowed to stand for 2 h at 4 °C with occasional mixing to maximize extraction and was subsequently centrifuged at 5000 × g for 30 min. Aqueous extracts were then subjected to dialysis at 4 °C against deionized water for 36 h using a 3500 MWCO SnakeSkin pleated dialysis tubing (ThermoFisher Scientific, Rockford, Ill., USA). Dialyzed extracts were then centrifuged at 5000 × g for 30 min to remove large insoluble particles and frozen at -80 °C. Frozen extracts were lyophilized using Labconco FreeZone 12 L Freeze Dry System (Labconco, Kansas City, Missouri, USA) to concentrate them. Lyophilized extracts were stored at room temperature in a sealed container until testing.

The lyophilized aqueous extract was subsequently extracted with 10%, 20%, 30%, 40%, 50%, 60%, 70%, 80%, and 90% solvent (methanol or acetonitrile). Following solvent extraction, samples were centrifuged at 13,000 × g for 30 min which separated them into two fractions: the pellet (not soluble in solvent concentration) and the supernatant (soluble in solvent concentration). Fractions were subsequently dried using a SpeedVac Concentrator (Savant Industries, Inc., Farmingdale, N.Y., USA). Lyophilized solvent-extracts were weighed, resuspended in sterile water to a concentration of 40 mg/ml and stored at -20 °C until testing. The GC-MS chromatograms of one initial active and one inactive methanol extract were used to select compounds found in the active extract but absent in the inactive extract, and likely to contribute to antibacterial activity (sugars were not selected).

Antimicrobial susceptibility tests

MRSA strains ATCC 33591 and ATCC 33593 were purchased from American Type Culture Collection (ATCC; Manassas, Va., USA). Methicillin-sensitive *Staphylococcus aureus* (SA)

strains ATCC 27708 and SA 113 were obtained from the Center Environmental Biotechnology at the University of Tennessee, Knoxville (courtesy of Steven Ripp). Bacteria were selected on Baird-Parker medium (Becton, Dickinson and Co., Sparks, Md., USA) and stock cultures were prepared by isolating a single colony, growing in tryptic soy broth (TSB; Becton, Dickinson and Co.) and stored at -20 °C in glycerol.

Solvent extracts were tested for antimicrobial activity by the disk diffusion method against MRSA and non-resistant *S. aureus* (SA). Pure cultures of each bacterial strain were sub-cultured at least once in Mueller-Hinton broth (Becton Dickinson & Co.) by inoculating 50 ml broth with 200 µl stock cultures for 24 h incubation at 35-37 °C. Following incubation, ca. 9.0 $\log_{10}$ CFU/ml cultures were diluted to ca. 6.0 $\log_{10}$ CFU/ml and each diluted bacterial suspension was swabbed onto Mueller-Hinton agar plates prior to disk placement. Twenty microliters of the extract or water control were placed on each 6 mm sterile blank disk (Becton Dickinson & Co.), and subsequently plated in duplicate on Mueller-Hinton agar. Plates were incubated for 24 h at 37 °C and the zones of inhibition of bacteria were measured.

Two sets of activity assays were performed with authentic standards. The first used concentrations based on the approximated ratios of compounds observed in our initial two-sample GC-MS data (glycolic acid 1 µg/ml, 3,4-dihydroxybenzaldehyde 0.01 µg/ml, citric acid 31 µg/ml , caffeic acid 46 µg/ml, kaempferol 2 µg/ml, chlorogenic acid 285 µg/ml, 4-*O*-caffeoylquinic acid 210 µg/ml, 5-*O*-caffeoylquinic acid 311 µg/ml, and each of these concentrations at 10x). The second set of activity assays tested compounds alone at 10 µg/ml, 20 µg/ml, and 100 µg/ml. Activity assays for authentic standards alone and in combination were carried out using a micro-broth dilution assay. Sterile 96-well microtiter plates with a well capacity of 300 µl were used. A total volume of 250 µl was used consisting of 125 µl double

strength tryptic soy broth (TSB), 10 µl chemical diluted in 1% dimethyl sulfoxide (DMSO) in water, and 25 µl of inoculum (ca. 6.0 $\log_{10}$ CFU/mL). For the second set of activity assays, samples were randomly assigned within central, intermediate, and edge locations on each plate to minimize edge effects. Only center samples were used in the final analysis. For all tests, microtiter plates were covered with a sterile lid and incubated for 24 h to 48 h at 37 ^{o}C and the absorbance (630 nm) of each well was read at 0 h, 8 h, 24 h, and 48 h (for the second bioassay) with a microtiter plate spectrophotometer (El_x800 Universal Microplate reader, BioTek Instruments, Winooski, Vermont, USA). The micro-broth dilution assays were performed in triplicate. Statistical analysis of the data was performed using analysis of variance with mixed models in SAS 9.4 (SAS Institute Inc., Cary, N.C., USA) using a randomized block design (RBD) blocked on replicate for each single strain separately at 48 h or 24 h. Least squares means were separated using Tukey's significant difference test. Levene tests for equal variance ($P>0.05$) and Shapiro-Wilks tests for normality ($W>0.80$) were performed using R, and boxplots were constructed (R Foundation for Statistical Computing, Vienna, Austria).

GC-MS sample preparation and instrument parameters

The samples rehydrated to 40 mg/ml were filtered using 0.2 µm nylon membrane filters (13 mm Acrodisc; Pall Corporation, Ann Arbor, Mich., USA). Fifty microliters of each sample (or the whole sample if less than 50 µl) and 15 µl of 1 mg/ml liquid sorbitol solution were then dried under a stream of sterile flowing nitrogen. Two samples that contained < 50 µl were multiplied by a correction factor after feature detection and retention time correction to approximate a 50 µl sample. Several samples contained insufficient material for rehydration, filtration, and derivitization. We analyzed a total of 60 samples by GC-MS, 34 of which were unique (some biological duplicates generated different amounts of material). Dried samples were derivitized by

adding 500 µl HPLC grade acetonitrile followed by 500 µl N-methyl-N-trimethylsilyltrifluoroacetamide (MSTFA) with 1% trimethylchlorosilane (TMCS) (Thermo Fisher Scientific) and incubating at 70 °C for 60 min. After 2 d, 1 µl of each sample was injected by an autosampler into a GC-MS instrument (Agilent Technologies Inc., Santa Clara, Calif., USA) with a 5975C inert XL gas chromatograph-mass spectrometer, fitted with an Rtx-5MS with Integra-guard (5% diphenyl/95% dimethyl polysiloxane) capillary column 30 m by 250 µm by 0.25 µm of film thickness). This standard quadrupole GC-MS was operated with electron impact (EI) ionization at 70 eV, six 50 Da to 650 Da scans per second, and helium gas flow rate of 1.33 ml/min with the injection port in splitless mode. Temperatures were held at 250 °C for the injection port, 230 °C for the mass spectrometer source, and 150 °C for the mass spectrometer quad. The oven was programmed to start at 50 °C for 2 min, ramp up to 325 °C at 20 °C per min, hold for 11 min, and then cycle back down to 50 °C. Data files were exported to AIA format in MSD ChemStation (Agilent Technologies, Inc., Santa Clara, Calif, USA) for subsequent analysis.

Data analysis

In an initial assessment of methanolic fractions of yerba mate extract, we selected two comparable samples, one with antimicrobial activity against MRSA and one without antimicrobial activity against MRSA, for GC-MS analysis. The resulting spectra were overlayed and GC peaks that were higher in the active samples and lower in the inactive samples were identified with the aid of MS libraries when possible.

The software program XCMS (C. A. Smith, Want, O'Maille, Abagyan, & Siuzdak, 2006) was used for both feature detection and retention time correction with parameters based on the "GC –EI, Single Quadrupole MS" default values from XCMSOnline (Gowda et al., 2014;

Tautenhahn & Patti, 2012). The effectiveness of the feature detection of different parameter sets was assessed by plotting detected features onto a heatmap of a single sample with all known reference compounds present (Figure S 1). The presence of features at particular reference ions of known compounds was assessed alongside general trends of the heatmap topology in order to select optimal parameters. The same method was used to evaluate the effectiveness of correcting retention time drift by plotting corrected features and uncorrected features on the same single sample heatmap. Final feature detection and retention time correction parameters for XCMS are listed in Table S 1. Correction factors for the 2 samples with concentrations less than 50 µl were multiplied by intensity values to create a modified matrix that was used for all subsequent analyses. There was variation in the sorbitol (internal standard) 319 m/z peak height relative to the intensities of other peaks in some samples, which was likely the result of ion suppression and/or sample matrix interactions. Therefore, spectral peaks were further adjusted based on the 319 m/z peak of sorbitol, so that adjusted ion peak = ion peak * average sorbitol 319 m/z peak across all spectra/sorbitol 319 m/z peak of current spectrum.

Linear discriminant analysis (LDA) was implemented as a pseudo-inverse matrix calculation using the Python linear algebra library numpy.linalg.pinv. The data matrix from XCMS was normalized by subtracting the mean and dividing by the standard deviation for each attribute column. To construct a proper discriminant function, a 'bias' feature was added in the form of a column of ones. With this, the Python Numpy pseudo-inverse function was used to train and test the data with leave-one-out cross-validation sets. Finally, the whole dataset was used in training to generate an optimized weight for each attribute. The weight coefficient for each attribute in the discriminant function can be seen as an estimate of that attribute's

importance in computing the antimicrobial activity. Hence, attributes were ranked from largest to smallest weight and assessed for the numbers of known antimicrobial compounds with high rank. MetaboAnalyst was used to generate additional ranked peaklists using different methods. Using MetaboAnalyst software (Xia, Mandal, Sinelnikov, Broadhurst, & Wishart, 2012), we prioritized peaks in ranked lists from fold-change analysis (using proportions of change between two sample groups), t-test (using comparison of means between two groups), principal component analysis (PCA; using an unsupervised measure across data axis with the most spread), partial least squares linear discriminant analysis (PLS-DA; using a supervised measure across data axes with most variation), recursive support vector machine (R-SVM; using the supervised data-separating hyperplanes of several SVMs to rank the top 50 attributes from the t-test), significance analysis of microarray (SAM; using significance scores and thresholds to determine the significance of single features), empirical Bayesian analysis of microarray (EBAM; using a two group mixture model to separate null and significant features based on a delta value of 0.9), and random forests (using set of weak decision tree learners which form a strong voting system for classification) analyses. MetaboAnalyst parameters for no missing data and autoscaling for normalization were selected.

Lists from PCA were ordered from largest to smallest absolute values of the first principal component loading values to assess an unsupervised approach. PLS-DA, LDA, and random forests lists were ordered from largest to smallest (not absolute value) since they were supervised, and positive values were associated with attributes that discriminated the positive class (active) from the negative class (inactive). Lists from statistical tests were kept in order of statistical significance (smallest to largest p-values (t-test), smallest to largest log2s (fold

change), largest to smallest z-values (EBAM), and largest to smallest d-values (SAM)). Ranking weights and statistical values are reported in Table S 2.

JMP Pro 10 (SAS Institute Inc., Cary, N.C., USA 1989-2007) was used to run logistic regression analyses on the top-ranked spectral peaks of quinic acid, quercetin, and 5-hydroxy-pipecolic acid using peak intensity as a continuous variable to predict a binary outcome of inactive or active against MRSA. Each model was evaluated based on the whole model test Prob<ChiSq p-value and lack of fit Prob<ChiSq p-value being less than 0.05. The parameter estimate of the model was then used to reverse predict the classes of the dataset based on the spectral peak to get a predictive accuracy.

Prioritized peak lists were compared in a pairwise fashion using a rank biased overlap function implemented with the Python function rbo.py (Agrawal, 2013; Webber, Moffat, & Zobel, 2010). This function scored the similarity between the single top-ranked element of each list, then scored the similarity between the top two-ranked elements of each list, and so on, in overlapping sections to generate an overall score. These scores gave greater weight to the more highly ranked elements by using a convergent series of weights, specifically the geometric series (Webber et al., 2010).

The Golm Metabolome Database (GMD) was used to predict functional groups for unknown compounds. Each functional group had its own decision tree classifier with a cross-validation accuracy obtained from the GMD (Hummel, Strehmel, Selbig, Walther, & Kopka, 2010) that was used to gauge predictive accuracy. The Python library urllib2 was used to interface with the GMD in an automated fashion.

Retention index was calculated from a best-fit line of known compounds based on their retention indices in GMD GC-EI-TMS spectra, and their retention times in our data. This

calculation was devised from the knowledge that any set of compounds with known retention indices can be used to index other compounds from the same spectra (Ettre, 2003). Predicted functional groups were summarized for each dataset compilation by counting occurrences of each unique predicted group for all unique retention times and for the top ten unique retention times.

Results

Yerba mate extracts fractionated by varying proportions of acetonitrile (Table S 3) or methanol (Table S 4) in water had variable activity against MRSA and SA. In general, fractions with higher antimicrobial activity were observed in supernatants extracted with 80% or less methanol and 70% or less acetonitrile and in the pellets remaining from the extractions using higher percent methanol (>80%) (Table S 4) or acetonitrile (>70%) fractions (Table S 3). The resulting activity data was used to label each fraction as ‘active’ (any measure of bacterial growth inhibition) or ‘inactive’ (no bacterial growth inhibition) (Table S 3, Table S 4).

Our initial GC-MS analysis of one spectrum from an antibacterial extract and one spectrum from a non-antibacterial extract generated a differential list of 8 non-carbohydrate compounds (Figure 3), 4 of which were already known to inhibit MRSA, based on literature sources (Table S 5). For our automated spectral analysis of a more robust dataset, our feature detection parameters with XCMS resulted in 2204 m/z peaks at unique retention times. Visual examination of detected features on a m/z vs. retention time heatmap (Figure S 1) revealed that features generally aligned well with high intensity m/z regions of the heatmap. A check for the existence of major ions from our 8 known compounds showed that at least one major ion peak from caffeic acid, citric acid, and the chlorogenic acids was present. The extracted ion peaks our group used for 3,4-dihydroxybenzaldehyde and kaempferol were not detected, but other

characteristic peaks of these compounds were observed at their respective retention times. Peaks for glycolic acid were not detected.

In a check for proper retention time correction, features from two different sampling time periods were visually observed to improve based on overlays before and after retention time correction plotted on a sample heatmap (Figure S 1). Although there was significant improvement, retention time drift correction could still be improved further, as evidenced by non-overlapping dots in the corrected plot.

In general, spectra from extracts of different solvent fractionation methods contained many of the same GC peaks, so differences in quantitative information were more relevant to this analysis than differences in qualitative information. The ability to rank influential compounds would be improved and perhaps more reliable with fractionation methods that generated extracts with very qualitatively different compositions. Nevertheless, our analysis of this dataset revealed an additional set of three identifiable, and potentially antibacterial, compounds (quinic acid, quercetin, and 5-hydroxy-pipecolic acid) in addition to the unknown compounds that ranked with known antimicrobials. Since the list ranked by random forests contained the most antimicrobial compounds that were known in high ranks, we additionally surveyed compounds at ranks between 10 and 20. We identified one unknown (rank 13) compound predicted to be aromatic in the 10-20 ranks of the random forests list. This unknown compound would be of interest to further characterize as a potential novel antimicrobial (Table 2). In our analysis of activity against just SA, 3-*O*-feruloylquinic acid was identified as an additional compound of interest.

We evaluated the following eight pure compounds that were identified in our initial GC-MS data overlay for antimicrobial activity alone and in selected combinations at concentrations based on GC-MS quantification (in sorbitol equivalents) to assess approximate antimicrobial

ratios of the compounds: citric acid, caffeic acid, 3,4-dihydroxybenzaldehyde, 3-*O*-caffeoylquinic acid (chlorogenic acid), 4-*O*-caffeoylquinic acid, 5-*O*-caffeoylquinic acid, kaempferol, and glycolic acid. We observed a significant reduction ($P<0.05$) in means relative to a positive growth control sample (mean of 0.99 absorbance units, standard error of mean (SE) 0.08) with caffeic acid at 460 µg/ml (0.62 absorbance units, SE 0.08) with SA 27708. We also observed a significant reduction ($P<0.05$) in means relative to a positive growth control sample (0.87 absorbance units, SE 0.05) with MRSA 33593 for 3,4-dihydroxybenzaldehyde at 0.01 µg/ml (0.70 absorbance units, SE 0.05), glycolic acid at 1 µg/ml (0.66 absorbance units, SE 0.05), and caffeic acid at both 46 µg/ml (0.73 absorbance units, SE 0.05) and 460 µg/ml (0.72 absorbance units, SE 0.05). Of our selected combinations of compounds, only the sample containing the combination of most components (caffeic acid, citric acid, 3,4-dihydroxybenzaldehyde, chlorogenic acid, kaempferol, and glycolic acid at 10x concentrations listed in Figure 3) showed antimicrobial activity (0.55 absorbance units, SE 0.05) against MRSA, and only against MRSA 33593 (Figure 4).

Each of the previously-identified compounds were also tested at concentrations of 10 µg/ml, 20 µg/ml, and 100 µg/ml, although only 3,4-dihydroxybenzaldehyde was observed to significantly reduce MRSA growth (from positive control mean of 0.74 absorbance units, SE 0.03, to 0.66 absorbance units, SE 0.03), and only at 100 µg/ml (Figure 5). Assumptions of normality, equal variance, and no block-by-treatment interaction were upheld with the exception of SA 113 (Figure 5A), in which a significant block-by-treatment interaction was observed ($P < 0.05$), which meant that no conclusion could be drawn from Figure 5A.

A total of 12 ranked peak lists were produced using statistical tests and classification analyses from MetaboAnalyst software and LDA. Among the lists generated by supervised

learning (PLS-DA, random forests, LDA), the accuracies were similar, with an accuracy of 0.83 for both LDA and random forests with the MRSA data, and accuracies of 0.86 for SA LDA and 0.80 for SA RF. PLS-DA had an accuracy of 0.77 for both MRSA and SA (confusion matrices in Table S 6). There was no obvious similarity between misclassified samples, although several samples had relatively low intensities.

The relationship between result lists from different classification methods was assessed using a rank biased overlap analysis (Webber et al., 2010) and are summarized in Table 3. The lists generated by t-test, SAM, and EBAM were nearly identical (RBO > 0.99 similarity), so only the t-test list is displayed in Table 4. PCA, fold-change, and SVM lists were most different from each other and other lists (RBO < 0.1). The fold-change list was additionally noted to contain many derivitization artifacts with high rank (7 of the top 10 were derivitization artifacts). Random forests, PLS-DA, and t-test results were more similar to each other with RBO values ranging from 0.2 to 0.6 (RBO similarity scale 0 to 1, 1 = identical). Many of the same compounds appeared in the top 10 elements of each list, summarized in Table 4. These compounds included citric acid, 3-*O*-caffeoylquinic acid, 4-*O*-caffeoylquinic acid, caffeic acid, quinic acid, quercetin, and unknown compounds (retention times and major m/z peaks listed in Table 4).

Contributions of the newly-identified potential antimicrobial compounds quinic acid, quercetin, and 5-hydroxy-pipecolic acid were further assessed with a logistic regression analysis of a single representative m/z peak for each. Using m/z peaks 537, 471, and 244 for quinic acid, quercetin, and 5-hydroxy-pipecolic acid, respectively, we evaluated the area under receiver operating characteristic (ROC) curves for the logistic regression analysis of each compound (Table 5). The area under the ROC curve followed the ranked order of the compounds with

quinic acid at 0.86, quercetin at 0.78, and 5-hydroxy-pipecolic acid at 0.72. All of these values are > 0.50, and so there exists some predictive ability over random chance.

Additional compounds that could not be identified might also contribute to antimicrobial activity. To gain further information about the highly-ranked unknown compounds, functional groups were predicted by GMD decision trees for the fragments detected at each unique retention time in the random forests list (Table 6, Table 7). For the 315 unique retention times found in our dataset, the major predicted functional groups were carboxylic acid derivatives (228), alpha amino acids (106), aromatics (119), and carboxylic acids (292) (Table 5). Of particular interest was the unknown compound in the random forests top-10 list, but the GMD decision trees predicted it to be a carboxylic acid and a carboxylic acid derivative rather than a functional group commonly associated with antibacterial activity. In examining the top-20 list from random forests, we found an unknown compound (rank 13) that was predicted to contain an aromatic group that would be of interest for further characterization as a potentially novel antimicrobial compound (Table 2).

The reliability of these functional group predictions was based on the "VAR5" cross-validation assessment of each training model done by the Golm group (Hummel et al., 2010), with the resulting functional group predictions having an F-measure threshold of at least 0.65 based on a precision-recall plot (Hummel et al., 2010). The predicted functional group cross-validation error was 13.54% for "hydroxy", 9.65% for "aromatic", and 3.31% for "phenol" groups (Hummel et al., 2010).

Discussion

Hyphenated chromatography-mass spectrometry techniques have yielded a number of downstream data analysis pipelines (reviewed in Hoffmann and Stoye, 2012), from which we

implemented functions from XCMS, MetaboAnalyst, and Python's Numpy. We obtained GC-MS data for 60 fractions of aqueous yerba mate extract (including biological duplicates) and monitored the data-processing steps of XCMS. Since each fraction had a known bioactivity against MRSA, we computationally predicted compounds with significant contribution to the grouping, or class, of 'active' fractions and then assessed the classification using MICs found in the literature, as well as our own set of bioassays using authentic standards.

In our first bioassay, we aimed to assess the effect of key compounds alone and in combination using concentrations that approximated the relative content of compounds that were visible using GC-MS. We observed caffeic acid to be inhibitory at 46 µg/ml, which is similar to the 62.5 µg/ml previously observed for caffeic acid against SA, but smaller than the minimum inhibitory concentration (MIC) of 240 µg/ml reported against MRSA (Luís, Silva, Sousa, Duarte, & Domingues, 2014). Citric acid and chlorogenic acid were previously shown to have MICs of 900 µg/ml (Nagoba, Gandhi, Wadher, Potekar, & Kolhe, 2008) and 500 µg/ml or higher (Alves et al., 2013; Luís et al., 2014; Su, Ma, Wen, Wang, & Zhang, 2014) for MRSA, respectively, although we did not observe these compounds to inhibit MRSA. We did observe the inhibition of MRSA by glycolic acid at 1 µg/ml, which is in the activity range of bacterial antibiotics (Tegos & Stermitz, 2002). However, glycolic acid was not found with our peak detection parameters, and so was not included in our peak ranking analysis or second bioassay. Kaempferol and quercetin were previously observed to be active against MRSA at pharmacologically-relevant concentrations of 13 µg/ml (Hazni, Ahmad, Hitotsuyanagi, Takeya, & Choo, 2008) and from 10 µg/ml to 125 µg/ml (Rodríguez Vaquero, Alberto, & Manca de Nadra, 2007; Su et al., 2014), respectively. However, we observed no significant growth inhibition for kaempferol or quercetin

against MRSA at these concentrations (Figure 5). This lack of inhibition might result from the incomplete solubilization in 1% DMSO and, thus, loss of chemicals during filtration.

A major challenge of analyzing GC-MS data is dealing with the large number of attributes relative to the small number of samples. Data with more attributes than samples are easily overfit by nonlinear methods, so linear analysis methods are preferred. Since the purpose of the automated analysis was to rank attributes by their contribution to antimicrobial activity, we required a method capable of classifying and ranking samples. After a pre-processing step of feature detection and correction using XCMS software, we found that LDA was a method that fit both of these requirements, which has already been implemented in studies of mass spectral analysis (Covington et al., 2013; Santos, Nardini, Cunha, Barbosa, & De Almeida Teixeira, 2014). MetaboAnalyst software also hosts a set of easily implemented techniques for the comparative analysis of mass spectral data that resulted in useful comparisons with LDA. This work suggested that LDA did not do well at prioritizing antimicrobial compounds with our data since none of the known antimicrobial compounds were ranked in the top-10 list (Table 4). The limitations of LDA with highly collinear data could have contributed to its poor rankings, as suggested previously (Varmuza, He, & Fang, 2003). Random forests classification implemented with MetaboAnalyst did, however, prioritize antimicrobial compounds well, ranking 4 of the known antimicrobials in the top-10 list. The superiority of random forests over SVM and LDA in a GC-MS classification application was previously observed (Chen et al., 2013). Despite this apparent success of MetaboAnalyst's random forests implementation, it also identified sugars in the top-10 list. This occurred in other lists too, as well as did derivization artifacts, or peaks that were present in the derivitization blank.

The highly-ranked matches to sugar compounds that we observed with multiple methods likely resulted from a coincidental correlation of sugar concentration with the yerba mate fractions observed to have antimicrobial activity. There are background sugar peaks at many unique retention times that could be glycosides attached to the active components we have identified, but the data generated did not give enough information to categorize them as glycosides or background sugar peaks. It is interesting to note that the presence of sugar has been observed to promote the activity of antimicrobial compounds (Allison, Brynildsen, & Collins, 2011).

Of the potential anti-MRSA compounds identified by our analysis that we were unable to experimentally test, 5-hydroxy-pipecolic acid and 3-*O*-feruloylquinic acid have strong potential for antimicrobial activity as hydroxylated phenolic compounds, even though we did not find any literature in which these compounds have been tested against MRSA. Quinic acid is a common plant metabolite in the shikimic acid pathway that has been reported to have antimicrobial activity against SA at 16 µg/ml, but it was not observed to have activity against MRSA at concentrations up to 28 µg/ml (Ozçelik, Kartal, & Orhan, 2011).

In the top-10 unique retention times predicted by random forests, there were an additional two aromatic, phenol, and hydroxyl groups predicted in the MRSA data over the SA data (Table 6). This identification suggests that aromatic and hydroxylated groups may play a role in the MRSA antimicrobial activity of the active fraction, although further analysis would be required to test this hypothesis. Aromatic compounds have antimicrobial activity dependant on hydroxyl groups (reviewed in Saleem et al., 2010)), including derivatives of caffeic acid and caffeoylquinics, which have previously been observed to inhibit MRSA (Luís et al., 2014).

Conclusion

The increasing resistance of MRSA to existing antimicrobials demands the development of new antimicrobial options. Here we have assembled a pipeline that took advantage of the large amounts of data generated by GC-MS by implementing existing GC-MS tools for an automated analysis that resulted in a ranked list of compounds likely to contribute to the antimicrobial activity of aqueous yerba mate extract against MRSA. We tested the results of this analysis by assaying the antimicrobial activity of pure compounds at a pharmacologically-relevant concentration. 3,4-dihydroxybenzaldehyde was the only compound we assayed with activity at a concentration of 100 µg/ml or less. We also determined that 5-hydroxy-pipecolic acid, quercetin, quinic acid, and one unidentified compound could be possible contributors to yerba mate antimicrobial activity against MRSA using LDA and a random forests analysis. The unique combination of existing methods and tools used in this study generated prioritized lists of compounds likely to contribute to the antimicrobial activity of yerba mate extract, of which citric acid, caffeic acid, chlorogenic acid, kaempferol, quercetin were observed to inhibit MRSA in previous studies (Fattouch & Caboni, 2007; Hazni et al., 2008; Hirai et al., 2010; Luís et al., 2014; Nagoba et al., 2008; Su et al., 2014). 5-hydroxy pipecolic acid, 3-*O*-feruloylquinic acid, and the unknown compound ranked 13 from the random forests list would be useful for further characterization in order to understand which natural compounds in yerba mate might serve as useful antimicrobials against both MRSA and SA.

Acknowledgements

We would like to thank Nancy Engle (NLE) at ORNL for her assistance with and advice for running GC-MS. We thank Steven Ripp for sharing bacteria strains. This research was supported by SCALE-IT IGERT NSF IRE, the Ivan Racheff Chair of Excellence endowment,

and the Tennessee Agricultural Experiment Station. TJT and NLE were supported by the Genomic Science Program (project ‘Plant-Microbe Interactions’), U.S. Department of Energy, Office of Science, Biological and Environmental Research under the contract DE-AC05-00OR22725.

References

Agrawal, R., 2013. rbo.py.

Allison, K., Brynildsen, M., Collins, J., 2011. Metabolite-enabled eradication of bacterial persisters by aminoglycosides. Nature 473, 216–220.

Alves, M.J., Ferreira, I.C.F.R., Froufe, H.J.C., Abreu, R.M. V, Martins, a, Pintado, M., 2013. Antimicrobial activity of phenolic compounds identified in wild mushrooms, SAR analysis and docking studies. J. Appl. Microbiol. 115, 346–57.

Burris, K.P., Davidson, P.M., Stewart, C.N., Harte, F.M., 2011. Antimicrobial activity of yerba mate (*Ilex paraguariensis*) aqueous extracts against *Escherichia coli* O157:H7 and *Staphylococcus aureus*. J. Food Sci. 76, M456–62.

Burris, K.P., Davidson, P.M., Stewart, C.N., Zivanovic, S., Harte, F.M., 2012. Aqueous extracts of yerba mate (*Ilex paraguariensis*) as a natural antimicrobial against *Escherichia coli* O157:H7 in a microbiological medium and pH 6.0 apple juice. J. Food Prot. 75, 753–7.

Burris, K.P., Higginbotham, K.L., Stewart, C.N., 2015. Aqueous extracts of yerba mate as bactericidal agents against methicillin-resistant *Staphylococcus aureus* in a microbiological medium and ground beef mixtures. Food Control 50, 748–753.

Chen, T., Cao, Y., Zhang, Y., Liu, J., Bao, Y., Wang, C., Jia, W., Zhao, A., 2013. Random forest in clinical metabolomics for phenotypic discrimination and biomarker selection. Evidence-based Complement. Altern. Med. 2013, 1–11.

Covington, J.A., Westenbrink, E.W., Ouaret, N., Harbord, R., Bailey, C., O'Connell, N., Cullis, J., Williams, N., Nwokolo, C.U., Bardhan, K.D., Arasaradnam, R.P., 2013. Application of a novel tool for diagnosing bile acid diarrhoea. Sensors 13, 11899–912.

Cowan, M.M., 1999. Plant products as antimicrobial agents. Clin. Microbiol. Rev. 12, 564–82.

Ettre, L.S., 2003. Retention Index Expressions. Chromatographia 58, 491–494.

Fattouch, S., Caboni, P., 2007. Antimicrobial activity of Tunisian quince (*Cydonia oblonga Miller*) pulp and peel polyphenolic extracts. J. Agric. Food Chem. 55, 963–969.

Gowda, H., Ivanisevic, J., Johnson, C.H., Kurczy, M.E., Benton, H.P., Rinehart, D., Nguyen, T., Ray, J., Kuehl, J., Arevalo, B., Westenskow, P.D., Wang, J., Arkin, A.P., Deutschbauer, A.M., Patti, G.J., Siuzdak, G., 2014. Interactive XCMS Online: simplifying advanced metabolomic data processing and subsequent statistical analyses. Anal. Chem. 86, 6931–9.

Hazni, H., Ahmad, N., Hitotsuyanagi, Y., Takeya, K., Choo, C.Y., 2008. Phytochemical constituents from *Cassia alata* with inhibition against methicillin-resistant *Staphylococcus aureus* (MRSA). Planta Med. 74, 1802–1805.

Heck, C.I., de Mejia, E.G., 2007. Yerba Mate Tea (*Ilex paraguariensis*): a comprehensive review on chemistry, health implications, and technological considerations. J. Food Sci. 72, R138–51.

Hirai, I., Okuno, M., Katsuma, R., Arita, N., Tachibana, M., Yamamoto, Y., 2010. Characterisation of anti-*Staphylococcus aureus* activity of quercetin. Int. J. Food Sci. Technol. 45, 1250–1254.

Hoffmann, N., Stoye, J., 2012. Generic software frameworks for GC-MS based metabolomics. In: Roessner, D.U. (Ed.), Metabolomics. InTech, Rijeka, pp. 73–98.

Hummel, J., Strehmel, N., Selbig, J., Walther, D., Kopka, J., 2010. Decision tree supported substructure prediction of metabolites from GC-MS profiles. Metabolomics 6, 322–333.

Luís, Â., Silva, F., Sousa, S., Duarte, A.P., Domingues, F., 2014. Antistaphylococcal and biofilm inhibitory activities of gallic, caffeic, and chlorogenic acids. Biofouling 30, 69–79.

Martin, J.G.P., Porto, E., Alencar, S.M. De, Glória, E.M., Corrêa, C.B., Cabral, I.S.R., 2013. Antimicrobial activity of yerba mate (*Ilex Paraguariensis* St. Hil.) against food pathogens. Rev. Argent. Microbiol. 45, 93–98.

Nagoba, B.S., Gandhi, R.C., Wadher, B.J., Potekar, R.M., Kolhe, S.M., 2008. Microbiological, histopathological and clinical changes in chronic infected wounds after citric acid treatment. J. Med. Microbiol. 57, 681–2.

Ozçelik, B., Kartal, M., Orhan, I., 2011. Cytotoxicity, antiviral and antimicrobial activities of alkaloids, flavonoids, and phenolic acids. Pharm. Biol. 49, 396–402.

Rodríguez Vaquero, M.J., Alberto, M.R., Manca de Nadra, M.C., 2007. Antibacterial effect of phenolic compounds from different wines. Food Control 18, 93–101.

Saleem, M., Nazir, M., Ali, M.S., Hussain, H., Lee, Y.S., Riaz, N., Jabbar, A., 2010. Antimicrobial natural products: an update on future antibiotic drug candidates. Nat. Prod. Rep. 27, 238–54.

Santos, V.S., Nardini, V., Cunha, L.C., Barbosa, F., De Almeida Teixeira, G.H., 2014. Identification of species of the *Euterpe* genus by rare earth elements using inductively coupled plasma mass spectrometry and linear discriminant analysis. Food Chem. 153, 334–9.

Smith, C.A., Want, E.J., O'Maille, G., Abagyan, R., Siuzdak, G., 2006. XCMS: processing mass spectrometry data for metabolite profiling using nonlinear peak alignment, matching, and identification. Anal. Chem. 78, 779–87.

Su, Y., Ma, L., Wen, Y., Wang, H., Zhang, S., 2014. Studies of the *in vitro* antibacterial activities of several polyphenols against clinical isolates of methicillin-resistant *Staphylococcus aureus*. Molecules 19, 12630–9.

Tautenhahn, R., Patti, G., 2012. XCMS Online: a web-based platform to process untargeted metabolomic data. Anal. Chem. 84, 5035–5039.

Tegos, G., Stermitz, F., 2002. Multidrug pump inhibitors uncover remarkable activity of plant antimicrobials. Antimicrob. Agents Chemother. 46, 3133–3141.

Varmuza, K., He, P., Fang, K., 2003. Boosting applied to classification of mass spectral data. J. Data Sci. 1, 391–404.

Webber, W., Moffat, A., Zobel, J., 2010. A similarity measure for indefinite rankings. ACM Trans. Inf. Syst. 28, 1–38.

World Health Organization, 2014. Antimicrobial resistance: global report on surveillance. Geneva.

Xia, J., Mandal, R., Sinelnikov, I. V, Broadhurst, D., Wishart, D.S., 2012. MetaboAnalyst 2.0--a

comprehensive server for metabolomic data analysis. Nucleic Acids Res. 40, W127–33.

Appendix

Figures

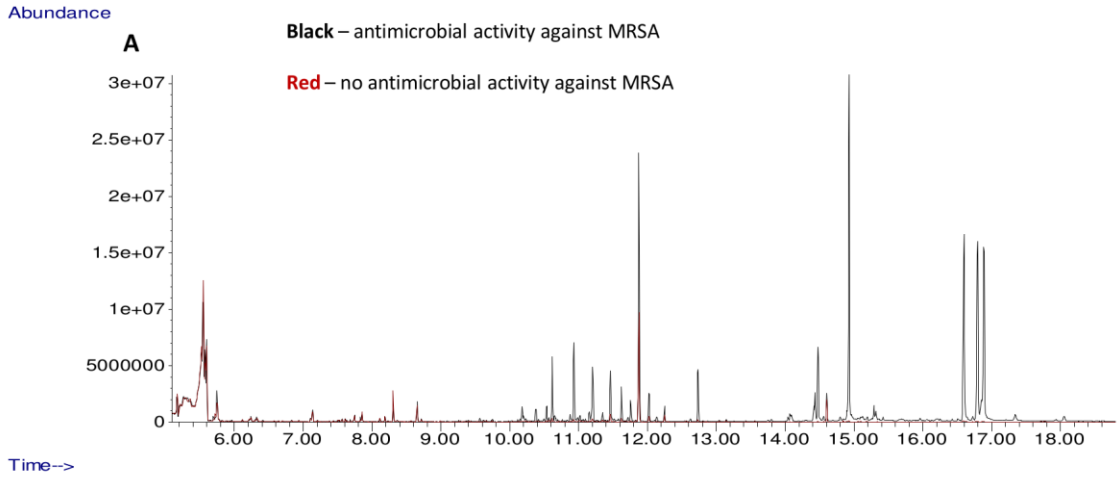

Retention Time	6.41	10.11	11.20	12.74	16.42	16.60	16.79	16.89
Compound	glycolic acid	3,4-dihydroxy-benzaldehyde	citric acid	caffeic acid	kaempferol	chlorogenic acid	4-*O*-caffeoyl-quinic acid	5-*O*-caffeoyl-quinic acid
Quantification (µg/ml sorbitol equivalents)	1	0.01	31	46	2	285	210	311

Figure 3. Overlay of initial yerba mate extract fraction chromatograms. A) The black chromatogram corresponds to a yerba mate extract fraction that demonstrated antibacterial activity against methicillin-resistant *Staphylococcus aureus* (MRSA); the red chromatogram corresponds to a yerba mate fraction that had no antibacterial activity against MRSA. B) Retention times of identified compounds and quantification in sorbitol equivalents were reported.

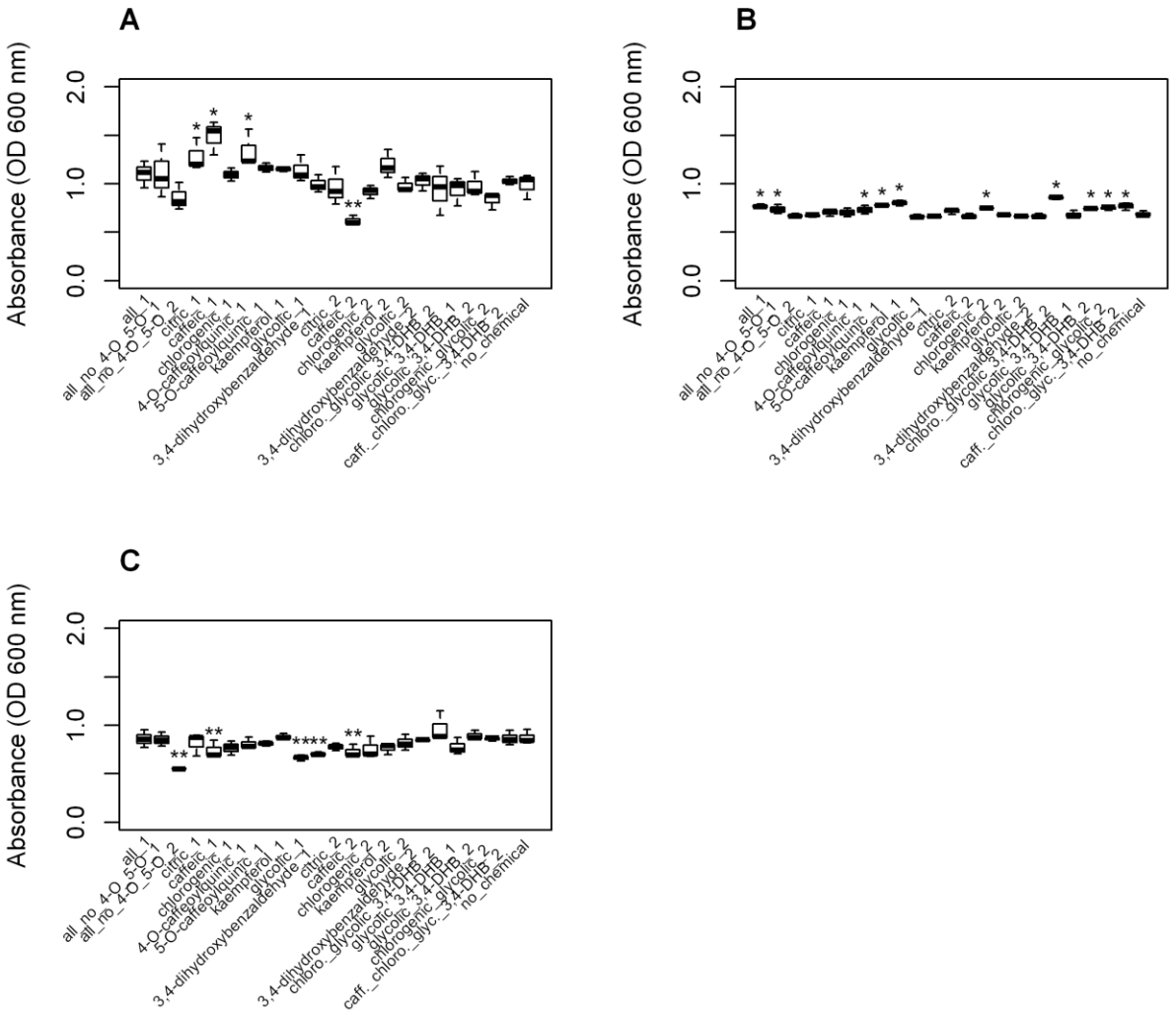

Figure 4. Growth of methicillin-sensitive (SA) and methicillin-resistant *Staphylococcus aureus* (MRSA) in the presence of single or multiple pure compounds at proportions approximated from GC-MS quantification. Growth with compounds alone or together was compared to the positive growth control (no chemical added) to determine inhibitory activity. Statistically significant differences greater (*) or less (**) than control are marked by asterisks. Concentrations follow the GC-MS quantification values in Figure 3, but in µg/ml. Growth of A. SA 27708, B. MRSA 33591, and C. MRSA 33593 are reported at 24 h.

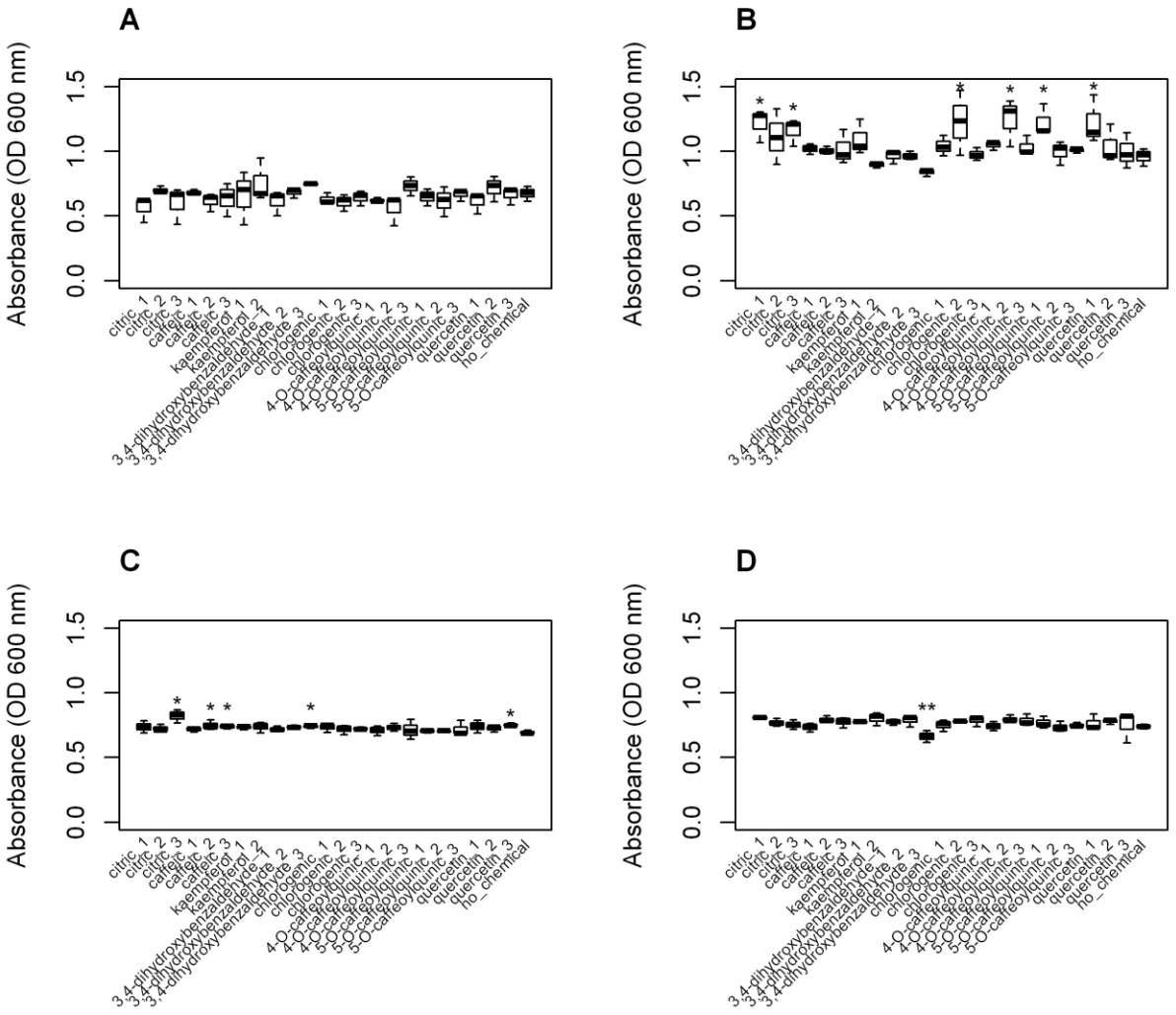

Figure 5. Growth of methicillin-sensitive (SA) and methicillin-resistant *Staphylococcus aureus* MRSA) in the presence of pure compounds. At concentrations of 10 µg/ml (chemical_1), 20 µg/ml (chemical_2) and 100 µg/ml (chemical_3), growth with compounds was compared to the positive growth control (no chemical added) to determine inhibitory activity. Statistically significant differences greater (*) or less (**) than control are marked by asterisks. Growth of A. SA 113, B. SA 27708, C. MRSA 33591, and D. MRSA 33593 are reported at 48 h. SA113 had a significant block by treatment interaction, so no conclusions can be drawn from it.

Tables

Table 2. Top 20 unique retention times ranked by antimicrobial significance against MRSA using random forests.

Rank	Retention Time (min.)	Known Active Concentration (µg/ml)	Major Ion Peaks	Name
1	11.44	---	147, 255, 345	Quinic acid
2	11.18	900	147, 273	Citric acid
3	12.71	250	219, 396	Caffeic acid
4	14.92	---	147, 217, 361	Sucrose
5	16.41	10	396, 559	Kaempferol
6	16.82	125	307	Quercetin
7	10.8	---	394	Unknown
8	16.58	500	147, 255, 307, 345	3-*O*-caffeoylquinic acid
9	18.03	---	103, 129, 204, 217, 361 , 427	Raffinose
10	5.61	---	144, 158	DA
11	10.58	---	55, 57, 69, 75, 81, 83, 97, 99, 123, 204, 217	Unknown
12	16.78	---	193, 255, 257, 324, 372, 489	4-*O*-caffeoylquinic acid
13	12.58	---	143	Unknown, predicted aromatic
14	6.23	---	295	DA
15	5.11	---	59, 86, 100, 133, 160, 174, 175, 221, 223	DA
16	14.47	---	_	Unknown
17	15.28	---	103, 129, 204, 217, 305, 361	Unknown
18	16.85	---	133, 191, 239, 283, 357, 419, 447	5-*O*-caffeoylquinic acid
19	10.07	---	262	Unknown
20	11.85	---	275	DA

Known active concentrations were obtained from either literature or our bioassays.
DA derivitization artifact
--- no known inhibitory concentration found
_ no peaks above cut-off

Table 3. Rank biased overlap comparison of lists.

Average RBO MRSA									
	PCA	Fold Change	PLS-DA	SAM	SVM	T-test	LDA	EBAM	RF
PCA	1	3.08E-11	0.000366	0.000192	0.002276	0.001582	0.000109	0.001605	0.008998
Fold Change	3.08E-11	1	0.011483	0	0	7.34E-06	0.075296	1.23E-09	0.000891
PLS-DA	0.000366	0.011483	1	0.618936	0.05196	0.612391	0.012616	0.612037	0.136071
SAM	0.000192	0	0.618936	1	0.002872	0.999874	0.00313	1	0.224733
SVM	0.002276	0	0.05196	0.002872	1	0.004933	0.04423	0.004054	0.024031
T-test	0.001582	7.34E-06	0.612391	0.999874	0.004933	1	0.002991	0.999644	0.220768
LDA	0.000109	0.075296	0.012616	0.00313	0.04423	0.002991	1	0.002995	0.009479
EBAM	0.001605	1.23E-09	0.612037	1	0.004054	0.999644	0.002995	1	0.220807
RF	0.008998	0.000891	0.136071	0.224733	0.024031	0.220768	0.009479	0.220807	1
Average RBO SA									
	PCA	Fold Change	PLS-DA	SAM	SVM	T-test	LDA	EBAM	RF
PCA	1	1.59E-12	2.95E-05	1.13E-05	6.17E-09	0.000676	0.000333	0.00068	0.010393
Fold Change	1.59E-12	1	0.044871	0	0	3.28E-05	0.098322	1.86E-11	0.001522
PLS-DA	2.95E-05	0.044871	1	0.395548	0.28188	0.388904	0.081874	0.388895	0.149397
SAM	1.13E-05	0	0.395548	1	0.527674	1	0.015228	1	0.186309
SVM	6.17E-09	0	0.28188	0.527674	1	0.542135	0.051292	0.542135	0.122868
T-test	0.000676	3.28E-05	0.388904	1	0.542135	1	0.0154	0.999991	0.182801
LDA	0.000333	0.098322	0.081874	0.015228	0.051292	0.0154	1	0.015403	0.021609
EBAM	0.00068	1.86E-11	0.388895	1	0.542135	0.999991	0.015403	1	0.182803
RF	0.010393	0.001522	0.149397	0.186309	0.122868	0.182801	0.021609	0.182803	1

Table 3 notes continued
Values range from 0, dissimilar, to 1, identical. For comparison between MRSA and SA lists, rank biased overlap between MRSA RF and SA RF = 0.19; MRSA LDA and SA LDA = 0.057; PCA = 1; PLS-DA = 0.399; T-test = 0.518, EBAM = 0.518; SVM = 0; Fold Change = 0.63.

Table 4. Top ten results for each attribute ranking method. (attachment)

Table 5. Classification accuracy of a single major mz peak for each of the 3 identified compounds of interest.

Area under receiver operating characteristics curve		
	MRSA	SA
quinic acid mz 537	0.83	0.86
quercetin mz 471	0.78	0.78
5-hydroxy-pipecolic acid mz 244	0.72	0.68

Quinic acid, quercetin, and 5-hydroxy-pipecolic acid classification accuracies are reported as the area under the curve (AUC) of a receiver operating curve (ROC) for the logistic regression of each single m/z peak MRSA or SA. Accuracy ranges from 0 (no samples accurately classified) to 1 (all samples accurately classified).

Table 6. Predicted functional groups from Golm

Unique Retention Time Counts from	MRSA Top 10	SA Top 10	All Retention Times
Carboxylic Acid Deriv	4	6	228
Alkene	0	0	3
Prim Aliph Amine	0	0	3
Alcohol	4	5	18
Alpha Aminoacid	0	0	106
Carbonyl	0	0	1
Prim Amine	0	0	4
Aromatic	5	3	119
Prim Alcohol	1	2	9
Phenol	2	0	3
1 2 Diol	3	2	9
Sec Alcohol	2	3	9
Phosphoric Acid Deriv	0	0	1
Carboxylic Acid	7	7	292
Hydroxy	2	0	10
Acetal	1	0	3
Amine	0	0	3

Summary of predicted functional groups from only the top 10 unique retention times and from all 315 unique retention times of the random forests ranked list.

Supporting Information

Supporting figures

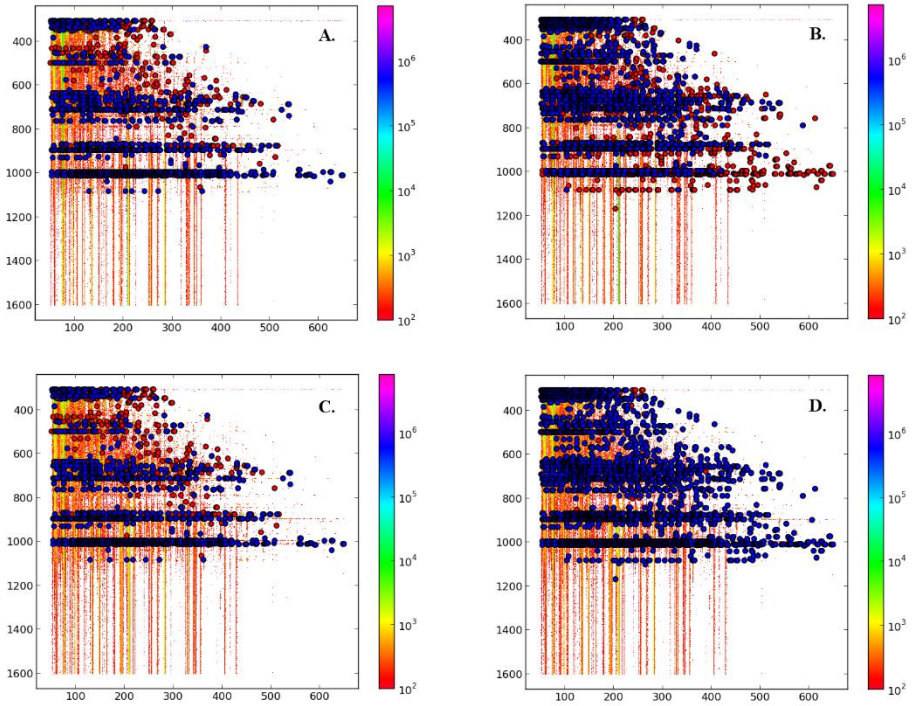

Figure S 1. Heatmaps showing feature detection and retention time correction of GC-MS data. A and B correspond to methicillin-resistant *Staphylococcus aureus* (MRSA) and C and D correspond to methicillin-sensitive *S. aureus* (SA). Blue and red dots are from samples obtained at different times that are in need of retention time correction. The A and C heatmaps display data points before retention time correction and the B and D heatmaps display data points after retention time correction. The complete overlap of blue over red would show perfect retention time correction.

Supporting tables

Table S 1. Final parameters implemented with XCMS for feature detection and retention time correction of mass spectral data.

Feature Detection		
XCMS Parameters	**Value**	**Function**
method	matchedFilter	Feature detection method using a matched filter algorithm that compares two classes of spectra to identify features
snthresh	10	Signal to noise threshold
max	100	Max peaks selected per mass chromatogram
step	1.0	Step size between masses (increased to match the unit mz resolution of our instrument)
bin	2	Steps per bin
mzdiff	1	Minimum difference in mz for peaks with overlapping retention times
Retention Time Correction		
XCMS Parameters	**Value**	**Function**
method	peakgroups	"well behaved" peak groups are used to calculate retention time deviation, which is used for alignment
missing	2	Allowed missing peakgroups
extra	2	Allowed extra peakgroups
smoothing	loess	Loess smoothing method implemented
family	Gaussian	Check for Gaussian fit and symmetry; outlier check
span	0.20	degree of smoothing for regression fitting
group() Function to group peaks with below parameters		
mzwid	1	Width of overlapping mz slices
minfrac	1	Minimum fraction of samples for peak group to be in, in at least one sample group
minsamp	1	Minimum number of samples for peak group to be in
bw	5 before rtcorr, 3 after rtcorr	Bandwidth of Gaussian smoothing kernel

Table S 2. Ranking values of top 10 attributes for each ranking method. (attachment)

Table S 3. Antimicrobial activity assays of aqueous yerba mate acetonitrile fractions**.**

Sample number	Sample type (Supernatant)	Activity			
		SA 27708		MRSA 33591	
		A	B	A	B
1	Water super	Active	Active	Active	Active
2	100% MeOH super	Active	None	Active	Active
3	90% MeOH super	Active	None	None	Active
4	80% MeOH super	Active	None	Active	Active
5	70% MeOH super	Active	Active	Active	Active
6	60% MeOH super	Active	Active	Active	Active
7	50% MeOH super	Active	Active	Active	Active
8	40% MeOH super	Active	Active	Active	Active
9	30% MeOH super	Active	Active	Active	Active
10	20% MeOH super	Active	None	Active	Active
11*	Water pellet	None	None	None	None
12	100% MeOH pellet	Active	Active	Active	Active
13	90% MeOH pellet	Active	None	Active	Active
14	80% MeOH pellet	Active	None	None	Active
15	70% MeOH pellet	None	None	None	None
16	60% MeOH pellet	None	None	None	None
17	50% MeOH pellet	Active	Active	None	None
18	40% MeOH pellet	None	None	None	None
19	30% MeOH pellet	Active	None	None	None
20	20% MeOH pellet	Active	Active	None	None

Shaded boxes indicate that not enough extract was obtained to perform bioassays.

Table S 4. Antimicrobial activity assays of aqueous yerba mate methanol fractions.

Sample number	Sample type (Supernatant)	Activity			
		SA 27708		MRSA 33591	
		A	B	A	B
1	Water super	Active	Active	Active	Active
2	10% Acetonitrile super	Active	Active	Active	Active
3	20% Acetonitrile super	Active	Active	Active	Active
4	30% Acetonitrile super	Active	Active	Active	Active
5	40% Acetonitrile super	Active	Active	Active	Active
6	50% Acetonitrile super	Active	Active	Active	Active
7	60% Acetonitrile super	Active	Active	Active	Active
8	70% Acetonitrile super	None	Active	Active	Active
9	80% Acetonitrile super	None	None	None	None
10	90% Acetonitrile super	None	None	None	None
11*	100% Acetonitrile super	None			
12	Water pellet				
13*	10% Acetonitrile pellet	None	None		
14	20% Acetonitrile pellet	None	None		
15	30% Acetonitrile pellet	None	None	None	None
16	40% Acetonitrile pellet	None	None	None	None
17	50% Acetonitrile pellet	None	None	None	None
18	60% Acetonitrile pellet	None	None	None	None
19	70% Acetonitrile pellet	None	None	Active	None
20	80% Acetonitrile pellet	Active	Active	Active	Active
21	90% Acetonitrile pellet	Active	Active	Active	Active
22	100% Acetonitrile pellet	Active	Active	None	None

Shaded boxes indicate that not enough extract was obtained to perform bioassays.
A and B are replicates.
Any size zone of inhibition was considered active.

Table S 5. Summary of compounds identified as potential antibacterials from GC-MS data and MIC concentrations against methicillin-sensitive *Staphylococcus aureus* (SA) and methicillin-resistant *S. aureus* (MRSA) from literature.

Compound	SA MIC	MRSA MIC	References
Caffeic acid	62.5 ug/ml	250 ug/ml	LuÍs et al. 2013
Citric acid	not found	900 ug/ml; 0.05-0.2 gm%	Nagoba et al. 1998; Thool et al. 2014
Chlorogenic acid	200 ug/ml; 500 ug/ml	500 ug/ml	Zhu et al. 2004; LuÍs et al. 2013
Kaempferol	not found	10 ug/ml; MIC_{50} = 13 ug/ml	Fattouch et al. 2007; Hazni et al. 2008
Quercetin	10 ug/ml	50uM; 125 ug/ml	Hirai et al. 2010; Su et al. 2014
Quinic acid	16 ug/ml	>28 ug/ml	Özçelik et al. 2011

Table S 6. Accuracies of classification methods shown in confusion matrices.

MRSA						**SA**					
LDA			**RF**			**LDA**			**RF**		
Predicted			**Predicted**			**Predicted**			**Predicted**		
	-1	**1**		**-1**	**1**		**-1**	**1**		**-1**	**1**
-1	11	4	**-1**	9	6	**-1**	8	10	**-1**	11	7
1	6	39	**1**	4	41	**1**	5	37	**1**	5	37
PLS-DA accuracy						**PLS-DA accuracy**					
0.77						0.77					

Table S 7. Predicted functional groups listed for the top 10 compounds with retention time (RT), retention index (RI) and name if known.

Rank	RT	RI	Name	Predicted Functional Groups
A. MRSA				
1	11.43	1983.451	quinic acid	Carboxylic Acid, Alcohol, Carboxylic Acid Deriv., Aromatic
2	11.18	1930.634	citric acid	Sec Alcohol, Carboxylic Acid, Alcohol, Carboxylic Acid Deriv.
3	12.72	2254.577	caffeic acid	Hydroxy, Aromatic, Carboxylic Acid, Phenol, Carboxylic Acid Deriv.
4	14.92	2719.366	sucrose	None
5	16.42	3036.268	kaempferol	Carboxylic Acid, Aromatic
6	16.82	3120.775	quercetin	1 2 Diol, Carboxylic Acid, Aromatic
7	10.8	1849.648	unknown	Carboxylic Acid, Carboxylic Acid Deriv.
8	16.58	3071.479	3-O-caffeoylquinic	Carboxylic Acid, Hydroxy Aromatic, 1 2 Diol, Phenol Alcohol
9	18.03	3377.817	raffinose	1 2 Diol Sec Alcohol, Acetal, Alcohol, Prim Alcohol
10	5.62	754.5775	derivitization artifact	none
B. SA				
1	11.18	1930.634	citric acid	Sec Alcohol, Carboxylic Acid, Alcohol, Carboxylic Acid Deriv.
2	11.43	1983.451	quinic acid	Carboxylic Acid, Alcohol, Carboxylic Acid Deriv., Aromatic
3	10.67	1821.479	unknown	Carboxylic Acid, Carboxylic Acid Deriv.
4	13.78	2479.93	unknown	Carboxylic Acid, Carboxylic Acid Deriv., Aromatic
5	11.85	2071.479	derivitization artifact	Carboxylic Acid, Aromatic

Table S 7 continued

Rank	RT	RI	Name	Predicted Functional Groups
6	10.52	1789.789	unknown	Carboxylic Acid, Alcohol, Carboxylic Acid Deriv
7	10.35	1754.577	unknown	1 2 Diol Sec Alcohol, Alcohol, Prim Alcohol,
8	16.5	3053.873	3-O-caffeoylquinic	Carboxylic Acid, Aromatic,
9	10.32	1747.535	unknown	Carboxylic Acid, Carboxylic Acid Deriv.
10	10.58	1803.873	unknown	Sec Alcohol, Alcohol, 1 2 Diol Prim Alcohol

CHAPTER IV
METABOLITES ACCUMULATED DURING *SALMONELLA ENTERICA* SEROVAR TYPHIMURIUM AND *LACTOBACILLUS CASEI* YERBA MATE TREATMENT AND THE RESCUING EFFECT OF EXOGENOUS IRON SULFATE ON *S.* TYPHIMURIUM

This manuscript reports on a learning experience that will remain unpublished.

CS Rempe led this project based on previous work by KP Burris, designed the experiments, and carried out all experiments aside from the initial *Salmonella* Typhimurium growth experiments, which were done by K Higgenbotham and KP Burris. TJ Tschaplinski assisted with the metabolomics experimental design and analysis. KP Burris and CN Stewart, Jr. assisted with the development and direction of the project.

Abstract

Plant extracts are a potential source of novel antimicrobials that could kill both pathogenic and probiotic bacteria. This study assessed the *in vitro* effect of aqueous yerba mate extract on the growth of *Salmonella enterica* serovar Typhimurium and three *Lactobacillus* strains. *S.* Typhimurium was significantly inhibited at 64 mg/ml aqueous yerba mate extract while a biologically insignificant effect of < 3 log fluctuation in growth was observed in the *Lactobacillus* strains. An untargeted metabolomics approach was used to further investigate *S.* Typhimurium and *L. casei in vitro* growth alone or in the presence of yerba mate extract in order to monitor any decreases in yerba mate phenolic compounds from culture supernatants that could signify bacterial metabolism. A gas chromatography – mass spectrometry analysis of derivitized cell culture extracts was used to monitor the accumulation of metabolites in *L. casei* and in *S.* Typhimurium with starting inoculums that were not susceptible to the antibacterial effects of yerba mate extract. In both *S.* Typhimurium and *L. casei* the major metabolites that accumulated differently between treatments were sugars present in the yerba mate extract and common constituents of citric acid metabolism. The differences in oxalomalate when *S.* Typhimurium was grown with or without yerba mate led to the hypothesis that yerba mate impacts iron homeostasis, which was tested by supplementing cultures of *S.* Typhimurium and an inhibitory

concentration of yerba mate extract with iron sulfate. The partial recovery of *S.* Typhimurium with exogenous iron sulfate suggests that disruption of iron, sulfate, or the stability of iron-sulfate clusters is involved in the antibacterial activity of yerba mate extract against *S.* Typhimurium.

Introduction

Plants produce a complex mixture of biologically active chemicals from which herbal medicines, modern drugs, antimicrobials, and pesticides have been developed. Phenolic compounds are abundant in plants and plant-derived food products. When ingested, phenolic compounds are not readily available to the human system, but they do encounter microbes in the gut that have the opportunity to metabolize phenolic compounds into derivative molecules (reviewed by de Souza et al. 2015) that may or may not exert an effect on other microbes or on the human system. Phenolic plant extracts are known to inhibit a broad range of bacterial enteropathogens (reviewed by Cowan, 1999), yet they stimulated the growth of *Lactobacillus acidophilus* (Hervert-Hernández, Pintado, Rotger, & Goñi, 2009) and had no effect on several indigenous gut bacteria (Lee, Jenner, Low, & Lee, 2006). The ability to target bacterial pathogens and bypass other bacterial strains could reduce or prevent the rise of diarrhea-causing pathobionts like *Clostridium difficile,* which thrive when normal gut-microbe populations are reduced in size and diversity by antibiotics (briefly reviewed by Cervantes, 2016). A better understanding of microbial metabolism of phenolic compounds is needed in order to assess health benefits or risks of consuming certain phenolic sources. Furthermore, a deeper understanding of the mechanisms behind inhibition or stimulation of phenolic compounds could reveal new means of treating bacterial pathogens with resistance to common antibiotics.

Yerba mate is a traditional South American beverage made from aqueous extracts of a plant known by the same name (*Ilex paraguariensis*; family Aquifoleaceae). Yerba mate extracts have antimicrobial activity against a wide range of foodborne bacterial pathogens (Burris et al., 2011, 2012), including the globally relevant enteropathogen, *Salmonella enterica* serovar Typhimurium. *S.* Typhimurium contributes to thousands of infections and about 30 deaths annually in the U.S. *S.* Typhimurium strains, including the definitive phage type (DT) 104 strain 2576 used in this study, are also known to be resistant to several antibiotic drugs (CDC, 2013; S. M. Crim et al., 2014; Scallan et al., 2011). Yerba mate has a high phenolic content and shares compounds with grape pomace and tea extracts that have been previously observed to stimulate *Lactobacillus acidophilus* or leave native gut strains unaffected (Heck & de Mejia, 2007; Hervert-Hernández et al., 2009; Lee et al., 2006). *Lactobacillus* strains have also been noted to metabolize phenolic compounds (Filannino et al., 2015; Rodríguez et al., 2008; Sánchez-Maldonado et al., 2011). The degradation of aromatic compounds and their breakdown metabolites were previously observed for several gut bacteria, including *Lactobacillus casei* and *Salmonella enteridis* (Lee et al., 2006). Though *S.* Typhimurium DT104 has been observed to be strongly inhibited by phenolic compounds (Lee et al., 2006), it is predicted to contain some enzymes capable of acting on aromatic compounds, including a salicylate hydroxylase, flavin reductase, and alcohol dehydrogenase (KEGG database).

While many studies have examined the impact of antimicrobial plant extracts on probiotics, we have not encountered any metabolomic analyses of *S.* Typhimurium or *L. casei* growth in the presence of yerba mate extract prior to this dissertation. The aims of this study were to 1) determine the growth effects of different concentrations of yerba mate extract on the foodborne pathogen *S.* Typhimurium and 3 *Lactobacillus* strains and 2) identify any phenolic

compounds that decreased over time from the supernatants of *S.* Typhimurium or *L. casei* during growth with yerba mate extract. Since no identifiable phenolic compounds were observed to significantly decrease over time, the limitations of this experimental design were used to improve the experimental plan for the final chapter of this dissertation. Despite the lack of identifiable phenolic compounds, oxalomalate was a non-phenolic compound that accumulated when *S.* Typhimurium was grown with yerba mate extract. The accumulation of oxalomalate, which is known to interfere with iron-sulfur clusters of aconitase (Ruffo, Testa, Adinolfi, & Pelizza, 1962), combined with knowledge that phenolics tend to chelate metals, motivated the testing of iron chelation as a mode of action of yerba mate extract.

Materials and methods

Yerba mate aqueous extraction

A commercial brand of yerba mate tea (Taragui; 100% leaves, Argentina), was purchased from a local international supermarket (Knoxville, Tenn, USA) and ground with an Oster blender (Boca Raton, Fl. USA) to a particle size of <1 mm. The ground tea was then extracted in ten times its mass of water at 4 °C for 3.5 h, 0.45 µm vacuum filtered, frozen at -80 °C, and lyophilized using a FreeZone, 12 L freeze dryer (Labconco, Kansas City, Mo. USA). Dried extracts were stored at room temperature in a sealed container until testing.

Phenolic content determination

Phenolic content of the extract was determined using Folin-Ciocalteu's phenol reagent (Montreau, 1972). Extracts were resuspended in water (1 mg/ml) and filtered through Whatman No. 4. The phenolic content was quantified using gallic acid as the standard and expressed in mg gallic acid equivalents (GAE)/g dry tea extract after the absorbance was read at 765 nm.

Bacterial culture maintenance

L. bulgaricus ATCC 11842 was purchased from the American Type Culture Collection (ATCC; Manassas, Va., USA), *L. acidophilus* (LA-5) and *L. casei* 431 were generously donated by Chr. Hansen (Milwaukee, Wi. USA), and *S.* Typhimurium DT104 strain 2576 was obtained from the Department of Food Science and Technology at the University of Tennessee. Stock cultures of *L. bulgaricus* and *S.* Typhimurium strains were stored in glycerol at -20 °C. *L. casei* and *L. acidophilus* were received and stored at -80 °C as frozen pellets. Cultures were maintained by re-inoculation in ultra-high temperature (UHT) nonfat skim milk (<0.05% fat; Diversified Foods, Inc., Metairie, LA, USA) or nutrient broth daily and starting new cultures from frozen stocks weekly. Prior to subculturing and growth experiments UHT milk was centrifuged at 5,000 × g for 30 min at 4 °C, then sterilely decanted into 50 ml tubes for storage at 4 °C.

Bacterial growth experiments

Yerba mate extracts were reconstituted in MilliQ water and syringe filtered through 0.22 µm Express PES Membrane (Millipore, Billerica, Ma., USA) prior to microbial susceptibility testing. All growth experiments were performed in 125 ml flasks containing 12.5 ml UHT milk, 10 ml reconstituted yerba mate extract or water, and 2.5 ml dilute bacteria ca. 5-6 log CFU/ml or UHT milk (*Lactobacillus* strains) or sterile 0.1% peptone (*S.* Typhimurium) for a total volume of 25 ml. We observed that the *Lactobacillus* strains grew much faster in milk than in other media, so all our experiments (including *S.* Typhimurium experiments) were conducted in milk to optimize growth time. Experiments were conducted at 37 °C for *L. casei, L. bulgaricus,* and *S.* Typhimurium and at 40 °C for *L. acidophilus*. Controls were prepared similarly using milk or water in place of bacteria (negative) or extract (positive) respectively.

Initial growth experiments performed with *S.* Typhimurium, *L. acidophilus*, and *L. casei* were all assessed at concentrations of 0, 0.4, 2, 4, 8, 16, 32, and 64 mg/ml yerba mate extract with time points at 0, 10, 24, and 48 h. *L. casei* was additionally monitored at 72 h since growth was slower. *L. bulgaricus* was monitored only at the concentrations deemed most relevant from previous experiments (0, 32, and 64 mg/ml for 0, 10, 24, 48, and 72 h). For metabolomics experiments, starting cultures were diluted to ca. 6-7 log CFU/ml and samples were only taken at 0 h and 48 h in a triplicate experiment with treatments of bacteria + yerba mate extract, only bacteria, and only yerba mate extract. For iron supplementation experiments, samples were taken at 0, 10, 24, and 48 h.

At each time point, a sample from each flask was serially diluted in 0.1% sterile peptone and pour-plated in duplicate using de Man, Rogosa, and Sharpe (MRS) or tryptic soy agar (TSA). *Lactobacillus* plates were grown anaerobically using AnaeroGen (Oxoid, Cambridge, UK) packets in airtight containers at 37 °C for 3 d. *S.* Typhimurium plates were grown aerobically at 37 °C for 24 h. Following incubation, colony forming units were enumerated. The pH was additionally monitored for *Lactobacillus* strains with 1 ml samples taken at each time point and measured in duplicate with an UltraBasic UB-10 pH meter (Denver Instruments, Bohemia, NY., USA).

Metabolomics

A 100 µl sample was taken from each treatment flask at each time point, quenched in 900 µl 80% methanol, vortexed, centrifuged at 20,000 × g for 5 min., and then the supernatant was collected. This was repeated with the pellet in 900 µl DI water to lyse cells, then in another 900 µl 80% methanol for a final extracted volume of 2700 µl in methanol and water that was stored at -20 °C in glass tubes. Plastic microcentrifuge tubes were used for initial extraction, so all

samples should have been equally contaminated with extracted plastic components. 50 µl of each extract and 10 µl of 0.1000 g/100 ml gallic acid (internal standard) were transferred to scintillation vials and dried under sterile flowing nitrogen. Each sample was then trimethylsilyl derivitized with 500 µl acetonitrile and 500 µl MSTFA at 70 °C for 1 hour. After 3 days (*Lactobacillus*) or 2 days (*S.* Typhimurium) an autosampler was used to inject samples into a GC-MS instrument (Agilent Technologies Inc., Santa Clara, Calif., USA) with a 5975C inert XL gas chromatograph-mass spectrometer, fitted with an Rtx-5MS with Integra-guard (5% diphenyl/95% dimethyl polysiloxane) capillary column 30 m by 250 µm by 0.25 µm of film thickness). This standard quadrupole GC-MS instrument was operated as was detailed in Rempe and Burris et al. 2015, with electron impact (EI) ionization at 70 eV, six 50 Da to 650 Da scans per second, and helium gas flow rate of 1.33 ml/min with the injection port in splitless mode. Temperatures were kept at 250 °C for the injection port, 230 °C for the mass spectrometer source, and 150 °C for the mass spectrometer quad. The oven was programmed to start at 50 °C for 2 min, ramp up to 325 °C at 20 °C per min, hold for 11 min, and then cycle back down to 50 °C.

Data analysis

Initial growth experiments were each set up and analyzed as a randomized block design, blocked on replicate with sampling in duplicate. Treatment design was repeated measures with concentration applied to each flask and time applied within each flask. Experiments were replicated three times. Bacterial growth data were analyzed by analysis of variance (ANOVA) using mixed models (SAS 9.3, SAS Institute, Cary, N.C., USA). Least significant differences (LSD) were used to compare treatment mean values when significant differences ($P<0.05$) were found. Error bars in preliminary growth data represent the standard error of the mean across both

concentration and time using LSD. Error bars in iron supplemented growth data represent standard deviations of triplicate experiments.

Metabolomic data was normalized to the gallic acid internal standard, then XCMS software (C. A. Smith et al., 2006) was used for peak selection and retention time correction with parameters based on the GC-MS default settings from XCMS Online (Tautenhahn & Patti, 2012).

To investigate treatment and time differences, the unscaled data matrix was analyzed as a randomized block design, blocked on replicate, with split plots since only two time points (0 h and 48 h) were sampled within each flask. The three flask treatments were bacteria and yerba mate extract, bacteria only, and yerba mate extract only. ANOVA assumptions were tested in R with the Levene test for equal variance ($P>0.05$) and the Shapiro-Wilks test for normality ($W>0.80$). If these assumptions were not met, means were compared with the non-parametric Kruskal-Wallis test, otherwise data were analyzed using linear mixed models (package nlme, R Foundation for Statistical Computing, Vienna, Austria). P-values illustrating differences in treatment means, time point means, and interactions between treatment and time point means were adjusted for multiple comparisons (false discovery rate 0.05, R function p.adjust) and used to sort metabolite ions. The Wiley GC-MS library and an in-house library were used to attempt to identify the compounds containing ions with significant main effects of time and treatment, or significant main effects of either time or treatment and a significant interaction between time and treatment (adjusted $P<0.05$).

Iron assays

Fe^{2+} and Fe^{3+} were obtained from iron sulfate heptahydrate and iron chloride, respectively. New, unused plasticware and autoclaved milliQ water were used for chemical assessments of yerba

mate iron chelation. Reactions were done in 96-well plates with 250 µl total volumes. Dilutions of 0.22 µm filtered yerba mate extract were made from a fresh 160 mg/ml stock solution and $FeSO_4$ solutions were made by diluting a fresh 100 mM stock solution. A 100 mM $FeCl_3$ solution was kept at 4 ^{0}C and used for all Fe^{3+} assays since $FeCl_3$ is stable in solution. Chlorogenic acid and EDTA were diluted to 1 mM from 100 mM stock solutions and then added for a final concentration of 0.1 mM. Yerba mate extract was added at final concentrations of 0.32 mg/ml ("high") and 0.16 mg/ml ("low") in saturation assays and in competition assays before the addition of ferrozine. Milk was added at 12 µl milk per ml final volume in saturation assays and in competition assays (not including volume of ferrozine). Competition assays tested the ability of ferrozine to compete with the tested chemicals for iron binding. The tested chemicals were added to the well first (100 µl), then $FeSO_4$ or $FeCl_3$ (25 µl), and then ferrozine (12.5 µl) or water (12.5 µl; control) was added last. Absorbance was monitored at 562 nm (absorbance peak of ferrozine-Fe^{2+} complex) one hour after the addition of ferrozine. Since the binding of phenolics to iron is visible with UV-vis spectroscopy, saturation assays were done to tentatively observe where the iron-phenolic complex becomes saturated (100 µl dilute test compound + 25 µl dilute iron solution). No ferrozine was used in these assays and only phenolic chemicals were tested since others do not have a visible absorbance shift with iron binding. Absorbance at 380 nm, where a slight increase in absorbance was observed with increasing concentrations of iron (Figure S 2), was recorded after one hour.

Growth assays of *S.* Typhimurium were supplemented with $FeSO_4$ added at concentrations of 0, 3.2, and 9.6 mM $FeSO_4$ based on putative saturation regions observed in the chemical iron binding assessments at 0.1, 1, and 3 mM $FeSO_4$ (Figure S 3). 25 ml total volume flasks were used with tea in final concentrations of 32 mg/ml or 64 mg/ml and iron in final

concentrations of 0, 3.2, and 9.6 mM $FeSO_4$. The tea and iron solutions were solvated with pH 5.5 phosphate buffer and adjusted to pH 5.5 before 0.22 µm syringe filtering and subsequent addition of sterile milk and dilute overnight culture (ca. 5-6 log CFU/ml). Flasks were not acid-washed, so trace amounts of iron likely contributed to experimental error. Data was analyzed to compare buffered and unbuffered samples without iron in random block design blocked on replicate with buffer vs. water treatments using repeated measures with time (0, 10, 24, 48 h) and subsampling. Iron supplemented growth data was analyzed at each time point separately using a random block design blocked on replicate with iron (0, 3.2, 9.6 mM $FeSO_4$) and tea treatments (0, 32, 64 mg/ml extract).

Results

Extract and phenolic content

For every 10 g of ground tea, approximately 2.2 g of freeze dried extract was obtained. This means our initial cold water extract concentration was about 22 mg/ml of the final lyophilized extract. The lyophilized extract was easily resuspended in water. The highest concentration of extract (64 mg/ml) in milk had an average starting pH of 5.5, and the phenolic content was determined to be ca. 81 ± 3.4 mg GAE/g freeze-dried extract.

Bacterial growth with yerba mate extract

Our data demonstrated that a 64 mg/ml aqueous extract of yerba mate was capable of *in vitro* inactivation of *S.* Typhimurium in milk by 48 h (Figure 6A) while minimally affecting the growth of *L. casei*, *L. acidophilus*, and *L. bulgaricus* (Figure 6B, C, and D, respectively). *S.* Typhimurium growth was significantly reduced by ca. > 5 log CFU/ml at 64 mg/ml by 48 h while we observed fluctuations of < 3 log CFU/ml in the growth of *L. casei*, *L. acidophilus*, and *L. bulgaricus* relative to their controls (Figure 6).

Metabolomics

Using adjusted p-values from the ANOVA model, 22 *S*. Typhimurium metabolites (11 tentatively identified) and 46 *L. casei* metabolites (16 tentatively identified) were found to be significantly different across treatment or time. The compounds with significantly different treatment means, time means, and/or interaction between treatment and time are listed in Table 7 (*L. casei*) and Table 8 (*S.* Typhimurium). The identifiable compounds with significantly altered accumulation patterns between treatment and/or time groups tended to be either sugars consumed from the yerba mate extract or compounds involved in common metabolic pathways, including the citric acid cycle. The only putatively identified phenolic compound was sinapyl alcohol in the *L. casei* supernatant, but it accumulated in the bacteria treatments both with and without yerba mate extract.

Iron binding assays

Using ferrozine to monitor Fe^{2+}, the expected linear relationship was observed between 562 nm absorbance (ferrozine-Fe^{2+} complex) and the concentration of added $FeSO_4$ in water. This linear relationship was clearly seen with water, chlorogenic acid, and tea samples, indicating they did not effectively compete with ferrozine to bind Fe^{2+} (Figure 7A). The EDTA control and all the samples containing milk showed a delayed absorbance as EDTA or milk bound to Fe^{2+} and removed it from ferrozine (Figure 7A). At about 0.5 mM $FeSO_4$, though, there was sufficient iron to interact with ferrozine and a linear relationship between absorbance (Fe^{2+} complex formation) and iron concentration was observed from that point (Figure 7A).

There was no signal with added $FeCl_3$ in water, with EDTA, or with milk, as expected since $FeCl_3$ supplies Fe^{3+} which cannot interact with ferrozine (Figure 7C). Chlorogenic acid and all the samples containing tea did show a delayed absorbance though, indicating that they are

capable of converting Fe^{3+} to Fe^{2+} (Figure 7C). Controls without ferrozine showed no observable interference at 562 nm (Figure 7A, Figure 7D).

In saturation assays the native absorbance was monitored at 380 nm, a wavelength where absorbance was observed to vary between yerba mate extracts with high and low iron concentrations (Figure S 2). The tea and milk trends showed very little difference with both $FeCl_3$ and $FeSO_4$. When tea and milk were combined in growth assay proportions, a clear curve was visible with the absorbance signal showing theorized iron saturation at about 1-1.5 mM Fe (Figure S 3).

Bacterial growth with iron supplementation

S. Typhimurium with 32 mg/ml tea extract grew at all concentrations of added iron with no significant difference at 48 h. With 64 mg/ml, *S*. Typhimurium was killed by 48 h in the treatments with 0 mM $FeSO_4$ (differed from all other treatments with $P<0.05$), but survived with a mean of 7.5 log CFU/ml when supplemented with 9.6 mM $FeSO_4$, which was not significantly different from the ca. 8.5 log CFU/ml means of the 0 and 32 mg/ml tea treatments with and without iron at 48 h (Figure 8). The treatment with 64 mg/ml tea and 3.2 mM iron grew with a mean of ca. 4.5 log CFU/ml at 48 h, which was significantly different from all the other treatments at 48 h ($P < 0.05$).

Discussion

A 64 mg/ml concentration of the aqueous extract of yerba mate significantly inhibited the growth of *S.* Typhimurium but did not have a major effect on the growth of *L. casei, L. acidophilus,* or *L. bulgaricus in vitro*. Although 64 mg/ml is higher than the 14.6 mg/ml previously observed to inhibit *S*. Typhimurium in tryptic soy broth (TSB) (Gonzalez-gil et al., 2014), growth in milk rather than TSB has been observed to reduce *S*. Typhimurium susceptibility to antibiotics

(Branen & Davidson, 2004). 64 mg/ml is also greater than the original cold water extract we obtained, which was 22 mg/ml. 22 mg/ml might be comparable to a commonly ingested concentration of yerba mate since a range of 21.7-34.5 mg/ml was obtained from aqueous yerba mate leaf extracts in another study (Sambiassi, Escalada, & Schmalko, 2002), or higher than an ingested concentration since the "soluble solids" obtained from yet another set of hot and cold water extractions ranged from 4.8-7.8 mg/ml (Bastos, Fornari, De Queiroz, Soares, & Torres, 2005).

Yerba mate extract is rich in phenolic compounds (Heck & de Mejia, 2007); this evaluation found ca. 81 ± 3.4 mg GAE/g dry extract, comparable to the 110.5 ± 14.3 mg GAE/g observed previously (Deladino et al., 2013). Since phenolics are known to have antibacterial properties, GC-MS with TMS-derivitized samples was used to profile any changes in phenolic compounds and common bacterial metabolites.

The first goal of this metabolomics analysis was to assess whether any phenolic compounds present in the tea extract were metabolized by the bacteria. Although the changes in *L. casei* growth patterns were not biologically meaningful, they were statistically significant ($P<0.05$) and showed a growth lag between 10 h and 24 h in comparison to controls. This trend could be explained by a particular compound in the extract initially inhibiting growth, but then later being degraded or utilized by *L. casei.* However, we did not observe any identifiable phenolic compounds with a significant change between 0 h and 48 h except for sinapyl alcohol, which appeared to be produced by *L. casei* or be a breakdown product of milk components. Either way, the changes in this compound putatively identified as sinapyl alcohol were independent of yerba mate extract. Most of the compounds observed to decrease over time in the

tea samples were sugars with both *L. casei* and *S*. Typhimurium, which were likely metabolized as carbon sources.

Since there were no identifiable phenolic compounds with significant changes across time and yerba mate treatment, the *S.* Typhimurium pathways altered by yerba mate extract were further investigated in literature searching in order to create hypotheses about yerba mate's antibacterial mechanism(s). The metabolomics analysis revealed a significant difference in oxalomalate between *S.* Typhimurium treatments, so it was investigated further and found to compete with iron-sulfur clusters for binding to eukaryotic aconitase, which is structurally very similar to aconitase A of *Salmonella*, and to bacterial isocitrate lyase (Baothman, Rolfe, & Green, 2013; Walden, Selezneva, & Dupuy, 2006). Oxalomalate is often formed non-enzymatically by the interaction of oxaloacetate and glyoxylate. It is not clear whether the oxalomalate observed was produced non-enzymatically or enzymatically by the bacteria.

Since phenolic components of yerba mate extract are already known to have a strong ability to chelate metal ions, including iron (Guo et al., 2007; Kono & Kashine, 1998), we decided to test the hypothesis that the yerba mate extract chelates iron and so starves *S.* Typhimurium of this necessary element. This hypothesis was also in accord with our observation that 3 *Lactobacillus* strains are generally unaffected by yerba mate extract since *Lactobacilli* use manganese rather than iron and they lower the pH of their environment to levels that generally deter the chelation of any metal ions (Imbert & Blondeau, 1998). However, metabolic signs of iron stress through increased amounts of enterobactin and pyruvic acid (Reissbrodt et al., 1997), were not apparent since neither of these compounds were identifiable in the GC-MS spectra.

In order to probe the relationship of iron to our antibacterial tea system, the iron binding capabilities of yerba mate extract were assayed, followed by EDTA, chlorogenic acid, milk, and

combinations of tea and milk (Figure 7). It is clear that the milk alone and the milk and tea combination are capable of binding Fe^{2+} from the ferrozine competition assay, which we expected since milk contains the iron storage protein lactoferrin. However, the ferrozine assay did not show any binding capabilities of chlorogenic acid or yerba mate extract. Chlorogenic acid has been previously observed to chelate iron in 1:1 and 3:1 ratios, with visible UV-vis absorbance shifts at 324 nm and 355 nm (Kono & Kashine, 1998). Yerba mate was observed to have shifts at 320 nm and 380 nm that could be representative of single phenolics depleting and an iron-phenolic complex forming (Figure S 2). With this observation and claims of yerba mate iron chelation in the literature (Huang et al., 2014; Salkić & Ćavar Zeljković, 2014), it is possible that ferrozine is able to bind more strongly to Fe^{2+} than either chlorogenic acid or any of the yerba mate phenolics. By further monitoring the native absorbance shift of both the tea and chlorogenic acid at 380 nm, saturation curves were observed that could be interpreted as the formation of an iron-phenolic complex (Figure S 3). Using the proportions of iron to tea found where the saturation curve plateaued, we selected two iron concentrations that might provide enough uncomplexed iron for the bacteria to survive low iron stress. These concentrations were close to the start of the plateau since bacteria generally require only 10^{-7} to 10^{-5} M iron for optimal growth (Andrews, Robinson, & Rodríguez-Quiñones, 2003).

The supplementation of $FeSO_4$ at 9.6 mM clearly rescued *S.* Typhimurium from the antibiotic effects of 64 mg/ml yerba mate extract, although growth was still significantly below the level of the treatments with no tea and the 32 mg/ml tea. This supports the hypothesis that the iron chelation of yerba mate extract plays a major role in its antibacterial function. Although many other studies hypothesize iron as a potential factor in the antimicrobial activity of phenolic plant extracts, to our knowledge we are the first to test it with a whole plant extract. A similar

assay with tannic acid found that exogenous iron prompted the recovery of bacterial pathogens (Chung et al., 1998). A possibility remains that milk components acted synergistically with phenolics to withhold iron since direct evidence of yerba mate binding to iron was not observed. Future experiments are needed to assess whether a major portion of yerba mate extract's antibacterial activity against *S.* Typhimurium is simply from chelating iron or if a more complex mechanism is at work.

Conclusion

The effects of yerba mate extract on the growth of three *Lactobacillus* strains and the pathogen *S.* Typhimurium was evaluated, the metabolic effects of yerba mate extract on *L. casei* and *S.* Typhimurium was surveyed, and finally the hypothesis that iron is involved in the antibacterial effect of yerba mate extract against *S.* Typhimurium was tested. It was found that the addition of ferrous iron sulfate rescued *S.* Typhimurium from the antibacterial effect of yerba mate extract. Additional experiments are needed to assess whether it was chelation of iron by yerba mate or a different mechanism that is the main source of the antibacterial effect, but this study has verified that iron has an influence.

Acknowledgements

We are very grateful for the use of Dr. P. Michael Davidson's BSL-2 laboratory, equipment, and storage space. We would also like to thank Dr. Hayriye Bozkurt for assistance with BSL-2 lab equipment, Dr. Arnold Saxton for statistics advice, and Nancy Engle for assistance with GC-MS methods. Additionally, we would like to acknowledge the generous donation of *Lactobacillus* strains by Chr. Hansen.

References

Andrews, S.C., Robinson, A.K., Rodríguez-Quiñones, F., 2003. Bacterial iron homeostasis. FEMS Microbiol. Rev. 27, 215–237.

Baothman, O. a S., Rolfe, M.D., Green, J., 2013. Characterization of *Salmonella enterica* serovar Typhimurium aconitase A. Microbiology 159, 1209–16.

Bastos, D.H.M., Fornari, A.C., De Queiroz, Y.S., Soares, R.A.M., Torres, E.A.F.S., 2005. The chlorogenic acid and caffeine content of yerba mate (*Ilex paraguariensis*) beverages. Acta Farm. Bonaer. 24, 91–95.

Branen, J.K., Davidson, P.M., 2004. Enhancement of nisin, lysozyme, and monolaurin antimicrobial activities by ethylenediaminetetraacetic acid and lactoferrin. Int. J. Food Microbiol. 90, 63–74.

Burris, K.P., Davidson, P.M., Stewart, C.N., Harte, F.M., 2011. Antimicrobial activity of yerba mate (*Ilex paraguariensis*) aqueous extracts against *Escherichia coli* O157:H7 and *Staphylococcus aureus*. J. Food Sci. 76, M456–62.

Burris, K.P., Davidson, P.M., Stewart, C.N., Zivanovic, S., Harte, F.M., 2012. Aqueous extracts of yerba mate (*Ilex paraguariensis*) as a natural antimicrobial against *Escherichia coli* O157:H7 in a microbiological medium and pH 6.0 apple juice. J. Food Prot. 75, 753–7.

CDC, 2013. Antibiotic resistance threats in the United States, 2013. U. S. Dep. Heal. Hum. Serv. Centers Dis. Control Prev. 1–114.

Cervantes, J., 2016. Use your antibiotics wisely. Consequences to the intestinal microbiome. FEMS Microbiol. Lett. Adv. 53, 1689–1699.

Chung, K.T., Lu, Z., Chou, M.W., 1998. Mechanism of inhibition of tannic acid and related compounds on the growth of intestinal bacteria. Food Chem. Toxicol. 36, 1053–1060.

Cowan, M.M., 1999. Plant products as antimicrobial agents. Clin. Microbiol. Rev. 12, 564–82.

Crim, S.M., Iwamoto, M., Huang, J.Y., Griffin, P.M., Gilliss, D., Cronquist, A.B., Cartter, M., Tobin-D'Angelo, M., Blythe, D., Smith, K., Lathrop, S., Zansky, S., Cieslak, P.R., Dunn, J., Holt, K.G., Lance, S., Tauxe, R., Henao, O.L., 2014. Incidence and trends of infection with pathogens transmitted commonly through food - foodborne diseases active surveillance network, 10 U.S. sites, 2006-2013. MMWR. Morb. Mortal. Wkly. Rep. 63, 328–332.

Deladino, L., Teixeira, A.S., Reta, M., García, A.D.M., Navarro, A.S., Martino, M.N., 2013. Major phenolics in yerba mate extracts (*Ilex paraguariensis*) and their contribution to the total antioxidant capacity. Food Nutr. Sci. 4, 154–162.

Filannino, P., Bai, Y., Di Cagno, R., Gobbetti, M., Gänzle, M.G., 2015. Metabolism of phenolic compounds by Lactobacillus spp. during fermentation of cherry juice and broccoli puree. Food Microbiol. 46, 272–9.

Gonzalez-gil, F., Diaz-sanchez, S., Pendleton, S., Andino, A., Zhang, N., Yard, C., Crilly, N., Harte, F., Hanning, I., 2014. Yerba mate enhances probiotic bacteria growth in vitro but as a feed additive does not reduce *Salmonella* Enteritidis colonization *in vivo*. Poult. Sci. 93, 434–440.

Guo, M., Perez, C., Wei, Y., Rapoza, E., Su, G., Bou-Abdallah, F., Chasteen, N.D., 2007. Iron-binding properties of plant phenolics and cranberry's bio-effects. Dalton Trans. 4951–61.

Heck, C.I., de Mejia, E.G., 2007. Yerba mate tea (*Ilex paraguariensis*): a comprehensive review on chemistry, health implications, and technological considerations. J. Food Sci. 72, R138–51.

Hervert-Hernández, D., Pintado, C., Rotger, R., Goñi, I., 2009. Stimulatory role of grape pomace polyphenols on *Lactobacillus acidophilus* growth. Int. J. Food Microbiol. 136, 119–22.

Huang, W.Y., Lee, P.C., Hsu, J.C., Lin, Y.R., Chen, H.J., Lin, Y.S., 2014. Effects of water quality on dissolution of yerba mate extract powders. Sci. World J. 2014, 1–6.

Imbert, M., Blondeau, R., 1998. On the iron requirement of lactobacilli grown in chemically defined medium. Curr. Microbiol. 37, 64–66.

Kono, Y., Kashine, S., 1998. Iron chelation by chlorogenic acid as a natural antioxidant. Biosci. Biotechnol. Biochem. 62, 22–27.

Lee, H.C., Jenner, A.M., Low, C.S., Lee, Y.K., 2006. Effect of tea phenolics and their aromatic fecal bacterial metabolites on intestinal microbiota. Res. Microbiol. 157, 876–84.

Reissbrodt, R., Kingsley, R., Rabsch, W., Beer, W., Roberts, M., Williams, P.H., 1997. Iron-regulated excretion of alpha -keto acids by *Salmonella typhimurium* 179, 4538–4544.

Rodríguez, H., Landete, J.M., Rivas, B. de las, Muñoz, R., 2008. Metabolism of food phenolic acids by Lactobacillus plantarum CECT 748T. Food Chem. 107, 1393–1398.

Ruffo, A., Testa, E., Adinolfi, A., Pelizza, G., 1962. Control of the Citric Acid Cycle by Glyoxylate: 1. A new inhibitor of aconitase formed by the condensation of glyoxylate with oxaloacetate. J. Biochem. 85, 588–93.

Salkić, A., Ćavar Zeljković, S., 2014. Preliminary investigation of bioactivity of green tea (*Camellia sinensis*), rooibos (*Asphalatus linearis*), and yerba mate (*Ilex paraguariensis*). J. Herbs. Spices Med. Plants 21, 259–266.

Sambiassi, C., Escalada, A.M., Schmalko, M.E., 2002. Extraction optimization of soluble compounds of yerba maté. Brazilian Arch. Biol. Technol. 45, 189–193.

Sánchez-Maldonado, A.F., Schieber, A., Gänzle, M.G., 2011. Structure-function relationships of the antibacterial activity of phenolic acids and their metabolism by lactic acid bacteria. J. Appl. Microbiol. 111, 1176–1184.

Scallan, E., Hoekstra, R.M., Angulo, F.J., Tauxe, R. V., Widdowson, M.-A., Roy, S.L., Jones, J.L., Griffin, P.M., 2011. Foodborne illness acquired in the United States—major pathogens. Emerg. Infect. Dis. 17, 7–15.

Smith, C.A., Want, E.J., O'Maille, G., Abagyan, R., Siuzdak, G., 2006. XCMS: processing mass spectrometry data for metabolite profiling using nonlinear peak alignment, matching, and identification. Anal. Chem. 78, 779–87.

Tautenhahn, R., Patti, G., 2012. XCMS Online: a web-based platform to process untargeted metabolomic data. Anal. Chem. 84, 5035–5039.

Walden, W., Selezneva, A., Dupuy, J., 2006. Structure of dual function iron regulatory protein 1

complexed with ferritin IRE-RNA. Science. 314, 1903–1909.

Appendix

Figures

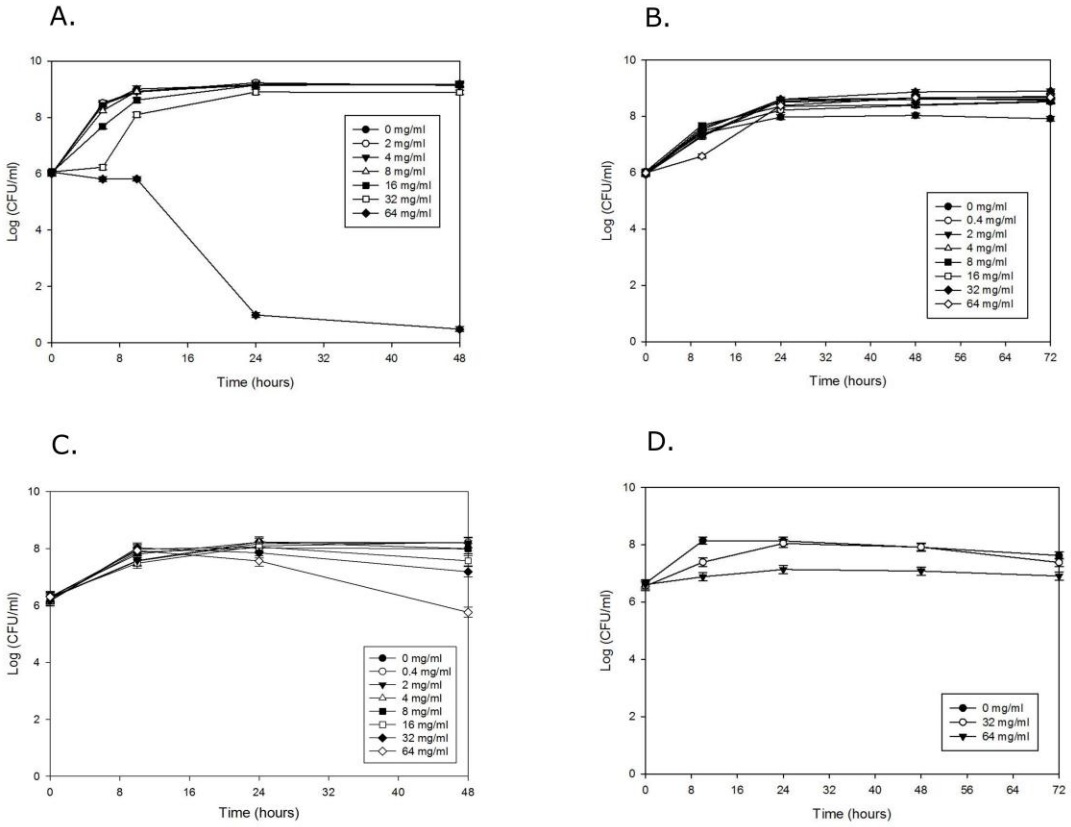

Figure 6. Growth trends (log CFU/ml) of A. *S. Typhimurium*, B. *L. acidophilus*, C. *L. casei*, and D. *L. bulgaricus* in UHT skim milk at different concentrations of yerba mate extract. Error bars represent ± 1 standard deviation (triplicate experiment).

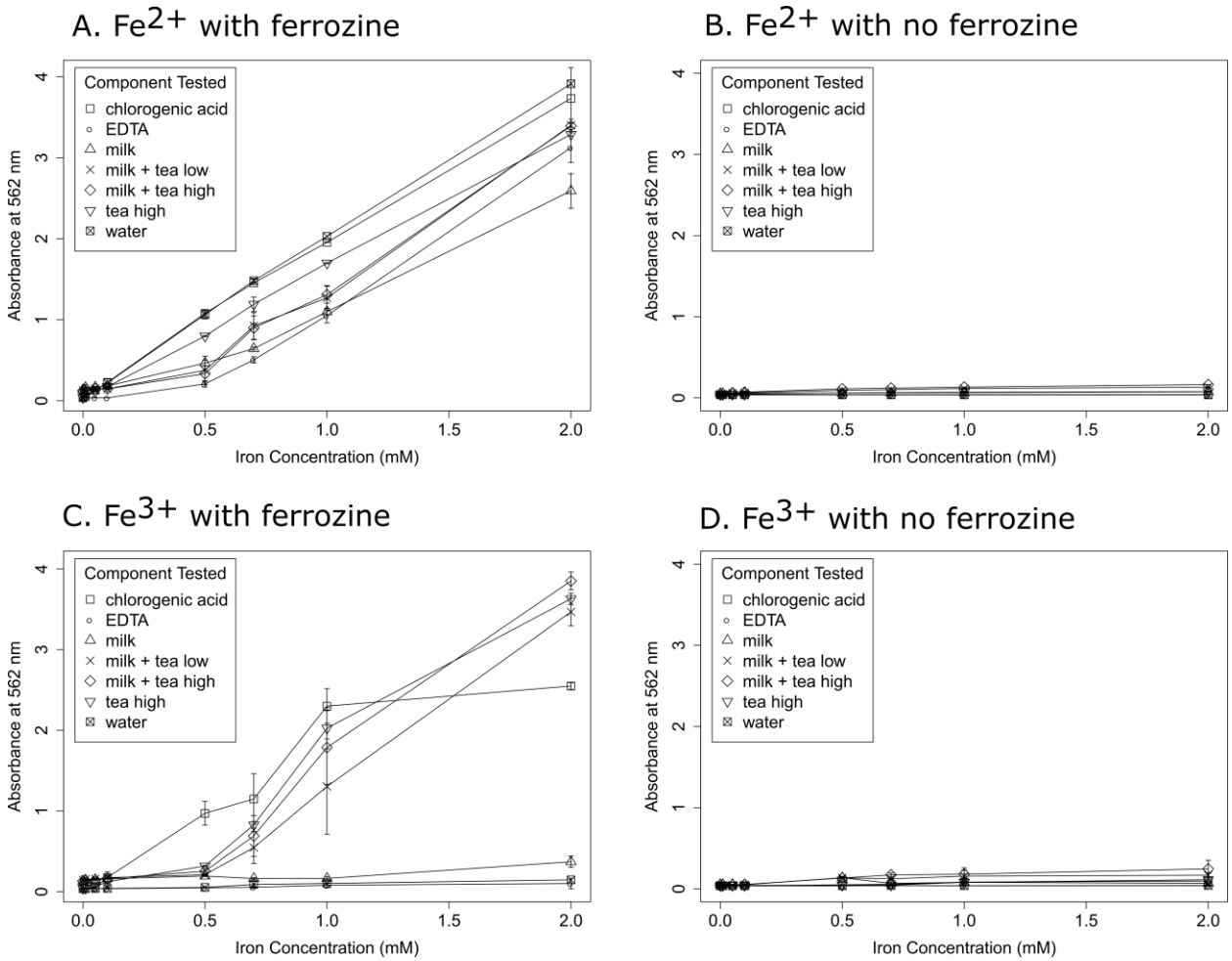

Figure 7. Plots show competition assays of ferrozine; A. Fe^{2+} ($FeSO_4$) and C. Fe^{3+} ($FeCl_3$) were tested and controls without ferrozine were also tested with B. Fe^{2+} and D. Fe^{3+}. Experiments were done at least in duplicate. Error bars represent standard deviation. Tea concentrations were 0.32 mg/ml ("high") and 0.16 mg/ml ("low).

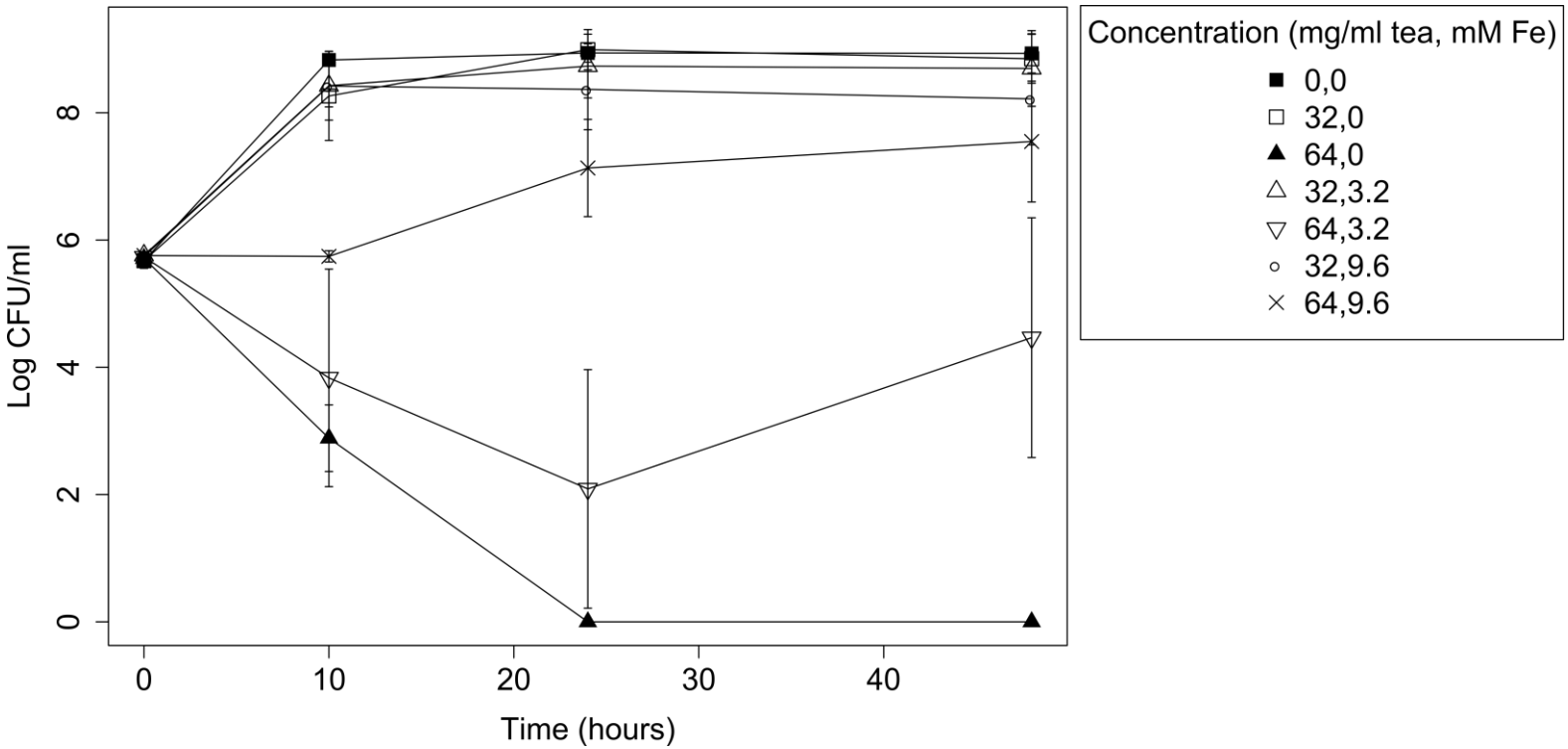

Figure 8. Growth of *S*. Typhimurium in 3 concentrations of iron ($FeSO_4$) and 2 concentrations of yerba mate extract ("tea") is plotted over time. Error bars show standard deviation for 3 replicates with the exception of the 10 h time point, which only had 2 replicates.

Tables

Table 7. *L. casei* metabolites found to be significantly different between treatments with ‘control_no_bacteria’ = milk+tea, ‘control_no_tea’ = milk+bacteria, and ‘tea’ = milk+tea+bacteria. Extracted ion intensity values normalized to a gallic acid internal standard are listed with data ranges in parentheses. (attached)

Table 8. *S.* Typhimurium metabolites found to be significantly different between treatments with ‘control_no_bacteria= milk+tea, ‘control_no_tea ’ = milk+bacteria, and ‘tea’ = milk+tea+bacteria. Extracted ion intensity values normalized to a gallic acid internal standard are listed with data ranges in parentheses. (attached)

Supporting information

Supporting figures

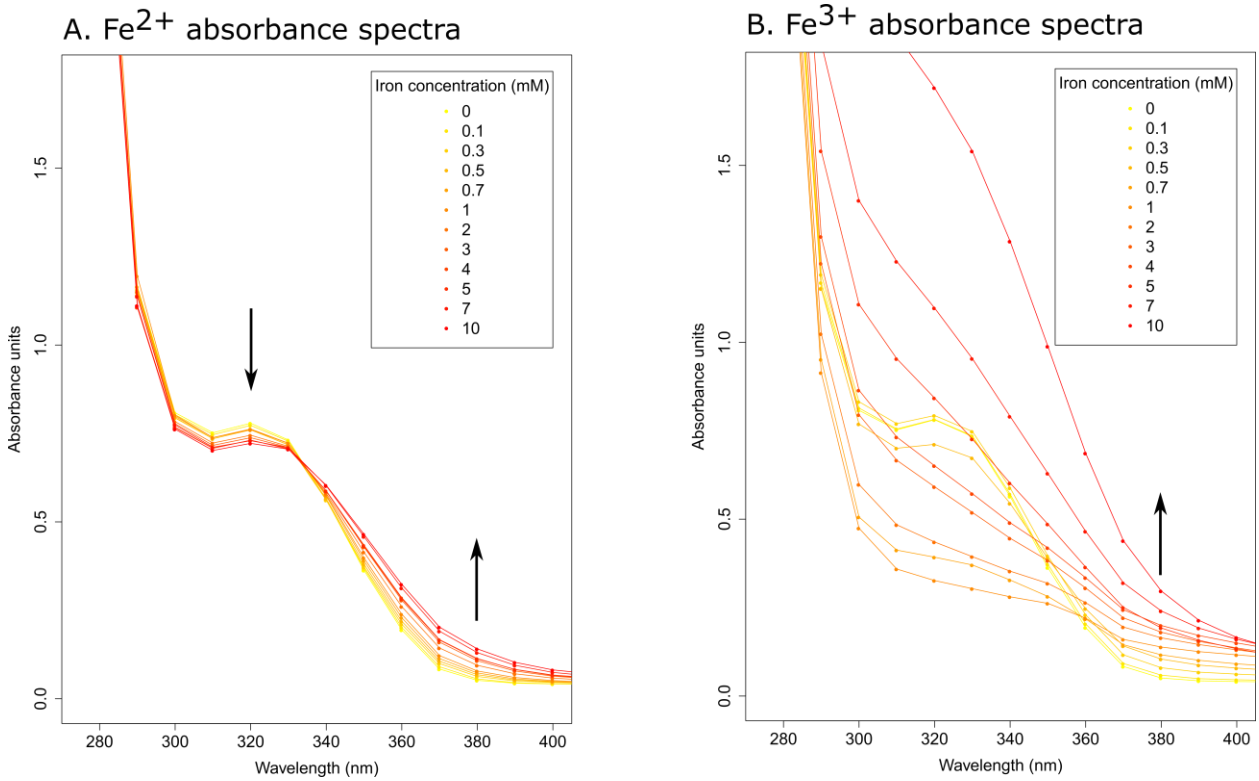

Figure S 2. Ultraviolet-visible spectra of yerba mate extract (0.16 mg/ml tea; "low" concentration) with $FeSO_4$ or $FeCl_3$ at varying concentrations. Points are the means of technical duplicates; one representative biological replicate is shown. Arrows indicate the tendency of absorbance to shift up or down corresponding with increasing or decreasing iron concentrations.

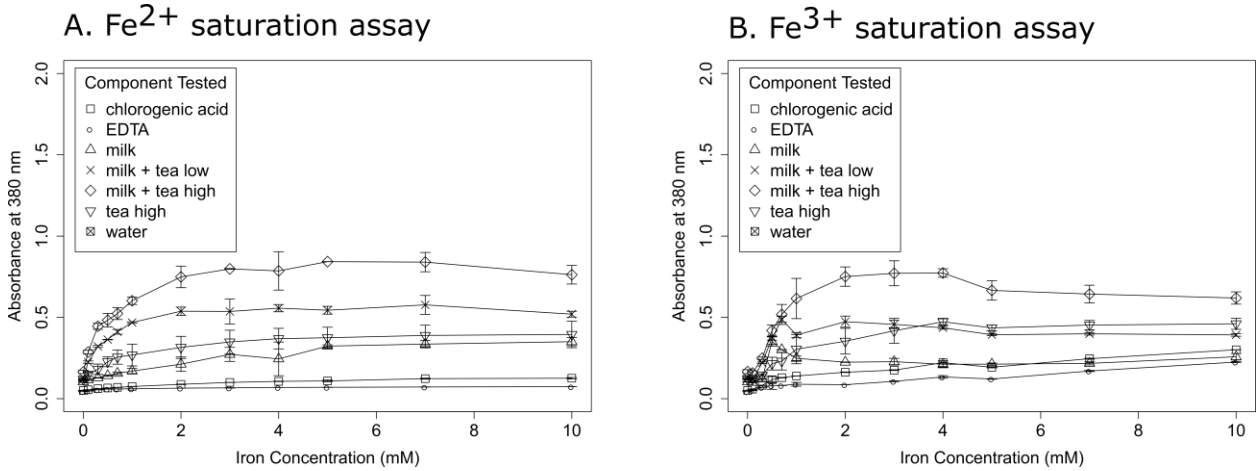

Figure S 3. Saturation assays are plotted for A. Fe^{2+} ($FeSO_4$) and B. Fe^{3+} ($FeCl_3$); absorbance was monitored at 380 nm. No ferrozine was added for this assay. Experiments were done at least in duplicate; error bars represent standard deviation. Tea concentrations were 0.32 mg/ml (“high”) and 0.16 mg/ml (“low).

CHAPTER V
METABOLIC ANALYSIS OF THE MECHANISMS OF ACTION OF YERBA MATE EXTRACT ON *SALMONELLA ENTERICA* SEROVAR TYPHIMURIUM

This manuscript will be submitted to the journal *Metabolomics* by Caroline S. Rempe, Scott C. Lenaghan, Kellie P. Burris, and C. Neal Stewart, Jr. to be considered for peer-reviewed publication.

CS Rempe, SC Lenaghan, KP Burris, and CN Stewart conceived and designed the study; CS Rempe conducted the experiments, CS Rempe and SC Lenaghan analyzed and interpreted the data; CS Rempe, SC Lenaghan, KP Burris, and CN Stewart wrote and edited the manuscript. All authors read and approved the final manuscript.

Abstract

Salmonella enterica serovar Typhimurium is a Gram-negative enteropathogen that infects millions of people worldwide each year; the rapid emergence of antibiotic resistant strains has heightened the urgency to develop effective treatments for this pathogen. Aqueous extracts of yerba mate (*Ilex paraguariensis*) provide effective therapy, *in vitro*, for the drug-resistant *S*. Typhimurium DT104. Unfortunately, while some of the chemical constituents that contribute to the extract's antibacterial activity have been identified, the mechanism of action of the extract is still unknown and of crucial importance to its future potential in combating antibiotic resistant bacteria. Yerba mate extract induced changes in central carbon metabolism in *S*. Typhimurium, reduced catalase activity by means other than direct inhibition, and did not change membrane integrity (except at the initial 0 time point, where differences were not resolved) despite a significant increase in the production of a cell wall precursor. Additional significant differences were observed in the global metabolic regulators alpha-ketoglutarate and acetylphosphate, the energy-related molecule NAD^+, and in an unexpected match to the antibacterial compound yohimbine. This work provides the first evaluation of the mechanism of action of yerba mate

extract on *S*. Typhimurium, revealing a major impact on central carbon metabolism, catalase activity, and possible metabolic links to interference in energy production and membrane integrity. The putative identification of the antibacterial compound yohimbine and the many unidentified compounds provides additional avenues for future investigations of novel yerba mate compounds capable of traversing or binding to *S*. Typhimurium's membrane.

Introduction

Nontyphoidal *Salmonella* species are widespread food-borne enteropathogens responsible for more than one million infections annually in the United States alone (S. Crim et al., 2015; Scallan et al., 2011). The cost of these infections places a significant burden on the U.S. healthcare system, leading to over 2,000 hospitalizations and 30 deaths per year (S. Crim et al., 2015; Scallan et al., 2011). Perhaps of even greater concern, *Salmonella enterica* serotype Typhimurium accounts for approximately 12% of serotyped *Salmonella* infections in the U.S. (S. Crim et al., 2015), and strains have emerged that are reported to be resistant to the most common antimicrobial agents (CDC, 2015). The emergence of drug resistance in this globally relevant pathogen highlights the need to identify new antibacterial agents, and serves as the motivation for this work.

One source of novel antibacterial agents is plants, which have evolved to produce numerous biologically active chemicals. At present, antibacterial agents derived from plants are not a major source for pharmaceutical-grade antibiotics, likely due to the generally higher minimum inhibitory concentrations compared to bacterial-derived antibiotics (discussed by Tegos & Stermitz, 2002), concerns over quality control (Yau, Goh, & Koh, 2015), and difficulties in obtaining intellectual property for natural products (Silins, Tan, & Chan, 2015). Despite these concerns, plants contain many weakly antibiotic compounds that may act

synergistically to increase the efficacy of other antibiotics (Lewis & Ausubel, 2006). One example of synergism in plant antibiotics are the barberry plants (*Berberis*), which produce the antibiotic berberine that is only effective in the presence of a multidrug resistance pump inhibitor, like the phytochemical 5'-methoxyhydnocarpin (Tegos & Stermitz, 2002). This synergistic mechanism of action shows a level of complexity not readily observed in synthetic pharmaceutical systems. In addition to synergistic mechanisms, single plant antibacterial compounds, such as eugenol (Devi, Nisha, Sakthivel, & Pandian, 2010), ferulic acid (Borges et al., 2013), and essential oils (Bakkali et al. 2008), have been shown to be involved in membrane disruption, production of reactive oxygen species (ROS), and inhibition of transcription, translation, and DNA replication (Abreu et al., 2012; Cowan, 1999; Radulović, Blagojević, Stojanović-Radić, & Stojanović, 2013; Upadhyay, Upadhyaya, Kollanoor-Johny, & Venkitanarayanan, 2014). In plant antibacterial compounds, the ability to disrupt the bacterial membrane/cell wall, as assayed by monitoring efflux of intracellular components, influx of hydrophobic dyes or antibiotics, or microscopic observation, has been frequently attributed to polyphenolics (Borges et al., 2015; Cushnie & Lamb, 2011; Devi et al., 2010; Di Pasqua et al., 2007; Gill & Holley, 2006; Helander et al., 1998; Lambert, Skandamis, Coote, & Nychas, 2001; Nohynek et al., 2006; Tyagi, Singh, Kumari, Kumari, & Mukhopadhyay, 2015). Similarly, plant polyphenols have been implicated in the formation of ROS in bacteria, based on colorimetric or fluorescent dyes (Dwyer, Collins, & Walker, 2015; Nakamura et al., 2015; Zhao, Hong, & Drlica, 2014). Inhibition of proteins, such as FtsZ (Hwang & Lim, 2015) and DNA gyrase (Plaper et al., 2003), or direct binding to DNA (Lou et al., 2012; Plaper et al., 2003) by plant extracts have been less studied, but have been shown to be important to the generation of antibacterial activity in some systems. As bacteria continue to develop resistance to current

pharmaceuticals, alternative compounds will be necessary to quell this threat, with plants providing a vast resource of novel compounds with various modes of action.

The goal of this study was to examine the mechanism of action of an aqueous extract of yerba mate, a leaf tea made from *Ilex paraguariensis*, on *Salmonella* Typhimurium. Previous studies have demonstrated the antibacterial activity of yerba mate against a wide range of foodborne bacterial pathogens (Burris et al., 2011, 2012, 2015; Hongpattarakere, 2000; Kubo & Muroi, 1993; Martin et al., 2013; Sari, Turkmen, Polat, & Velioglu, 2007; Tsai, Tsai, Chien, Lee, & Tsai, 2008). Yerba mate is known to contain numerous antibacterial phenolic compounds, including chlorogenic acids, quercetin, and ferulic acids (Heck & De Mejia, 2007). While pure phenolic compounds isolated from yerba mate have been investigated for their antibacterial modes of action (Martin et al., 2013), no studies have examined the antibacterial mechanism of the whole extract. In this work, membrane disruption, catalase activity, and the metabolomic profiles of *Salmonella* Typhimurum DT104 in response to a sub-lethal concentration of yerba mate extract was examined.

Results

At a starting *S.* Typhimurium concentration of ca. 6 log colony forming units (CFU)/ml, the minimum inhibitory concentration (MIC) of yerba mate was found to be 10 mg/ml based on killing at 24 hours (h) (Figure 9A). At concentrations < 2.5 mg/ml, a lag in growth was observed over the first 4 h of culture, with the cultures fully recovering by 8 h. This lag was more pronounced at 5 mg/ml with the cultures failing to reach the culture maximum over the 24 h period of the experiments. When the starting concentration of *S.* Typhimurium was increased to ca. 9 log in order to obtain sufficient cell quantities for subsequent assays, a MIC was not observed over the tested concentration range; however, at a dose of 80 mg/ml yerba mate, there

was a significant reduction in growth after 2 h, thus this dose was termed the sub-lethal dose (Figure 9B). For simplicity, the three *S.* Typhimurium treatment conditions with ca. 9 log CFU/ml starting culture conditions will be referred to as $control_{no\ tea}$ (0 mg/ml yerba mate extract with *S*. Typhimurium), tea (80 mg/ml yerba mate extract with *S*. Typhimurium), and $control_{no\ bacteria}$ (80 mg/ml yerba mate extract with phosphate buffered saline (PBS) pH 7.4 instead of *S*. Typhimurium) throughout the remainder of this paper.

No significant differences between $control_{no\ tea}$ and tea treatments were observed in measurements of optical density at 600 nm (OD_{600}), so the crystal violet assay was not adjusted to OD_{600} (Figure S 4). The crystal violet assay for membrane integrity showed no significant differences between $control_{no\ bacteria}$ compared to tea except at the initial timepoint (Figure 10B), so the significant differences that were observed between $control_{no\ tea}$ and tea can generally be explained by the interaction of yerba mate extract with crystal violet. Thus, no change in membrane integrity was detected with this assay except for a possible unresolved loss of membrane integrity immediately after the tea treatment was applied. Catalase activity, however, was observed to be reduced in the tea treatment as compared to the $control_{no\ tea}$ treatment. No effect of $control_{no\ bacteria}$ was observed on catalase (Figure 10A).

The intracellular metabolomics analysis showed that 20 to 34 identifiable metabolites were significantly different in each of the six displayed treatment comparisons (tea vs. $control_{no\ tea}$ at 0, 40, and 240 min and tea vs. $control_{no\ bacteria}$ at 0, 40, and 240 min) that focus on differences between the tea treatment and control treatments at each time point (Table 9, Table 10, Table 11, Table 12, Table 13, Table 14). The tricarboxylic acid (TCA) cycle (Figure 11) was the pathway most enriched by the identifiable compounds in Tables 9-14.

The pentose phosphate pathway (PPP) (Figure S 5), glycolysis pathways (Figure 12), and amino acid and nucleotide biosynthesis/metabolism (Figure S 6, Figure S 7) were also represented in the identifiable compounds with significant differences between tea and control treatments. Two identifiable compounds with significant differences between tea and controls, yohimbine and ornithine, were observed to be present only in tea and not in $control_{no\ tea}$ (Figure 13, Figure S 7). As seen in the plots of succinate/methylmalonate, fumarate, and malate, some common metabolic products are also clearly present in the tea treatment (Figure 11). In a brief summary of treatment differences, there were 7 compounds with significant differences between tea and both controls at 0 min, 15 compounds at 40 min, and 10 compounds at 240 min (Tables 9-14). Among these compounds, aconitate, citraconate, citrate/isocitrate, flavin mononucleotide (FMN), fumarate, and N-carbamoyl-L-aspartate were significantly different between tea and both control treatments at 0 min and at 40 min Acetylphosphate, alpha-ketoglutarate, sedoheptulose 1/7-phosphate, and valine were significantly different between tea and both controls at 40 min and at 240 min; there were no compounds significantly different between tea and both controls across all three time points (Tables 9-14).

Discussion

The MIC of yerba mate was 10 mg/ml with ca. 6 log CFU/ml starting culture based on killing at 24 h (Figure 9A). This was similar to the 7.4 mg/ml MIC previously observed (Gonzalez-gil et al., 2014) with aqueous yerba mate extract and *S.* Typhimurium DT104. An MIC of 10 mg/ml is much higher than the µg/ml-level MICs of antibiotics currently in use, but is comparable to the *S.* Typhimurium MICs of other plant extracts, which were observed to range from 0.78 to 6.25 mg/ml (Marasini et al., 2015). Variation between manufacturers' batches (Golozar et al., 2012) would be expected to contribute to differences in MIC between studies. There is a known

"inoculum effect" such that antibiotic susceptibility is reduced when the bacterial inoculum concentration is increased. This was observed when the *S.* Typhimurium inoculum concentration was increased to ca. 9 log CFU/ml in order to obtain enough biomass for assays in the current study (Figure 9B). The inoculum effect was previously observed with multiple antibiotic classes, including aminoglycosides, beta-lactams, and fluoroquinolones in studies that focused on *Escherichia coli* and *Staphylococcus aureus* (Greulich, Scott, Evans, & Allen, 2015; Udekwu, Parrish, Ankomah, Baquero, & Levin, 2009; zur Wiesch et al., 2015). *S.* Typhimurium inoculum effects have been characterized with beta-lactams (Eng, Cherubin, Smith, & Buccini, 1985) but recent work with inoculum effects has primarily focused on *E. coli* and *S. aureus*.

Yerba mate contains a diverse mixture of compounds, including polyphenolics, xanthines, alkaloids, and flavonoids, that likely contribute to its antioxidant, stimulant, antibacterial, and other bioactive properties (reviewed by Heck & De Mejia, 2007). The antibacterial mechanisms of many specific plant constituents such as eugenol or ferulic acid have been studied with assays for membrane integrity, reactive oxygen species, and binding to key proteins (Borges et al., 2013; Devi et al., 2010). Membrane integrity is traditionally assayed by monitoring efflux of intracellular components, influx of hydrophobic dyes or antibiotics, or microscopic observation and has generally been found to contribute to the antibacterial mechanism of polyphenolics (Borges et al., 2015; Cushnie & Lamb, 2011; Devi et al., 2010; Di Pasqua et al., 2007; Gill & Holley, 2006; Helander et al., 1998; Lambert et al., 2001; Nohynek et al., 2006; Tyagi et al., 2015), although quercetin has been observed to increase cell wall rigidity (T. Wu, He, et al., 2013). The crystal violet membrane integrity assay used in the current study revealed that the major differences between tea and $\text{control}_{\text{no tea}}$ treatments could be explained by a precipitate of the tea interacting with crystal violet dye, as evidenced by the $\text{control}_{\text{no bacteria}}$

treatment (Figure 10B). The only significant difference between tea and control$_{\text{no bacteria}}$ occurred at the initial 0 min time point (Figure 10B), which suggests that there could be a slight, immediate change in membrane integrity upon addition of the tea treatment (the tea treatment took up more crystal violet than the control$_{\text{no tea}}$ or control$_{\text{no bacteria}}$ treatments) that occurred too quickly for this experiment to resolve.

ROS assays based on colorimetric or fluorescent dyes are also common and generally conclude that phenolics promote ROS formation (Dwyer et al., 2015; Nakamura et al., 2015; Zhao et al., 2014). The current work hypothesized that yerba mate extract would follow a noted trend of increased ROS with antibacterial activity (Kohanski, Dwyer, Hayete, Lawrence, & Collins, 2007), which would in turn upregulate the expression of catalase. Catalase activity of bacterial cells, however, was determined to be significantly reduced with the tea treatment compared to the control$_{\text{no tea}}$ treatment at 0 h, 4 h, and 8 h (Figure 10A). Again, the difference at 0 h suggests fluctuation on a time scale smaller than this experiment was able to accurately measure. The consistently reduced catalase activity of *S.* Typhimurium in the tea treatment was not due to the direct inhibition of catalase by the tea extract (Table S 9), but could be a result of transcriptional, translational, or post-translational control of tea components. Since yerba mate extract is well known for its high antioxidant activity (Filip, Lotito, Ferraro, & Fraga, 2000; Valerga, Reta, & Lanari, 2012; Valerga, Shorthose, & Lanari, 2013), it is also possible that ROS species were reduced by the tea, thus triggering a downregulation of catalase by *S.* Typhiumurium.

Additional phenolic mechanisms of action of that were not tested in this work include binding to specific proteins like FtsZ (Hwang & Lim, 2015) and DNA gyrase (Plaper et al., 2003) or direct binding to DNA (Lou et al., 2012; Plaper et al., 2003). Complex plant extracts, including berries (reviewed by Puupponen-Pimiä et al. 2005) and essential oils (reviewed by

Bakkali et al. 2008) have been evaluated for mechanisms of action, especially membrane integrity, ROS production, and protein binding. Three edible medicinal plants (Yong, Ooh, Ong, Chai, & Wong, 2015) were recently evaluated for their mechanisms of action using proteomic analyses of bacterial pathogens, but to our knowledge, the current study was the first to survey the metabolome of pathogenic bacteria in order to gain an understanding of a plant extract's antibacterial mechanism(s). Bacterial metabolomics has been shown to be capable of differentiating classes of common pharmaceutical antibiotics (Belenky, Ye, Porter, Schwarz, et al., 2015; Dörries, Schlueter, & Lalk, 2014) and evaluating pure phytochemicals (Mousavi, Bojko, Bessonneau, & Pawliszyn, 2016) but has not previously been applied to plant extracts. The metabolomics assessment of *S.* Typhimurium (Table 9-14, Figures 11, 12, S 5-S7) must be interpreted carefully since the "intracellular" metabolites of cells collected on filters were evaluated, meaning that the $\text{control}_{\text{no bacteria}}$ sample consisted of tea components that adhered to the filter rather than all possible components in the tea. Thus, metabolites that are absent from $\text{control}_{\text{no bacteria}}$ may still be present in the tea extract; metabolites that are present in the $\text{control}_{\text{no bacteria}}$ treatment were definitely present in the tea extract, but not necessarily at the same concentration observed. Thus, the tea and control treatments have the potential to contain an intracellular metabolite, a metabolite bound extracellularly, and metabolites adhered to the filter. The metabolomics results are additionally limited by which metabolites are identifiable and the possibility that mechanisms of action may either non-specifically alter the metabolome or not impact the metabolome at all (as observed in Vincent, Ehmann, Mills, Perros, & Barrett, 2016). Based on the results from the metabolomics data, there are three categories that the significantly different metabolites could fall under: 1) influx from the tea extract, 2) general stress conditions, and/or 3) antibiotic specific stressors.

Influx from tea extract

A significantly larger mean in tea vs. $control_{no\ tea}$ followed by a decrease over time in the tea treatment, as in citrate/isocitrate and aconitate of the tricarboxylic acid (TCA) cycle (Table 9-11, Figure 11), is a common trend that may signify an immediate cellular response, but may also be due to the influx of that metabolite into the cell from the tea extract. Yohimbine in particular can be confidently explained by influx from the tea since it is not known to be produced by *S.* Typhimurium and is absent from the $control_{no\ tea}$ treatment. Succinate, fumarate, and malate may also be transported into the cell from the tea extract and either join in the TCA cycle or, more likely, inhibit the progression of the TCA cycle since most TCA cycle products act as inhibitors through feedback regulation.

General stress conditions

Lag and exponential growth phases differ, with lag phase showing slow growth and increased expression of metal uptake and oxidative stress systems (Rolfe et al., 2012), but this should not impact the results of the current study since both $control_{no\ tea}$ and tea are in lag phase at 40 min and late exponential phase at 4 h. Osmolarity, however, was expected to be a factor in the response of *S.* Typhimurium to the tea treatment, but common osmoprotectants like glutamate and proline (discussed by Frossard et al., 2012) were observed to have no significant differences between treatments, and other osmoprotectants were not identified. Additionally, oxidative stress effects were expected, but not observed in the metabolomics data. For example, glutathione to glutathione disulfide ratios, associated with oxidative stress conditions (reviewed by Pompella, Visvikis, Paolicchi, De Tata, & Casini, 2003), had no significant differences compared to the controls, and glutathione disulfide was not observed. Other key indicators of oxidative stress, like 8-oxo-guanine (reviewed by Farr & Kogoma, 1991), were not present in the library of

standards used for compound identification, thus it was not possible to analyze their levels. One generic stress response is the downregulation of genes needed for cell growth, but specific stressors tend to give specific responses, especially with metabolomics data (Jozefczuk et al., 2010). In general, the later stages of the TCA cycle (succinate/methylmalonate, malate, fumarate) were the only cell growth-related steps that appeared to be static. Without flux information, the static appearance of these compounds could be due to constant movement as they are converted to the next metabolite, or it could be due to no movement at that portion of the TCA cycle. There are few entirely generic metabolic stress responses, but downregulation of the latter portion of the TCA cycle is one that might be at work in the current study.

Antibiotic specific stressors

Stress-specific trends in antibiotic-treated bacteria have previously been used to identify mechanisms of the antibiotic (Belenky, Ye, Porter, Schwarz, et al., 2015; Dörries et al., 2014; Vincent et al., 2016). In *E. coli* treated with norfloxacin, kanamycin, or ampicillin, no key distinguishing features were visible at 30 min, but large increases in levels of citrate, succinate, and oxidized nicotinamide adenine dinucleotide (NAD^+) and decreases in nucleotide precursors (including ribose 5-phosphate) were observed for all the tested antibiotics (Belenky, Ye, Porter, Schwarz, et al., 2015). The current study did not observe any of these trends at 40 min. Similarly, trends in nucleotides, cell wall precursors, and other metabolites that were previously seen to define a thymidine kinase inhibitor and a 1-deoxy D-xylulose 5-phosphate (DXR) pathway inhibitor (Vincent et al., 2016) were not observed in the significantly different metabolites of the current work.

UDP-N-acetylglucosamine is a lipid precursor that normally favors conversion to acyl-ACP; however, in the presence of an inhibitor of LpxC, the enzyme at the following step of lipid

A synthesis, acyl-ACP accumulates and may push the reverse reaction to convert it back to UDP-N-acetylglucosamine (Barb & Zhou, 2008; reviewed by Mcclerren et al., 2005). In the current work, UDP-N-acetylglucosamine was significantly higher in the tea treatment at 40 min but not different at 240 min, so it is possible that lipid A synthesis was blocked, causing acyl-ACP (not in library of standards) accumulation and pushing a reverse reaction to UDP-N-acetylglucosamine, which might have transiently risen at 40 min before being shuttled to other pathways. Membrane integrity effects would be expected if lipid A synthesis was blocked, so concentrations of the inhibitor may have been too low relative to cell concentrations to have a visible membrane effect under the tested conditions. The difference in membrane integrity seen at 0 min supports an immediate membrane effect that is quickly overcome due to the large number of bacterial cells, but a faster membrane integrity assay is needed to resolve the time scale of any membrane effects and ensure equivalent starting conditions.

Significant differences in amino acids and nucleotides between $\text{control}_{\text{no tea}}$ and tea were only observed with valine (decreased in tea at 240 min) and cytidine monophosphate (increased in tea at 240 min), suggesting interference or specific regulation of enzymes unique to valine and CMP synthesis or metabolism. However, no enzymes were noted to be unique to valine or CMP synthesis based on KEGG pathways (Kanehisa & Goto, 2000). CMP might also increase due to higher levels of RNA degradation, but other nucleotides would be expected to increase if this were the case. UMP, AMP, GMP, and IMP had noisy spectral abundance data that might show significant trends with additional replication.

Respiration occurs in the plasma membrane of *Salmonella* species, and uses the membrane-bound NADH complex, succinate dehydrogenase, and lactate dehydrogenase to gather electrons. Electrons are then passed to ubiquinone or another electron acceptor, powering

proton pumps that create the gradient needed for ATP synthase to function. NADH use by the NADH complex is the most efficient electron source since it is furthest from the final electron acceptor, capable of generating 3 ATP compared to 2 from succinate dehydrogenase. Flavin mononucleotide (FMN) and flavin adenine dinucleotide (FAD) are also important in electron transfer and frequently serve as cofactors in biosynthesis functions. The NADH complex contains a FMN cofactor and the succinate dehydrogenase complex holds an FAD cofactor. FAD levels were not different between tea and $control_{no\ tea}$, and the slightly elevated FMN levels at 0 and 40 min could be explained by immediate influx from the tea extract. NAD^+, however, had a significant increase of 0.7 fold at 240 min, which, although a small fold-change, amounts to a 5 log difference in abundance based on spectral intensity units (Table 11, Figure 13). NADH was not visible in these data and so it is presumed to have been used immediately after being produced. The higher levels of NAD^+ observed in tea vs. $control_{no\ tea}$ might signify slowed NADH production. Most NADH is produced in glycolysis, the pentose phosphate pathway (PPP), and the TCA cycle, the pathways in which the most differences in metabolites between treatments were observed. All TCA cycle enzymes with the exception of isocitrate dehydrogenase are known to be downregulated during lag phase, which is associated with ROS stress (Rolfe et al., 2012). The TCA enzymes following isocitrate dehydrogenase, which produces alpha-ketoglutarate, have no significant changes and thus could be down-regulated by the stress of yerba mate extract. This would leave the TCA cycle to produce only a single NADH from isocitrate dehydrogenase. Glycolysis showed no significant differences in pyruvate or acetyl CoA, the substrate and product for the NADH formation step. In the PPP 6-phosphogluconate, the precursor to an NADH reaction, is elevated at 0 and 240 min, which might be expected to increase NADH production. Based on these results, a reduced TCA cycle

would have the greatest impact on NADH production, but flux data would be needed to test whether the TCA cycle has been truncated or has constant flux under the tea treatment conditions.

Additional significantly different metabolites of particular interest are alpha-ketoglutarate, phosphoenolpyruvate (PEP), and acetylphosphate. Alpha-ketoglutarate has an unusual trend in which it is significantly greater than the $control_{no\ tea}$ treatment at both 40 min (2.1 fold higher) and 240 min (1.3 fold higher). As a key regulator and signaling molecule for both carbon and nitrogen metabolism, alpha-ketoglutarate alterations can be very influential. Alpha-ketoglutarate inhibits glucose transporters (Doucette, Schwab, Wingreen, & Rabinowitz, 2011), PEP synthetase (Chulavatnatol & Atkinson, 1973), and citrate synthase (Pereira, Donald, Hosfields, & Harry, 1994), so it may be responsible for the decrease in citrate over time after an initial high production rate or influx from the tea. Citrate could also be decreasing over time due to efflux from the cell by pumps that remove citrate-iron complexes from ROS-stressed cells (Frawley et al., 2013). Glucose-6-phosphate, a direct product of glucose, was not observed to differ between tea and $control_{no\ tea}$, but PEP increased at 240 min, perhaps in response to the reduction of alpha-ketoglutarate in the tea treatment between 40 and 240 min. Since alpha-ketoglutarate is a key intermediate in amino acid synthesis and degradation, the elevated levels of alpha-ketoglutarate may also have been a response to high turnover in amino acids or simply an overload of citrate and isocitrate from the tea that fluxed to alpha-ketoglutarate. While amino acids other than valine, which is derived from pyruvate, showed no significant differences between treatments, the production and consumption could have been higher in the tea treatment and required additional alpha-ketoglutarate levels to be maintained.

PEP and pyruvate are also major intermediates that regulate flux into the TCA cycle and other cellular pathways. No significant differences in pyruvate were observed between treatments, but PEP accumulated in the tea treatment at 240 min. This was unexpected since increased pyruvate has been associated with recovery from environmental stressors (Morishige, Fujimori, & Amano, 2013; J. Wu, Li, Cai, & Jin, 2014), but here the precursor to pyruvate, PEP, and a product of pyruvate, acetylphosphate, were observed to significantly increase while pyruvate had no significant difference (though there is a non-significant trend of increasing pyruvate in tea vs. $\text{control}_{\text{no tea}}$) (Figure 11, Figure 12). When there is excess glucose, pyruvate tends to flow to acetylphosphate and then to acetate that is excreted in "overflow metabolism" (Wolfe 2005). When glucose is less abundant, acetate is taken back up and converted to acetylphosphate and then to pyruvate or acetyl-coA. Acetylphosphate also acts as a global signaling molecule for nitrogen assimilation and biosynthesis of flagella, pili, capsule, and biofilm components (reviewed for *E. coli* in Wolfe, 2005). The accumulation of acetylphosphate in tea at 240 min could mark the switch between glucose and glucose/acetate metabolism delayed from the 40 min accumulation of acetylphosphate in $\text{control}_{\text{no tea}}$. Another possible explanation is that acetylphosphate production was upregulated for its signaling functions, particularly those involving membrane proteins since UDP-N-acetylglucosamine levels were increased at the same time.

Overall, most of the changes in identifiable compounds revealed that *S.* Typhimurium with the tea treatment was forced to handle an abundance of metabolic intermediates, which may have prompted differential production of the major regulatory metabolites alpha-ketoglutarate and acetylphosphate. An immediate metabolic response or influx from the tea may have been responsible for elevated levels of metabolites, but neither can be verified without a flux analysis.

At lower inoculum levels, the relatively higher concentrations of metabolic intermediates may backlog the TCA cycle, glycolysis, and the PPP, since intermediates tend to act as feedback inhibitors, resulting in minimal levels of NADH production, reduced respiration, and thus reduced energy production. This cell state could leave *S.* Typhimurium more vulnerable to abnormalities in membrane synthesis and any toxic effects of unusual tea metabolites like yohimbine (Table 9) and the many unknown compounds that may have entered the cell (Table S 10). Yohimbine is known to have strong antibacterial activity against *E. coli* (MIC 4-32 µg/ml) and had no cytotoxic effects on two different cell lines (Ozçelik et al., 2011). The compound found in the current study is a match to yohimbine, but since yohimbine has not previously been found in any processed or unprocessed *Ilex paraguariensis* samples, it may be a related compound with the same chemical formula ($C_{21}H_{26}N_2O_3$). Vincamine (Pubchem compound identifier (CID) 15376), rauwolscine (CID 643606), corynanthine (CID 92766), and epivincamine (CID 637570) are all isomers of yohimbine; some are found in *Rauwolfia* ssp. (Chatterjee et al., 1956) and *Aspidosperma quebracho-blanco* (Ewins, 1914) in South America.

Conclusion

Yerba mate extract contains potentially novel components that are capable of killing major bacterial pathogens like *S.* Typhimurium, but only mechanistic information on previously known pure components, not the comprehensive whole extract (including potentially novel compounds), was available prior to this work. Now it is clear that yerba mate extract has a major impact on central carbon metabolism, including the TCA cycle, PPP, and glycolysis pathways, by either stimulating an immediate response or presenting the cells with large quantities of metabolic intermediates that could block NADH production. Furthermore, catalase activity was reduced in the presence of the tea at 240 min, but not directly inhibited, which suggests that catalase was

downregulated due to effects of tea components or reduced ROS in the cell. Finally, this study has found that membrane integrity was unaffected in the conditions tested, but UDP-N-acetylglucosamine, a cell wall precursor, and acetylphosphate, a global signaling compound that can regulate membrane proteins were both upregulated at 240 min. This suggests that membrane stress may be visible with a lower relative concentration of bacterial cells to tea compounds. This first step toward characterizing the antibacterial activity of yerba mate extract has ruled out several previously known mechanisms based on metabolomic trends and contributed information on cell membrane integrity, catalase activity, altered *S.* Typhimurium metabolism, and putatively identified yohimbine and a list of unidentifiable yerba mate components compounds capable of entering or binding to *S.* Typhimurium cells. Future studies can now build on this knowledge to generate more specific hypotheses of antibacterial mechanism for yerba mate extract and its constituents and examine yohimbine and the set of currently unidentified compounds for their individual and synergistic antibacterial mechanisms of action.

Materials and methods

Yerba mate aqueous extraction

A commercial brand of yerba mate tea (Taragui; 100% leaves, Argentina) was homogenized in a blender to a particle size of <1 mm to be consistent with previous aqueous yerba mate studies (Burris et al., 2012; Rempe et al., 2015). The homogenized tea was then extracted with ten times its mass of water at 4 °C for 3.5 h, 0.22 µm polyethersulfone (PES) vacuum filtered (Corning Life Sciences, Oneonta, NY, USA), frozen at -80 °C, and lyophilized using a FreeZone, 12 L freeze dryer (Labconco, Kansas City, Mo. USA). Dried extracts were stored at room temperature in a sealed plastic container prior to testing.

Bacterial culture maintenance

S. Typhimurium DT104 strain 2576 was obtained from the Department of Food Science and Technology at the University of Tennessee. Stock cultures of *S.* Typhimurium strains were stored in 25% glycerol at -20 °C. Cultures were started from frozen stocks and re-inoculated daily in tryptic soy broth (TSB) for 2-3 days before an experiment. To score the CFUs at a given time interval, 100 µl samples were serially diluted in 0.1% sterile peptone and pour-plated in duplicate using tryptic soy agar (TSA). *S.* Typhimurium plates were grown aerobically at 37 °C for 24 h. Following incubation, CFUs were enumerated.

Bacterial growth experiments

Yerba mate extract (12.5 mg to 2 g) was reconstituted in MOPS buffer pH 7.3, adjusted to a final pH of 7.3 with 1 M KOH, and syringe-filtered through 0.22 µm Express PES Membrane (Millipore, Billerica, Mass., USA) prior to microbial susceptibility testing. All growth experiments were performed in 125 ml flasks containing 12.5 ml TSB, 10 ml reconstituted yerba mate extract or MOPS buffer pH 7.3, and 2.5 ml bacteria for a total volume of 25 ml. Overnight bacterial cultures were diluted in 0.1 % sterile peptone to obtain 2.5 ml of ca. 5-6 log CFU/ml starting concentrations or 5 ml of ca. 20 h culture was pelleted at 15,000 x g for 1 min at 4 °C, the supernatant decanted, and the pellet resuspended in 5 ml PBS pH 7.4 to achieve a ca. 9 log CFU/ml starting concentration. A no-bacteria control contained 2.5 ml PBS pH 7.4. Experiments were conducted aerobically at 37 °C with shaking at 150 rpm. Initial growth experiments were assessed at yerba mate extract concentrations of 0, 1.25, 2.5, 5, 10, 15, and 20 mg/ml yerba mate extract with time points of 0, 4, 8, 12, and 24 h.

For mechanistic assays, experiments started with ca. 9 log CFU/ml cells to ensure sufficient cells for assays. At this high cell density, no difference in mechanistic assays or growth

was observed between yerba mate concentrations of 0 mg/ml, 10 mg/ml, 20 mg/ml, or 40 mg/ml, so 80 mg/ml yerba mate extract was the treatment used for all mechanistic assays. Time points ranged from 0-2 h for membrane integrity assays and 0-8 h for catalase activity assays. Up to 3 samples (1.5 ml for catalase activity, 700 µl for membrane integrity and biomass, and 100 µl for CFU counts) were taken from each flask for mechanistic assays. Metabolomics extractions were taken at times 0, 40 min (lag phase), and 4 h (exponential phase, significant difference in catalase activity) in addition to samples for catalase activity, OD_{600}, and CFU enumeration.

Crystal violet membrane integrity assay:

For membrane integrity and biomass, a 700 µl sample from a flask with or without bacteria treated with yerba mate extract or MOPS buffer was taken, pelleted at 15,000 × g at 4 °C for 1 min, and washed at least three times with 500 µl PBS pH 7.4. The final pellet was resuspended in 700 µl PBS pH 7.4 and thoroughly vortexed. Two 200 µl samples were taken from each resuspended pellet, put in a 96-well plate, and OD_{600} was read. The remaining 500 µl was again pelleted at 15,000 × g at 4 °C for 1 min, the supernatant removed, and the pellet resuspended in 500 µl of 0.001% crystal violet freshly diluted in PBS pH 7.4 from a 1% aqueous solution. The crystal violet tubes were vortexed and incubated for 10 min at 37 °C, pelleted at 15,000 × g, and two 100 µl samples of the supernatant were added to a 96-well plate and read at crystal violet's absorbance wavelength of 590 nm. A blank sample of the crystal violet solution was used to calculate percent of crystal violet uptake (((blank – sample)/blank) * 100)) (modified from Devi, Nisha, Sakthivel, & Pandian, 2010).

Catalase activity assay

A 1.5 ml sample from a flask with or without bacteria treated with yerba mate extract or MOPS buffer was pelleted at 15,000 × g for 1 min at 4 °C and washed 3 times with 500 µl PBS pH 7.4. The final pellet was resuspended in 300 µl PBS pH 7.4 and thoroughly vortexed. A simple foam assay (Iwase et al., 2013) was conducted, in which 100 µl PBS pH 7.4, 100 µl washed sample in PBS pH 7.4, 100 µl 1% Triton X-100 in PBS pH 7.4, and 100 µl of cold 30 % hydrogen peroxide were added to a glass tube and mixed well. Technical duplicates were made for each sample. A standard curve was made by reconstituting 0.0050 g catalase powder (Fisher, Nazareth, Penn., USA; 20000 U/g) in 1 ml PBS pH 7.4, then serially diluting to get 0, 2.5, 5, 7.5, and 10 catalase activity units. Foam height (cm) was measured after foam had stabilized.

Metabolomics

Starting cultures had ca. 9 log CFU/ml cells or PBS pH 7.4 for media controls and 0 or 80 mg/ml buffered yerba mate extract. At times 0, 40 min, and 4 h, 500 µl of cells were removed, diluted in 4.5 ml PBS pH 7.4, mixed, and vacuum filtered with 0.4 µm polycarbonate filters. The filters were placed face-down in 1.3 ml cold (20 °C) extraction solvent (4:4:2 AcN:MeOH:H2O) for 20 min at 20 °C. In a 4 °C cold room, any remaining cells were washed from the filter with 400 µl extraction solvent and pelleted at 16,200 × g for 5 min. All extraction solvent fractions for a single sample were combined, dried under flowing nitrogen, resuspended in 300 µl of milliQ water, and transferred to a centrifuge tube. Six biological replicates were done, but contamination found in CFU plates prompted the exclusion of 3 replicates.

All samples were randomized in a 4 ˚C autosampler tray, from which 10 µl aliquots were injected into a Synergi 2.5 micron Hydro-RP 100, 100 × 2.00 mm liquid chromatography column (Phenomenex) maintained at 25 ˚C. A gradient across solvents A (97:3 water:methanol, 10 mM

tributylamine, and 15 mM acetic acid) and B (methanol) was run with 0% B for 5 min, 20 % B for 8 min, 55% B for 2.5 min, 95% B for 3.5 min, and finally 0 % B for 6 min using a 200 µl/min flow rate. The column eluted to an electrospray ionization (ESI) source coupled to a mass spectrometer by a 0.1 mm internal diameter fused silica capillary tube. A Thermo Scientific Exactive Plus orbitrap mass spectrometer was run in fullscan mode with negative ionization using a published method (Lu et al., 2010). Instrument parameters were set to a spray voltage of 3 kV, a nitrogen sheath gas flow of 10 psi with a capillary temperature of 320 ˚C, an automatic gain control (AGC) target of 3e6, a resolution of 140,000, a scan window of 85 to 800 m/z from 0 to 9 min and a scan window of 110 to 1000 m/z from 9 to 24 min.

Data analysis

Growth experiments were each set up and analyzed as a randomized block design, blocked on replicate with sampling in duplicate. Treatment design was repeated measures with concentration applied to each flask and time applied within each flask. Experiments were replicated three times. Bacterial growth data were analyzed by analysis of variance (ANOVA) using mixed models (SAS 9.4, SAS Institute, Cary, N.C., USA). Least significant differences (LSD) were used to compare treatment mean values when significant differences ($P<0.05$) were found. Error bars in all growth plots represent standard deviations of at least 3 replicates.

Metabolomics data analysis

Data was converted from Thermo .raw files to .mzML using msconvert from ProteoWizard (Chambers, Maclean, & Burke, 2012). Peak selection was done with MAVEN (Melamud, Vastag, & Rabinowitz, 2010) version 767 using the default model. Additional parameters are listed in Table S 8. Peak intensity data in the resulting data matrix was normalized to biomass by

scaling the intensity for each sample. All samples were arbitrarily scaled to the intensity value of the first sample (7.35×10^8 CFU/ml counts). To investigate treatment and time differences, the data matrix was analyzed as a randomized block design, blocked on replicate, with split plots of time. A split plot analysis was considered sufficient when the change in Akaike information criterion (AIC) was less than 3 between a repeated measures model with an adjusted correlation structure (AR1) and a split plot model without a defined correlation structure. In 131 of the 7693 untargeted metabolites that were normal and had equal variance, the change in AIC was greater than 3, so a repeated measures correlation structure was used in those cases. The three flask treatments were $\text{control}_{\text{no tea}}$ (0 mg/ml yerba mate extract with *S.* Typhimurium), tea (80 mg/ml yerba mate extract with *S.* Typhimurium), and $\text{control}_{\text{no bacteria}}$ (80 mg/ml yerba mate extract with PBS pH 7.4 instead of bacteria). ANOVA assumptions were tested in R with the Levene test for equal variance ($P>0.05$) and the Shapiro-Wilks test for normality ($W>0.80$). If these assumptions were not met or if errors occurred in the lme analysis (i.e. “computationally singular matrix”), metabolites were not included in the analysis. Otherwise, data were analyzed using linear mixed models (package nlme, R Foundation for Statistical Computing, Vienna, Austria). P-values were collected from a Tukey’s honestly significant difference (HSD) analysis implemented with the R glht function from the multcomp package. Six contrast statements are displayed in the results tables to focus on differences between controls (no tea or no bacteria) and the tea treatment. Tukey HSD p-values were adjusted for multiple comparisons with the Benjamini-Hochberg method (false discovery rate 0.05, R function p.adjust) as a single family across all metabolites. ANOVA p-values across treatments were adjusted with the Benjamini-Hochberg correction as a separate group across all metabolites. Metabolites with an ANOVA p-value of $P< 0.05$ across all treatments that additionally had a Tukey HSD contrast p-value of $P<0.05$ were ranked by the

most positive to most negative fold-change in the results tables. Both targeted (limited to identifiable compounds) and untargeted analyses were performed, but only results from the targeted analysis are displayed in Tables 9-14. Additional information for the targeted results is in Table S 11 and all untargeted results are in Table S 10. Metabolites were identified based on an in-house library of 257 compounds that had been run as pure standards on the same instrument and with the same methods used for the samples. Names were matched to peaks within 5 ppm m/z and 1.5 min of the observed m/z and retention time of the pure standard. If multiple peaks were within the range of a single compound, the peak closest to the observed retention time that did not appear to be a shoulder peak was selected for Tables 9-14 and Figures 11-13, S 5-S 7). All original multiply assigned peaks are in Table S 10 and Table S 11.

Acknowledgements

We are very grateful for the use of Dr. P. Michael Davidson's BSL-2 laboratory, equipment, and storage space. We would also like to thank the Department of Food Science and Technology for the use of *S.* Typhimurium DT104 strain 2576, Dr. Hayriye Bozkurt for assistance with BSL-2 lab equipment, Dr. Arnold Saxton for statistics advice, and Dr. Shawn Campagna, Dr. Hector Castro Gonzalez, and Eric Tague for extracting and running samples for metabolomics. This research was supported by the Ivan Racheff Chair of Excellence endowment, the Department of Genome Science and Technology, and the NSF-IGERT program SCALE-IT.

References

Abreu, A.C., McBain, A.J., Simões, M., 2012. Plants as sources of new antimicrobials and resistance-modifying agents. Nat. Prod. Rep. 29, 1007–21.

Bakkali, F., Averbeck, S., Averbeck, D., Idaomar, M., 2008. Biological effects of essential oils--a review. Food Chem. Toxicol. 46, 446–75.

Barb, A.W., Zhou, P., 2008. Mechanism and inhibition of LpxC: an essential zinc-dependent deacetylase of bacterial lipid A synthesis. February 9, 9–15.

Belenky, P., Ye, J.D., Porter, C.B.M., Schwarz, E.G., Walker, G.C., Collins, J.J., 2015. Bactericidal antibiotics induce toxic metabolic perturbations that lead to cellular damage. CellReports 13, 1–13.

Borges, A., Ferreira, C., Saavedra, M.J., Simões, M., 2013. Antibacterial activity and mode of action of ferulic and gallic acids against pathogenic bacteria. Microb. Drug Resist. 19, 256–265.

Borges, A., Saavedra, M.J., Simões, M., 2015. Insights on antimicrobial resistance, biofilms and the use of phytochemicals as new antimicrobial agents. Curr. Med. Chem. 22, 2590–2614.

Burris, K.P., Davidson, P.M., Stewart, C.N., Harte, F.M., 2011. Antimicrobial activity of yerba mate (*Ilex paraguariensis*) aqueous extracts against *Escherichia coli* O157:H7 and *Staphylococcus aureus*. J. Food Sci. 76, M456–62.

Burris, K.P., Davidson, P.M., Stewart, C.N., Zivanovic, S., Harte, F.M., 2012. Aqueous extracts of yerba mate (*Ilex paraguariensis*) as a natural antimicrobial against *Escherichia coli* O157:H7 in a microbiological medium and pH 6.0 apple juice. J. Food Prot. 75, 753–7.

CDC, 2015. National Antimicrobial Resistance Monitoring System for Enteric Bacteria (NARMS): Human Isolates Final Report, 2013.

Chambers, M., Maclean, B., Burke, R., 2012. A cross-platform toolkit for mass spectrometry and proteomics. Nat. Biotechnol. 30, 918–920.

Chatterjee, A., Pakrashi, S.C., Werner, G., 1956. Recent developments in the chemistry and pharmacology of *Rauwolfia* alkaloids. In: Zechmeister, L. (Ed.), Progress in the Chemistry of Organic Natural Products. Springer, Pasadena, CA, pp. 346–443.

Chulavatnatol, M., Atkinson, D.E., 1973. Phosphoenolpyruvate synthetase form *Escherichia coli*. J. Biol. Chem. 248, 2712–2715.

Cowan, M.M., 1999. Plant products as antimicrobial agents. Clin. Microbiol. Rev. 12, 564–82.

Crim, S., Griffin, P., Tauxe, R., Marder, E., Gilliss, D., Cronquist, A., Cartter, M., Tobin-D'Angelo, M., Blythe, D., Smith, K., Lathrop, S., Zansky, S., Cieslak, P., Dunn, J., Holt, K., Wolpert, B., Henao, O., 2015. Preliminary incidence and trends of infection with pathogens transmitted commonly through food - foodborne diseases active surveillance network, 10 U.S. sites, 2006-2014. MMWR Morb. Mortal. Wkly. Rep. 64, 495–9.

Cushnie, T.P.T., Lamb, A.J., 2011. Recent advances in understanding the antibacterial properties of flavonoids. Int. J. Antimicrob. Agents 38, 99–107.

Devi, K.P., Nisha, S.A., Sakthivel, R., Pandian, S.K., 2010. Eugenol (an essential oil of clove)

acts as an antibacterial agent against *Salmonella typhi*, by disrupting the cellular membrane. J. Ethnopharmacol. 130, 107–115.

Di Pasqua, R., Betts, G., Hoskins, N., Edwards, M., Ercolini, D., Mauriello, G., 2007. Membrane toxicity of antimicrobial compounds from essential oils. J. Agric. Food Chem. 55, 4863–4870.

Dörries, K., Schlueter, R., Lalk, M., 2014. Impact of antibiotics with various target sites on the metabolome of *Staphylococcus aureus*. Antimicrob. Agents Chemother. 58, 7151–63.

Doucette, C.D., Schwab, D.J., Wingreen, N.S., Rabinowitz, J.D., 2011. Alpha-ketoglutarate coordinates carbon and nitrogen utilization via enzyme I inhibition. Nat. Chem. Biol. 7, 894–901.

Dwyer, D.J., Collins, J.J., Walker, G.C., 2015. Unraveling the physiological complexities of antibiotic lethality. Annu. Rev. Pharmacol. Toxicol. 313–332.

Eng, R.H.K., Cherubin, C., Smith, S.M., Buccini, F., 1985. Inoculum effect of β-lactam antibiotics on *Enterobacteriaceae*. Antimicrob. Agents Chemother. 28, 601–606.

Ewins, A.J., 1914. CCLV.-The alkaloids of quebracho bark. J. Chem. Soc. Trans. 2738–48.

Farr, S.B., Kogoma, T., 1991. Oxidative stress responses in *Escherichia coli* and *Salmonella Typhimurium*. Microbiol. Rev. 55, 561–585.

Filip, R., Lotito, S.B., Ferraro, G., Fraga, C.G., 2000. Antioxidant activity of *Ilex paraguariensis* and related species. Nutr. Res. 20, 1437–1446.

Frawley, E.R., Crouch, M. V, Bingham-Ramos, L.K., Robbins, H.F., Wang, W., Wright, G.D., Fang, F.C., 2013. Iron and citrate export by a major facilitator superfamily pump regulates metabolism and stress resistance in *Salmonella Typhimurium*. Proc. Natl. Acad. Sci. 110, 12054–12059.

Frossard, S.M., Khan, A. a., Warrick, E.C., Gately, J.M., Hanson, A.D., Oldham, M.L., Sanders, D.A., Csonka, L.N., 2012. Identification of a third osmoprotectant transport system, the osmU system, in *Salmonella enterica*. J. Bacteriol. 194, 3861–3871.

Gill, A.O., Holley, R.A., 2006. Disruption of *Escherichia coli*, *Listeria monocytogenes* and *Lactobacillus sakei* cellular membranes by plant oil aromatics. Int. J. Food Microbiol. 108, 1–9.

Golozar, A., Fagundes, R.B., Etemadi, A., Schantz, M.M., Kamangar, F., Abnet, C.C., Dawsey, S.M., 2012. Significant variation in the concentration of carcinogenic polycyclic aromatic hydrocarbons in yerba maté samples by brand, batch and processing method. Environ. Sci. Technol. 46, 13488–13493.

Gonzalez-gil, F., Diaz-sanchez, S., Pendleton, S., Andino, A., Zhang, N., Yard, C., Crilly, N., Harte, F., Hanning, I., 2014. Yerba mate enhances probiotic bacteria growth in vitro but as a feed additive does not reduce *Salmonella* Enteritidis colonization *in vivo*. Poult. Sci. 93, 434–440.

Greulich, P., Scott, M., Evans, M.R., Allen, R.J., 2015. Growth-dependent bacterial susceptibility to ribosome-targeting antibiotics. Mol. Syst. Biol. 11, 796.

Heck, C.I., De Mejia, E.G., 2007. Yerba mate tea (*Ilex paraguariensis*): A comprehensive review

on chemistry, health implications, and technological considerations. J. Food Sci. 72, 138–151.

Heck, C.I., de Mejia, E.G., 2007. Yerba Mate Tea (*Ilex paraguariensis*): a comprehensive review on chemistry, health implications, and technological considerations. J. Food Sci. 72, R138–51.

Helander, I.M., Alakomi, H.-L., Latva-Kala, K., Mattila-Sandholm, T., Pol, I., Smid, E.J., Gorris, L.G.M., von Wright, A., 1998. Characterization of the action of selected essential oil components on Gram-negative bacteria. J. Agric. Food Chem. 46, 3590–3595.

Hongpattarakere, T., 2000. Natural antimicrobial components isolated from yerba mate (*Ilex paraguariensis*) leaves. Madison, WI. University of Wisconsin.

Hwang, D., Lim, Y.-H., 2015. Resveratrol antibacterial activity against *Escherichia coli* is mediated by Z-ring formation inhibition via suppression of FtsZ expression. Sci. Rep. 5, 1–10.

Iwase, T., Tajima, A., Sugimoto, S., Okuda, K., Hironaka, I., Kamata, Y., Takada, K., Mizunoe, Y., 2013. A simple assay for measuring catalase activity: a visual approach. Sci. Rep. 3, 3081.

Jozefczuk, S., Klie, S., Catchpole, G., Szymanski, J., Cuadros-Inostroza, A., Steinhauser, D., Selbig, J., Willmitzer, L., 2010. Metabolomic and transcriptomic stress response of *Escherichia coli*. Mol. Syst. Biol. 6, 364.

Kanehisa, M., Goto, S., 2000. KEGG: Kyoto encyclopedia of genes and genomes. Nucleic Acids Res. 28, 27–30.

Kohanski, M.A., Dwyer, D.J., Hayete, B., Lawrence, C.A., Collins, J.J., 2007. A common mechanism of cellular death induced by bactericidal antibiotics. Cell 130, 797–810.

Kubo, I., Muroi, H., 1993. Antibacterial activity of long-chain alcohols against *Streptococcus mutans*. J. Agric. Food Chem. 2447–2450.

Lambert, R.J.W., Skandamis, P.N., Coote, P.J., Nychas, G.J.E., 2001. A study of the minimum inhibitory concentration and mode of action of oregano essential oil, thymol and carvacrol. J. Appl. Microbiol. 91, 453–462.

Lewis, K., Ausubel, F.M., 2006. Prospects for plant-derived antibacterials. Nat. Biotechnol. 24, 1504–1507.

Lou, Z., Wang, H., Rao, S., Sun, J., Ma, C., Li, J., 2012. *p*-Coumaric acid kills bacteria through dual damage mechanisms. Food Control 25, 550–554.

Lu, W., Clasquin, M.F., Melamud, E., Amador-Noguez, D., Amy, A., Rabinowitz, J.D., 2010. Metabolome analysis via reversed-phase ion-pairing liquid chromatography coupled to a stand alone orbitrap mass spectrometer. Anal. Chem. 82, 3212–3221.

Marasini, B.P., Baral, P., Aryal, P., Ghimire, K.R., Neupane, S., Dahal, N., Singh, A., Ghimire, L., Shrestha, K., 2015. Evaluation of antibacterial activity of some traditionally used medicinal plants against human pathogenic bacteria. Biomed Res. Int. 2015, 1–6.

Martin, J.G.P., Porto, E., Alencar, S.M. De, Glória, E.M., Corrêa, C.B., Cabral, I.S.R., 2013. Antimicrobial activity of yerba mate (*Ilex Paraguariensis* St. Hil.) against food pathogens.

Rev. Argent. Microbiol. 45, 93–98.

Mcclerren, A.L., Endsley, S., Bowman, J.L., Andersen, N.H., Rudolph, J., Raetz, C.R.H., 2005. A slow, tight-binding inhibitor of the zinc-dependent deacetylase LpxC of lipid A biosynthesis with antibiotic activity comparable to ciprofloxacin. Biochemistry 44, 16574–16583.

Melamud, E., Vastag, L., Rabinowitz, J.D., 2010. Metabolomic analysis and visualization engine for LC-MS data. Anal. Chem. 82, 9818–9826.

Morishige, Y., Fujimori, K., Amano, F., 2013. Differential resuscitative effect of pyruvate and its analogues on VBNC (viable but non-culturable) *Salmonella*. Microbes Environ. 28, 180–6.

Mousavi, F., Bojko, B., Bessonneau, V., Pawliszyn, J., 2016. Cinnamaldehyde characterization as an antibacterial agent towards *E. coli* metabolic profile using 96-blade solid phase microextraction coupled to liquid chromatography-mass spectrometry. J. Proteome Res. 15, 963–975.

Nakamura, K., Ishiyama, K., Sheng, H., Ikai, H., Kanno, T., Niwano, Y., 2015. Bactericidal activity and mechanism of photo-irradiated polyphenols against Gram-positive and -negative bacteria. J. Agric. Food Chem. 150206163810003.

Nohynek, L.J., Alakomi, H., Kähkönen, M.P., Heinonen, M., Ilkka, M., Puupponen-pimiä, R.H., Helander, I.M., 2006. Berry phenolics: antimicrobial properties and mechanisms of action against severe human pathogens. Nutr. Cancer 54, 18–32.

Ozçelik, B., Kartal, M., Orhan, I., 2011. Cytotoxicity, antiviral and antimicrobial activities of alkaloids, flavonoids, and phenolic acids. Pharm. Biol. 49, 396–402.

Pereira, D.S., Donald, L.J., Hosfields, D.J., Harry, W., 1994. Active site mutants of *Escherichia coli* citrate synthase. J. Biol. Chem. 269, 412–417.

Plaper, A., Golob, M., Hafner, I., Oblak, M., Šolmajer, T., Jerala, R., 2003. Characterization of quercetin binding site on DNA gyrase. Biochem. Biophys. Res. Commun. 306, 530–536.

Pompella, A., Visvikis, A., Paolicchi, A., De Tata, V., Casini, A.F., 2003. The changing faces of glutathione, a cellular protagonist. Biochem. Pharmacol. 66, 1499–1503.

Puupponen-Pimiä, R., Nohynek, L., Alakomi, H.-L., Oksman-Caldentey, K.-M., 2005. Bioactive berry compounds — novel tools against human pathogens. Appl. Microbiol. Biotechnol. 67, 8–18.

Radulović, N.S., Blagojević, P.D., Stojanović-Radić, Z.Z., Stojanović, N.M., 2013. Antimicrobial plant metabolites: structural diversity and mechanism of action. Curr. Med. Chem. 20, 932–52.

Rempe, C.S., Burris, K.P., Woo, H.L., Goodrich, B., Gosnell, D.K., Tschaplinski, T.J., Stewart, C.N., 2015. Computational ranking of yerba mate small molecules based on their predicted contribution to antibacterial activity against methicillin-resistant *Staphylococcus aureus*. PLoS One 10, e0123925.

Rolfe, M.D., Rice, C.J., Lucchini, S., Pin, C., Thompson, A., Cameron, A.D.S., Alston, M., Stringer, M.F., Betts, R.P., Baranyi, J., Peck, M.W., Hinton, J.C.D., 2012. Lag phase is a distinct growth phase that prepares bacteria for exponential growth and involves transient

metal accumulation. J. Bacteriol. 194, 686–701.

Scallan, E., Hoekstra, R.M., Angulo, F.J., Tauxe, R. V., Widdowson, M.-A., Roy, S.L., Jones, J.L., Griffin, P.M., 2011. Foodborne illness acquired in the United States—major pathogens. Emerg. Infect. Dis. 17, 7–15.

Silins, G., Tan, J., Chan, K., 2015. Intellectual property and patent issues with phytotherapy products. In: Ramzan, I. (Ed.), Phytotherapies: Efficacy, Safety, and Regulation. Wiley, Hoboken, New Jersey, pp. 573–593.

Tegos, G., Stermitz, F., 2002. Multidrug pump inhibitors uncover remarkable activity of plant antimicrobials. Antimicrob. Agents Chemother. 46, 3133–3141.

Tsai, T.-H., Tsai, T.-H., Chien, Y.-C., Lee, C.-W., Tsai, P.-J., 2008. *In vitro* antimicrobial activities against cariogenic streptococci and their antioxidant capacities: A comparative study of green tea versus different herbs. Food Chem. 110, 859–864.

Tyagi, P., Singh, M., Kumari, H., Kumari, A., Mukhopadhyay, K., 2015. Bactericidal activity of curcumin I is associated with damaging of bacterial membrane. PLoS One 10, e0121313.

Udekwu, K.I., Parrish, N., Ankomah, P., Baquero, F., Levin, B.R., 2009. Functional relationship between bacterial cell density and the efficacy of antibiotics. J. Antimicrob. Chemother. 63, 745–757.

Upadhyay, A., Upadhyaya, I., Kollanoor-Johny, A., Venkitanarayanan, K., 2014. Combating pathogenic microorganisms using plant-derived antimicrobials : a minireview of the mechanistic basis. Biomed Res. Int. 2014, 1–18.

Valerga, J., Reta, M., Lanari, M.C., 2012. Polyphenol input to the antioxidant activity of yerba mate (*Ilex paraguariensis*) extracts. LWT - Food Sci. Technol. 45, 28–35.

Valerga, J., Shorthose, R., Lanari, M.C., 2013. Antioxidant activity of yerba mate extracts: Interactions between the individual polyphenols. Eur. J. Lipid Sci. Technol. 115, 513–525.

Vincent, I.M., Ehmann, D.E., Mills, S., Perros, M., Barrett, M.P., 2016. Untargeted metabolomics to ascertain antibiotic modes of action. Antimicrob. Agents Chemother. 60, 2281–91.

Wolfe, A.J., 2005. The acetate switch. Microbiol. Mol. Biol. Rev. 69, 12–50.

Wu, J., Li, Y., Cai, Z., Jin, Y., 2014. Pyruvate-associated acid resistance in bacteria. Appl. Environ. Microbiol. 80, 4108–4113.

Wu, T., He, M., Zang, X., Zhou, Y., Qiu, T., Pan, S., Xu, X., 2013. A structure-activity relationship study of flavonoids as inhibitors of *E. coli* by membrane interaction effect. Biochim. Biophys. Acta 1828, 2751–6.

Yau, W.-P., Goh, C.H., Koh, H.-L., 2015. Quality control and quality assurance of phytomedicines: key considerations, methods, and analytical challenges. In: Ramzan, I. (Ed.), Phytotherapies: Efficacy, Safety, and Regulation. Wiley, Hoboken, New Jersey, pp. 18–48.

Yong, A.L., Ooh, K.F., Ong, H.C., Chai, T.T., Wong, F.C., 2015. Investigation of antibacterial mechanism and identification of bacterial protein targets mediated by antibacterial medicinal plant extracts. Food Chem. 186, 32–36.

Zhao, X., Hong, Y., Drlica, K., 2014. Moving forward with reactive oxygen species involvement in antimicrobial lethality. J. Antimicrob. Chemother. 1–4.

zur Wiesch, P.A., Abel, S., Gkotzis, S., Ocampo, P., Engelstädter, J., Hinkley, T., Magnus, C., Waldor, M.K., Udekwu, K., Cohen, T., 2015. Classic reaction kinetics can explain complex patterns of antibiotic action. Sci. Transl. Med. 7, 287ra73.

Appendix

Figures

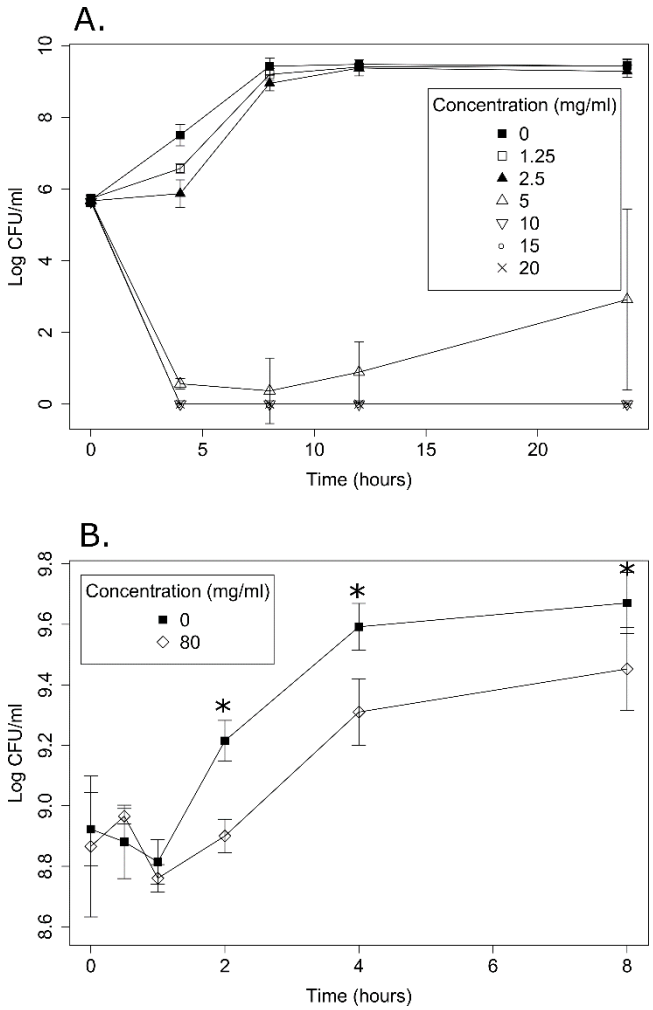

Figure 9. Growth of *S*. Typhimurium with A. ca. 6 log CFU/ml starting culture and 0 to 20 mg/ml yerba mate extract (n=3) or with B. ca. 9 log CFU/ml starting culture and 0 to 80 mg/ml yerba mate extract (n=3 for 0.5 and 1 h and n=7 for all other time points). Error bars show standard deviation. Statistically significant differences are marked by an asterisk for B only (RBD repeated measures ANOVA).

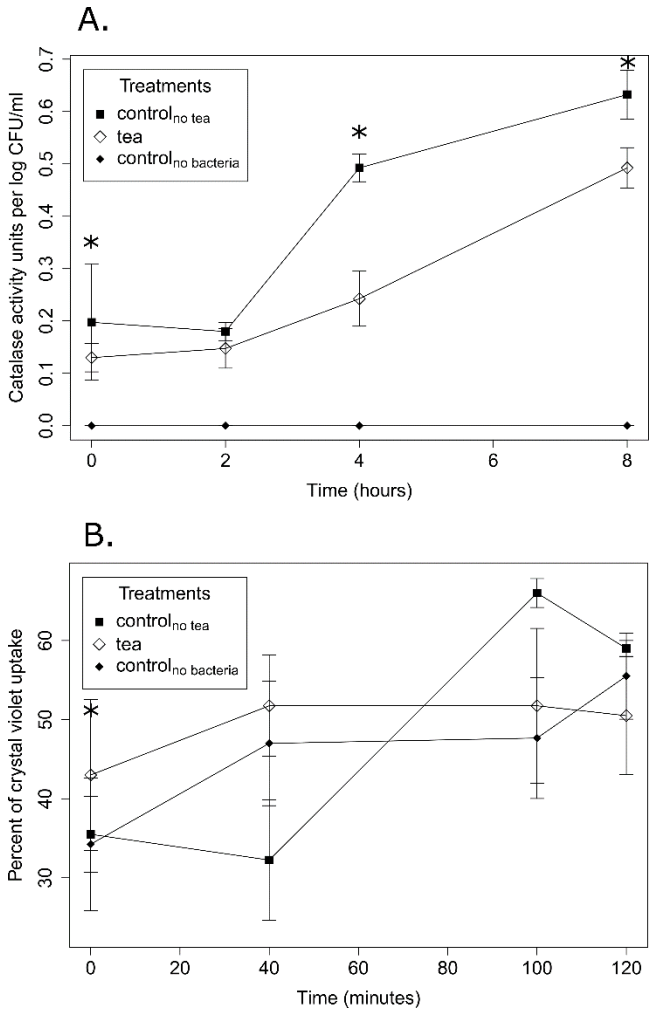

Figure 10. *S.* Typhimurium bioassays under control$_{\text{no tea}}$, tea, and control$_{\text{no bacteria}}$ treatments to test A. catalase activity with a simple foam assay and B. membrane integrity based on the uptake of crystal violet dye. Error bars show standard deviation. Statistically significant differences between control$_{\text{no tea}}$ and tea in A or between control$_{\text{no bacteria}}$ and tea in B are marked by an asterisk (RBD repeated measures ANOVA). n=4 for both A and B.

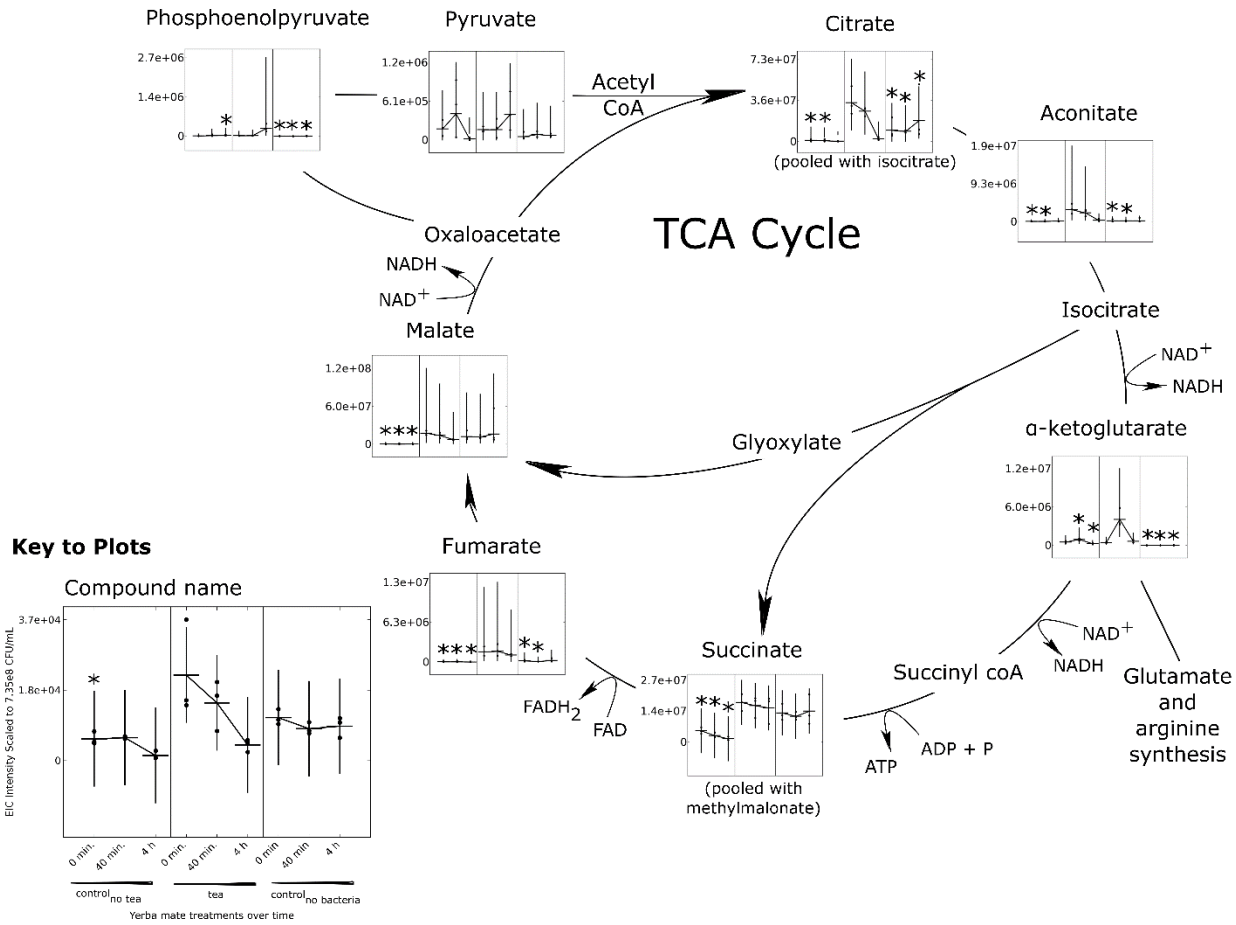

Figure 11. TCA cycle with plots displaying abundance of identifiable metabolites in three yerba mate extract treatments ($control_{no\ tea}$, tea, $control_{no\ bacteria}$) and at three timepoints (0, 40, 240 min). Asterisks mark significant differences between one control treatment at a single time point and the tea treatment at the corresponding time point. The citrate plot shows pooled results for citrate/isocitrate and the succinate plot shows pooled results for succinate/methylmalonate since these metabolite groups are indistinquishable with the methods used. Error bars represent 95% confidence intervals. n=3

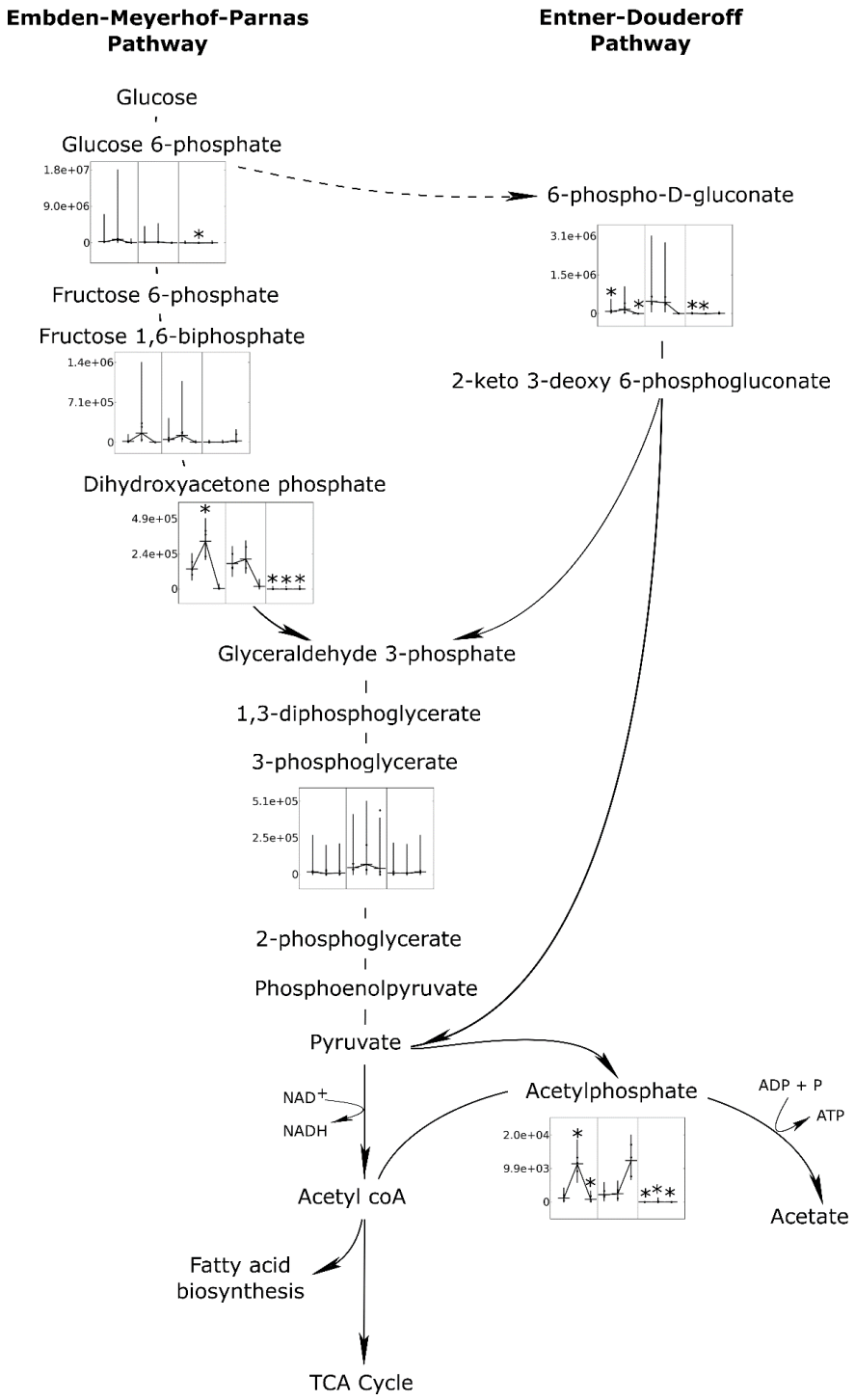

Figure 12. Glycolysis pathways with plots displaying abundance of identifiable metabolites in three yerba mate extract treatments ($control_{no\ tea}$, tea, $control_{no\ bacteria}$) and at three timepoints (0, 40, 240 min). Asterisks mark significant differences between one control treatment at a single time point and the tea treatment at the corresponding time point. Error bars represent 95% confidence intervals. n=3

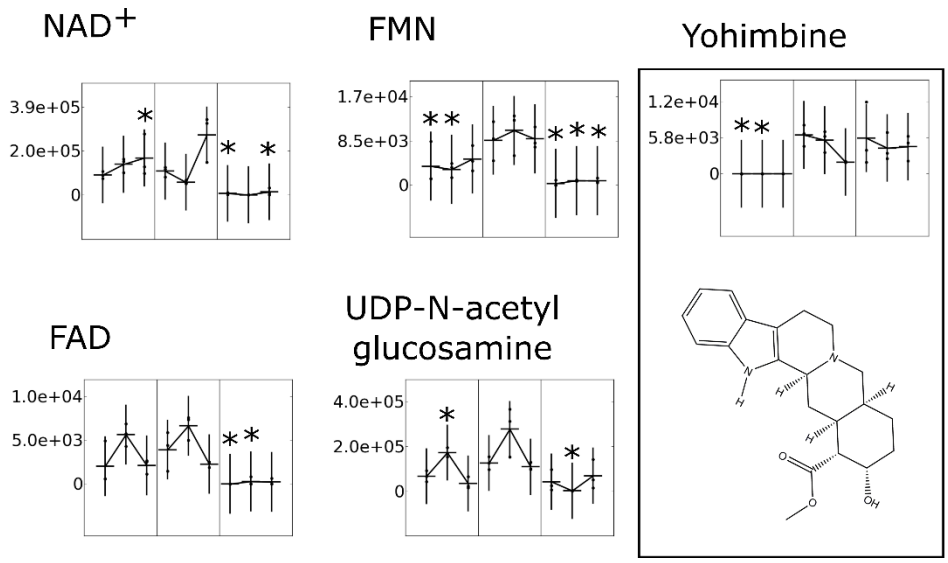

Figure 13. Metabolites that are included in the discussion but not in the TCA cycle or glycolysis pathways. Plots display abundance of identifiable metabolites in three yerba mate extract treatments ($control_{no\ tea}$, tea, $control_{no\ bacteria}$) and at three timepoints (0, 40, 240 min). Asterisks mark significant differences between one control treatment at a single time point and the tea treatment at the corresponding time point. Error bars represent 95% confidence intervals. n=3

Tables

Table 9. Significant differences between $control_{no_tea}$ and tea at 0 min

mz	rt	Putative name	Fold change	Mean diff.	Pathways/Notes
353.1861	12.25	Yohimbine	>6223	6223	Found in plant extracts
383.1158	5.49	S-Adenosyl-L-homocysteine	107.31	54606	Cysteine and methionine metabolism
179.0559	6.22	myo-Inositol	7.13	1007861	Galactose, ascorbate, aldarate metab
179.0346	12.96	Hydroxyphenylpyruvate	6.83	78289	Phe, Tyr, Trp, and quinone biosynth
209.0305	12.17	D-Glucarate	6.43	918498	Ascorbate and aldarate metabolism
195.0511	5.13	D-Gluconate	5.93	463201	Ascorbate and aldarate metabolism
168.9812	12.53	Sulfolactate	5.68	358020	Cysteine and methionine metabolism
133.0143	11.66	Malate	5.59	17120480	TCA
191.02	12.76	Citrate/isocitrate	5.5	33537521	TCA; Ala, Asp, Glu metabolism
173.0089	13.14	Aconitate	5.31	2896247	TCA
115.0033	12.55	Fumarate	5.01	1551875	TCA, Arg, Tyr, Phe, pyruvate, nicotinate metab.
157.0366	1.3	Allantoin	4.75	146091	Purine metabolism
175.0609	13.16	2-Isopropylmalate	4.63	272415	Pyruvate metab.; Val, Leu, Ile biosynth.
175.0244	6.47	Ascorbate	4.25	7640	Ascorbate and aldarate metab, PTS
213.0172	6.85	Deoxyribose phosphate	4.13	3983	PPP, pyrimidine metabolism
341.1095	1.34	Trehalose/Sucrose/Cellobiose	3.44	420093	Starch and sucrose metabolism
129.019	13.13	Citraconate	2.85	141501	Val, Leu, Ile biosynthesis
275.0177	12.41	6-Phospho-D-gluconate	2.43	393914	PPP
177.0401	6.86	Gluconolactone	2.37	27661	PPP
117.0191	10.91	Succinate/Methylmalonate	1.8	12531083	TCA, Ala, Asp, Glu, Tyr, Phe, pyruvate metab.
105.019	5.52	Glycerate	1.54	472651	PPP, Gly,Ser,Thr, metabolism
157.0255	6.52	Dihydroorotate	1.43	3289	Pyrimidine biosynthesis
565.0484	12.38	UDP-glucose	1.37	309874	Starch, sucrose; ascorbate, aldarate; pyrimidine metab.
455.0977	14.43	FMN	1.24	4980	Flavin biosynthesis, respiration
153.0193	12.55	2_3-Dihydroxybenzoate	1.07	20796	Aromatic amino acid, quinone, enterobactin metabolism
163.0399	15.03	Phenylpyruvate	-1.78	-9904	Phe biosynthesis
175.0358	11.46	N-Carbamoyl-L-aspartate	-2.36	-89246	Pyrimidine biosynthesis

mz = mass to charge ratio
rt = retention time
”tea” refers to *S.* Typhimurium treated with 80 mg/ml aqueous yerba mate extract
”$control_{no_tea}$“ refers to *S.* Typhimurium treated with buffer instead of tea
”$control_{no_bacteria}$” refers to tea with PBS pH 7.4 instead of bacteria
Fold change is expressed as log_2(control/tea)
Mean difference is the difference between the adjusted intensity means of control – tea

PPP = pentose phosphate pathway; TCA = tricarboxylic acid cycle; PTS = phosphoenolpyruvate transferase system

UDP = uridine diphosphate; FMN = Flavin mononucleotide; CMP = cytidine monophosphate; NAD = nicotinamide adenine dinucleotide

Table 10. Significant differences between control$_{no_tea}$ and tea at 40 min

mz	rt	Putative name	Fold change	Mean diff.	Pathways/Notes
383.1158	5.49	S-Adenosyl-L-homocysteine	108.01	73846	Cysteine and methionine metabolism
353.1861	12.25	Yohimbine	60.41	5392	Found in plant extracts
179.0346	12.96	Hydroxyphenylpyruvate	52.08	57363	Phe, Tyr, Trp, and quinone biosynth
157.0366	1.3	Allantoin	7.63	154804	Purine metabolism
179.0559	6.22	myo-Inositol	7.35	1027983	Galactose, ascorbate, aldarate metab
209.0305	12.17	D-Glucarate	6.84	972917	Ascorbate and aldarate metabolism
168.9812	12.53	Sulfolactate	6.4	279361	Cysteine and methionine metabolism
133.0143	11.66	Malate	5.75	13629865	TCA
195.0511	5.13	D-Gluconate	5.75	439500	PPP
191.02	12.76	Citrate/isocitrate	5.47	26177730	TCA; Ala, Asp, Glu metabolism
175.0244	6.47	Ascorbate	5.01	8597	Ascorbate and aldarate metab, PTS
115.0033	12.55	Fumarate	4.97	1659376	TCA, Arg, Tyr, Phe, pyruvate metabolism
173.0089	13.14	Aconitate	4.75	2074842	TCA, glyoxylate metabolism
175.0609	13.16	2-Isopropylmalate	3.45	103004	Val, Leu, Ile, pyruvate metabolism
341.1095	1.34	Trehalose/Sucrose/Cellobiose	3.2	333984	Starch and sucrose metabolism
117.0191	10.91	Succinate/Methylmalonate	2.49	13280583	TCA,Ala,Asp,Glu,Tyr,Phe,pyruvate metab,
129.019	13.13	Citraconate	2.19	95207	Val, Leu, Ile biosynthesis
177.0401	6.86	Gluconolactone	2.18	23413	PPP
145.0143	12.16	alpha-Ketoglutarate	2.13	3145953	TCA, amino acid and quinone biosynth
455.0977	14.43	FMN	1.79	7469	Flavin biosynthesis, respiration
105.019	5.52	Glycerate	1.61	411390	PPP, Gly,Ser,Thr, metabolism
116.0714	1.11	Valine	1.6	407	Val, Leu, Isoleu biosynth; pantothenate and coA biosynth
288.1204	7.56	Ophthalmate	0.86	110577	Cysteine and methionine metabolism
606.075	12.42	UDP-N-acetylglucosamine	0.68	105219	Lipopolysaccharide, peptidoglycan biosynth; amino and nucleotide sugar metab.
115.0398	12.39	2-Oxoisovalerate	-0.62	-100110	Val, Leu, Isoleu biosynth; pantothenate and coA biosynth
168.9906	9.32	Dihydroxyacetone phosphate	-0.68	-124034	Glycolysis, gluconeogenesis
131.0825	1.23	Ornithine	-1.29	-3130	Arg biosynth; Arg and Pro metabolism
368.9995	12.75	Sedoheptoluse bisphosphate	-1.36	-20176	PPP
319.0438	7.17	Octulose 8/1P	-1.37	-6145	Methylthiolincosamide biosynthesis
258.0388	1.49	Glucosamine phosphate	-1.67	-12173	Ala, Asp, Glu metab; PTS; amino and nucleotide sugar metab
157.0255	6.52	Dihydroorotate	-1.88	-7081	Pyrimidine biosynthesis
163.0399	15.03	Phenylpyruvate	-1.94	-32315	Phe biosynthesis
138.98	11.8	Acetylphosphate	-2.21	-8842	Taurine, pyruvate, carbon metab
175.0358	11.46	N-Carbamoyl-L-aspartate	-5.52	-1720323	Pyrimidine biosynthesis

mz = mass to charge ratio
rt = retention time
”tea” refers to *S.* Typhimurium treated with 80 mg/ml aqueous yerba mate extract
”control$_{no_tea}$“ refers to *S.* Typhimurium treated with buffer instead of tea

Table 10 notes continued

”$control_{no_bacteria}$” refers to tea with PBS pH 7.4 instead of bacteria
Fold change is expressed as log_2(control/tea)
Mean difference is the difference between the adjusted intensity means of control – tea
PPP = pentose phosphate pathway; TCA = tricarboxylic acid cycle; PTS = phosphoenolpyruvate transferase system
UDP = uridine diphosphate; FMN = Flavin mononucleotide; CMP = cytidine monophosphate; NAD = nicotinamide adenine dinucleotide

Table 11. Significant differences between $control_{no_tea}$ and tea at 240 min

mz	rt	Putative name	Fold change	Mean diff.	Pathways/Notes
179.0559	6.22	myo-Inositol	8.13	1745217	Galactose, ascorbate, aldarate metab
289.0333	7.24	Sedoheptulose 1/7-phosphate	6.26	654240	PPP, lipopolysaccaride biosynthesis
322.0449	9.04	CMP	5.77	267595	Pyrimidine metabolism
175.0244	6.47	Ascorbate	5.38	7728	Ascorbate and aldarate metab, PTS
115.0033	12.55	Fumarate	5.37	1092892	TCA, Arg, Tyr, Phe, pyruvate, nicotinate metab.
133.0143	11.66	Malate	4.28	6963500	TCA
138.98	11.8	Acetylphosphate	4.04	11563	Taurine, pyruvate, carbon metab
175.0609	13.16	2-Isopropylmalate	3.7	24484	Val, Leu, Ile, pyruvate metabolism
117.0191	10.91	Succinate/Methylmalonate	3.38	13699174	TCA,Ala,Asp,Glu,Tyr,Phe,pyruvate metab,
166.9751	13.06	Phosphoenolpyruvate	3.36	241253	TCA, glycolysis, gluconeogenesis, PTS, Phe, Tyr, Tryp biosynth
177.0401	6.86	Gluconolactone	3.04	13053	PPP
153.0193	12.55	2_3-Dihydroxybenzoate	2.98	28200	Aromatic amino acid, quinone, enterobactin metabolism
275.0177	12.41	6-Phospho-D-gluconate	2.31	4789	PPP
129.019	13.13	Citraconate	1.75	22694	Val, Leu, Ile biosynthesis
258.0388	1.49	Glucosamine phosphate	1.56	11003	Ala, Asp, Glu metab; PTS; amino and nucleotide sugar metab
115.0398	12.39	2-Oxoisovalerate	1.45	112597	Val, Leu, Isoleu biosynth; pantothenate and coA biosynth
145.0143	12.16	alpha-Ketoglutarate	1.35	391899	TCA, amino acid and quinone biosynth
662.1028	8.8	NAD^+	0.7	103153	Respiration, thiamine metabolism
173.0929	1.49	N-Acetylornithine	-2.08	-61697	Arginine biosynthesis
116.0714	1.11	Valine	-3.73	-1787	Val, Leu, Isoleu biosynth; pantothenate and coA biosynth

mz = mass to charge ratio
rt = retention time
”tea” refers to *S.* Typhimurium treated with 80 mg/ml aqueous yerba mate extract
”$control_{no_tea}$“ refers to *S.* Typhimurium treated with buffer instead of tea
”$control_{no_bacteria}$” refers to tea with PBS pH 7.4 instead of bacteria
Fold change is expressed as log_2(control/tea)
Mean difference is the difference between the adjusted intensity means of control – tea
PPP = pentose phosphate pathway; TCA = tricarboxylic acid cycle; PTS = phosphoenolpyruvate transferase system
UDP = uridine diphosphate; FMN = Flavin mononucleotide; CMP = cytidine monophosphate; NAD = nicotinamide adenine dinucleotide

Table 12. Significant differences between $control_{no_bacteria}$ and tea at 0 min

mz	rt	Putative name	Fold change	Mean diff.	Pathways/Notes
115.0398	12.39	2-Oxoisovalerate	-0.64	-55405	Val, Leu, Isoleu biosynth; pantothenate and coA biosynth
146.0459	4.72	Glutamate	-1.73	-6966631	Arg, Ala, Asp, Glu, Pro, His, Taurine, glutathione metabolism
191.02	12.76	Citrate/isocitrate	-1.8	-2.4E+07	TCA; Ala, Asp, Glu metabolism
175.0609	13.16	2-Isopropylmalate	-2.06	-215728	Pyruvate metab.; Val, Leu, Ile biosynth.
129.019	13.13	Citraconate	-2.28	-130526	Val, Leu, Ile biosynthesis
173.0929	1.49	N-Acetylornithine	-2.69	-18970	Arginine biosynthesis
166.9751	13.06	Phosphoenolpyruvate	-2.74	-13749	TCA, glycolysis, gluconeogenesis, PTS, Phe, Tyr, Tryp biosynth
288.1204	7.56	Ophthalmate	-2.91	-252922	Cysteine and methionine metabolism
175.0358	11.46	N-Carbamoyl-L-aspartate	-2.97	-18771	Pyrimidine biosynthesis
115.0033	12.55	Fumarate	-3	-1401927	TCA, Arg, Tyr, Phe, pyruvate, nicotinate metab.
565.0484	12.38	UDP-glucose	-3.78	-469416	Starch, sucrose; ascorbate, aldarate; pyrimidine metab.
173.0089	13.14	Aconitate	-4	-2785595	TCA
662.1028	8.8	NAD+	-4	-99637	Respiration, thiamine metabolism
455.0977	14.43	FMN	-4.71	-8292	Flavin biosynthesis, respiration
116.0714	1.11	Valine	-5.68	-9527	Val, Leu, Isoleu biosynth; pantothenate and coA biosynth
145.0143	12.16	alpha-Ketoglutarate	-5.69	-418654	TCA, amino acid and quinone biosynth
275.0177	12.41	6-Phospho-D-gluconate	-5.82	-474798	PPP
368.9995	12.75	Sedoheptoluse bisphosphate	-5.92	-10829	PPP
229.0119	7.15	Ribose phosphate	-6.13	-17148	PPP, purine metabolism
168.9906	9.32	Dihydroxyacetone phosphate	-9.46	-176509	Glycolysis, gluconeogenesis
784.152	15.1	FAD	-50.77	-3943	Riboflavin metabolism, respiration
138.98	11.8	Acetylphosphate	-103.07	-2147	Taurine, pyruvate, carbon metab
131.0825	1.23	Ornithine	-103.09	-546	Arg biosynth; Arg and Pro metabolism

mz = mass to charge ratio
rt = retention time
”tea” refers to *S.* Typhimurium treated with 80 mg/ml aqueous yerba mate extract
”$control_{no_tea}$“ refers to *S.* Typhimurium treated with buffer instead of tea
”$control_{no_bacteria}$” refers to tea with PBS pH 7.4 instead of bacteria
Fold change is expressed as log_2(control/tea)
Mean difference is the difference between the adjusted intensity means of control – tea
PPP = pentose phosphate pathway; TCA = tricarboxylic acid cycle; PTS = phosphoenolpyruvate transferase system
UDP = uridine diphosphate; FMN = Flavin mononucleotide; CMP = cytidine monophosphate; NAD = nicotinamide adenine dinucleotide

Table 13. Significant differences between control$_{no_bacteria}$ and tea at 40 min

mz	rt	Putative name	Fold change	Mean diff.	Pathways/Notes
115.0398	12.39	2-Oxoisovalerate	-0.95	-89485	Val, Leu, Isoleu biosynth; pantothenate and coA biosynth
116.0714	1.11	Valine	-1.43	-383	Val, Leu, Isoleu biosynth; pantothenate and coA biosynth
191.02	12.76	Citrate/isocitrate	-1.6	-1.8E+07	TCA; Ala, Asp, Glu metabolism
129.019	13.13	Citraconate	-1.69	-84205	Val, Leu, Ile biosynthesis
146.0459	4.72	Glutamate	-2.39	-7653190	Arg, Ala, Asp, Glu, Pro, His, Taurine, glutathione metabolism
455.0977	14.43	FMN	-3.57	-9620	Flavin biosynthesis, respiration
173.0089	13.14	Aconitate	-3.66	-1985077	TCA
163.0399	15.03	Phenylpyruvate	-3.7	-10513	Phe biosynthesis
322.0449	9.04	CMP	-3.9	-7209	Pyrimidine metabolism
115.0033	12.55	Fumarate	-3.98	-1605564	TCA, Arg, Tyr, Phe, pyruvate, nicotinate metab.
166.9751	13.06	Phosphoenolpyruvate	-4.38	-19162	TCA, glycolysis, gluconeogenesis, PTS, Phe, Tyr, Tryp biosynth
368.9995	12.75	Sedoheptoluse bisphosphate	-4.47	-12248	PPP
784.152	15.1	FAD	-4.6	-6412	Riboflavin metabolism, respiration
259.0227	6.66	Glucose 6-phosphate	-4.8	-205988	
289.0333	7.24	Sedoheptulose 1/7-phosphate	-4.88	-22783	PPP, lipopolysaccaride biosynthesis
175.0358	11.46	N-Carbamoyl-L-aspartate	-5.11	-37308	Pyrimidine biosynthesis
229.0119	7.15	Ribose phosphate	-5.83	-16429	PPP, purine metabolism
565.0484	12.38	UDP-glucose	-6.59	-797530	Starch, sucrose; ascorbate, aldarate; pyrimidine metab.
138.98	11.8	Acetylphosphate	-6.73	-2407	Taurine, pyruvate, carbon metab
606.075	12.42	UDP-N-acetylglucosamine	-6.81	-275975	Lipopolysaccharide, peptidoglycan biosynth; amino and nucleotide sugar metab.
275.0177	12.41	6-Phospho-D-gluconate	-6.86	-437177	PPP
288.1204	7.56	Ophthalmate	-7.58	-244381	Cysteine and methionine metabolism
145.0143	12.16	alpha-Ketoglutarate	-9.45	-4073374	TCA, amino acid and quinone biosynth
168.9906	9.32	Dihydroxyacetone phosphate	-10.51	-206741	Glycolysis, gluconeogenesis
321.0495	10.62	dTMP	-50.38	-914	Pyrimidine metabolism
131.0825	1.23	Ornithine	<-2177	-2177	Arg biosynth; Arg and Pro metabolism

mz = mass to charge ratio
rt = retention time
”tea” refers to *S.* Typhimurium treated with 80 mg/ml aqueous yerba mate extract
”control$_{no_tea}$“ refers to *S.* Typhimurium treated with buffer instead of tea
”control$_{no_bacteria}$” refers to tea with PBS pH 7.4 instead of bacteria
Fold change is expressed as $\log_2$(control/tea)
Mean difference is the difference between the adjusted intensity means of control – tea
PPP = pentose phosphate pathway; TCA = tricarboxylic acid cycle; PTS = phosphoenolpyruvate transferase system
UDP = uridine diphosphate; FMN = Flavin mononucleotide; CMP = cytidine monophosphate; NAD = nicotinamide adenine dinucleotide

Table 14. Significant differences between control$_{no\ bacteria}$ and tea at 240 min

mz	rt	Putative name	Fold change	Mean diff.	Pathways/Notes
213.0172	6.85	Deoxyribose phosphate	3.12	6161	PPP, pyrimidine metabolism
191.02	12.76	Citrate/isocitrate	3.07	16187946	TCA; Ala, Asp, Glu metabolism
177.0401	6.86	Gluconolactone	2.29	57692	PPP
116.0714	1.11	Valine	2.26	553	Val, Leu, Isoleu biosynth; pantothenate and coA biosynth
179.0346	12.96	Hydroxyphenylpyruvate	1.53	29855	Phe, Tyr, Trp, and quinone biosynth
105.019	5.52	Glycerate	1.51	486848	PPP, Gly,Ser,Thr, metabolism
341.1095	1.34	Trehalose/Sucrose/Cellobiose	1.45	242645	Starch and sucrose metabolism
115.0398	12.39	2-Oxoisovalerate	-0.65	-64809	Val, Leu, Isoleu biosynth; pantothenate and coA biosynth
179.0559	6.22	myo-Inositol	-1.22	-1001285	Galactose, ascorbate, aldarate metab
321.0495	10.62	dTMP	-1.53	-1093	Pyrimidine metabolism
157.0255	6.52	Dihydroorotate	-1.99	-3939	Pyrimidine biosynthesis
173.0929	1.49	N-Acetylornithine	-2.64	-16085	Arginine biosynthesis
455.0977	14.43	FMN	-3.36	-8022	Flavin biosynthesis, respiration
163.0399	15.03	Phenylpyruvate	-3.77	-29757	Phe biosynthesis
662.1028	8.8	NAD+	-4.33	-254901	Respiration, thiamine metabolism
168.9906	9.32	Dihydroxyacetone phosphate	-4.7	-18053	Glycolysis, gluconeogenesis
145.0143	12.16	alpha-Ketoglutarate	-5.51	-629579	TCA, amino acid and quinone biosynth
322.0449	9.04	CMP	-6.03	-268434	Pyrimidine metabolism
289.0333	7.24	Sedoheptulose 1/7-phosphate	-6.49	-655535	PPP, lipopolysaccaride biosynthesis
166.9751	13.06	Phosphoenolpyruvate	-6.83	-265009	TCA, glycolysis, gluconeogenesis, PTS, Phe, Tyr, Tryp biosynth
258.0388	1.49	Glucosamine phosphate	-8.21	-16604	Ala, Asp, Glu metab; PTS; amino and nucleotide sugar metab
175.0358	11.46	N-Carbamoyl-L-aspartate	-8.28	-879679	Pyrimidine biosynthesis
138.98	11.8	Acetylphosphate	-105.41	-12313	Taurine, pyruvate, carbon metab
131.0825	1.23	Ornithine	-106.24	-1211	Arg biosynth; Arg and Pro metabolism

mz = mass to charge ratio
rt = retention time
”tea” refers to *S.* Typhimurium treated with 80 mg/ml aqueous yerba mate extract
”control$_{no_tea}$“ refers to *S.* Typhimurium treated with buffer instead of tea
”control$_{no_bacteria}$” refers to tea with PBS pH 7.4 instead of bacteria
Fold change is expressed as $\log_2$(control/tea)
Mean difference is the difference between the adjusted intensity means of control – tea
PPP = pentose phosphate pathway; TCA = tricarboxylic acid cycle; PTS = phosphoenolpyruvate transferase system
UDP = uridine diphosphate; FMN = Flavin mononucleotide; CMP = cytidine monophosphate; NAD = nicotinamide adenine dinucleotide

Supporting information

Supporting figures

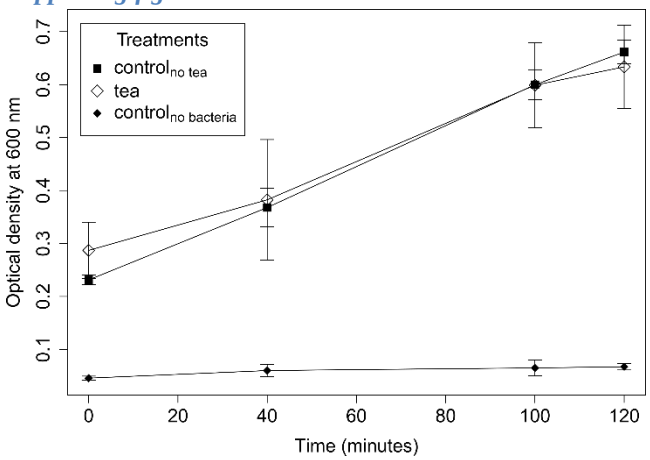

Figure S 4. Optical density at 600 nm of S. Typhimurium under 3 treatment types (control$_{no\ tea}$, tea, control$_{no\ bacteria}$). There were no significant differences between control$_{no\ tea}$ and tea treatments. Error bars represent standard deviation. n=4

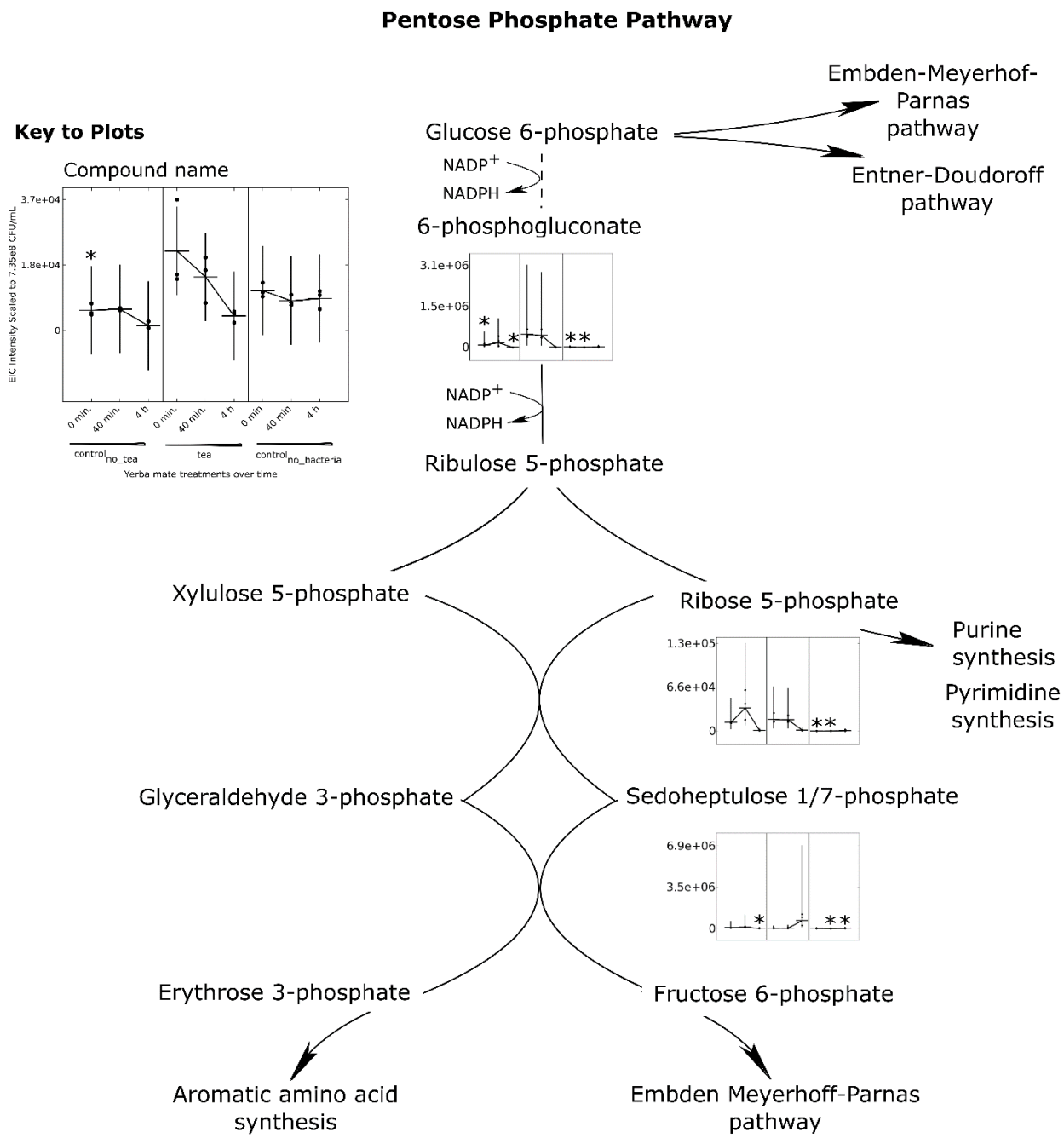

Figure S 5. Pentose phosphate pathway with plots displaying abundance of identifiable metabolites in three yerba mate extract treatments ($control_{no\ tea}$, tea, $control_{no\ bacteria}$) and at three timepoints (0, 40, 240 min). Asterisks mark significant differences between one control treatment at a single time point and the tea treatment at the corresponding time point. Error bars represent 95% confidence intervals. n=3

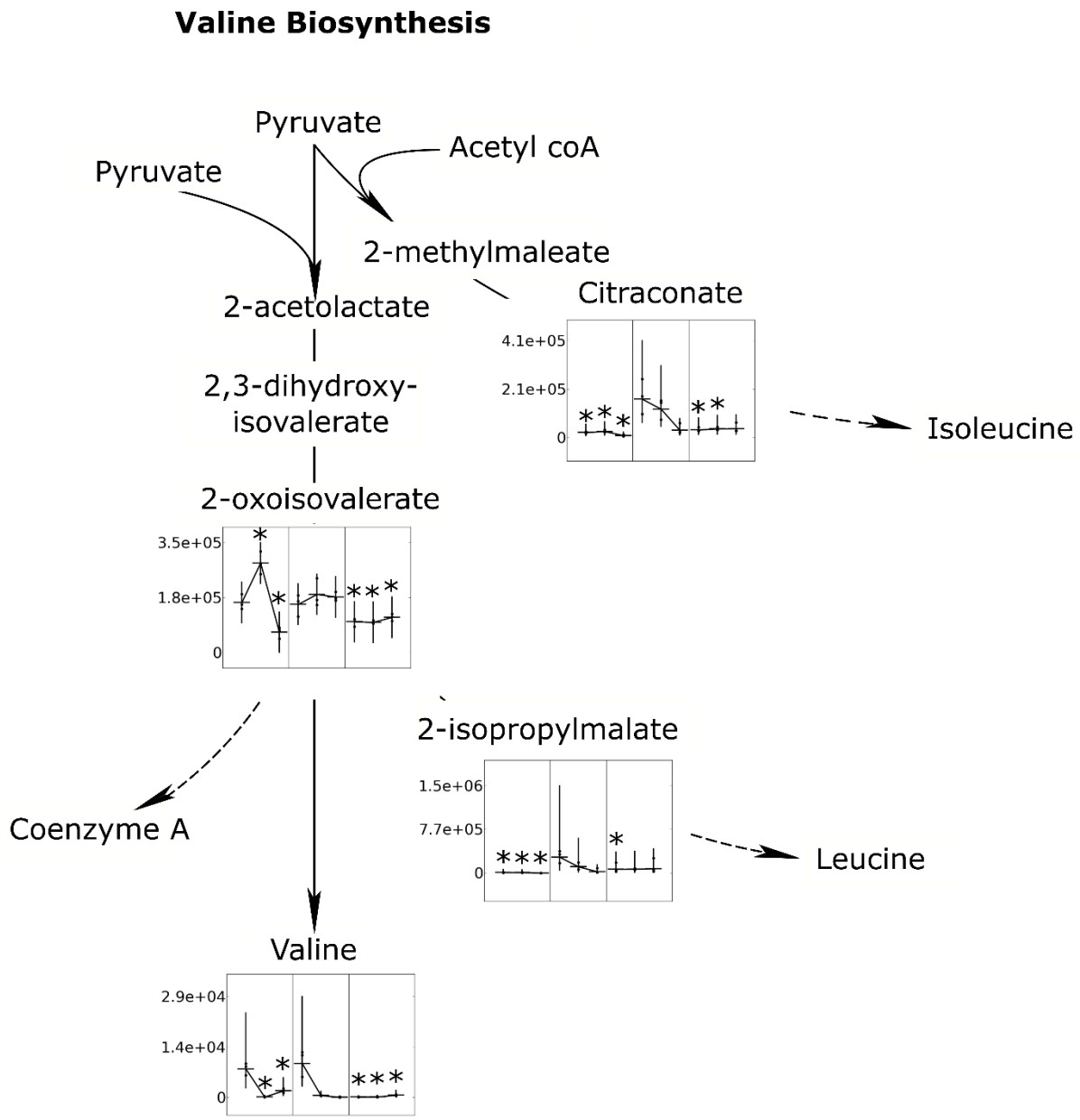

Figure S 6. Valine, leucine, and isoleucine biosynthesis pathway with plots displaying abundance of identifiable metabolites in three yerba mate extract treatments ($control_{no\ tea}$, tea, $control_{no\ bacteria}$) and at three timepoints (0, 40, 240 min). Asterisks mark significant differences between one control treatment at a single time point and the tea treatment at the corresponding time point. Error bars represent 95% confidence intervals. n=3

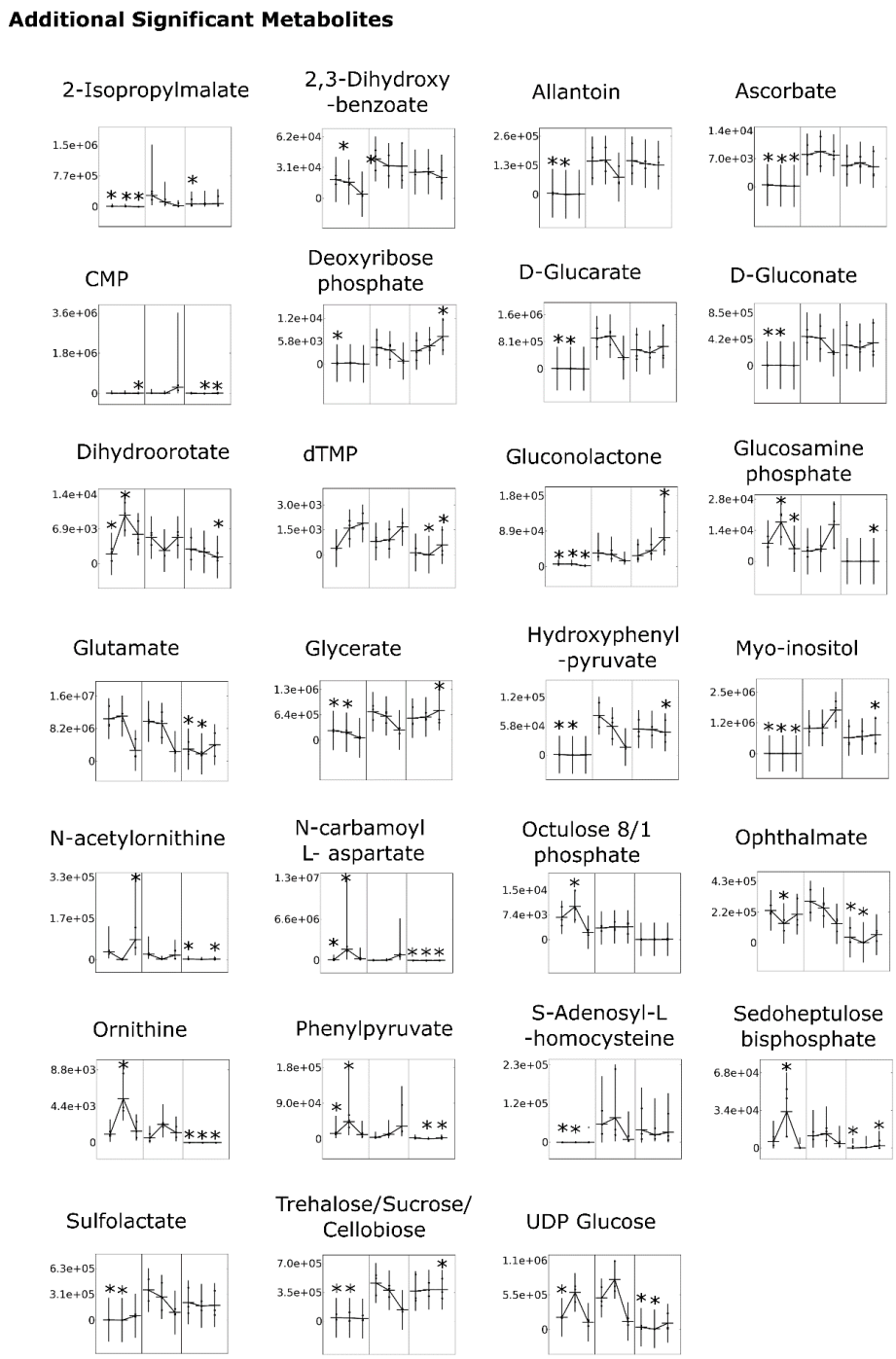

Figure S 7. Additional metabolites with significant differences between treatments; plots display abundance of identifiable metabolites in three yerba mate extract treatments (control$_{\text{no tea}}$, tea, control$_{\text{no bacteria}}$) and at three timepoints (0, 40, 240 min). Asterisks mark significant differences between one control treatment at a single time point and the tea treatment at the corresponding time point. Error bars represent 95% confidence intervals. n=3

Supporting tables

Table S 8. Peak-picking parameters for metabolomics data analysis with Maven software. These parameters were used for both targeted and untargeted analyses but targeted analyses were limited to identifiable compounds.

Parameter	**Value**
Mass domain resolution	5 ppm
Time domain resolution	10 scans
EIC smoothing	3 scans
Peak grouping (maximum group retention time difference)	0.50 min
Drop top x% intensities to get baseline	80%
Baseline smoothing	10 scans
Peak classifier model	default.model
Minimum good peaks/group	3
Minimum signal/baseline ratio	5
Minimum peak width	10 scans
Minimum signal/blank ratio	5
Minimum peak intensity	10000 ions

Table S 9. Pure catalase tested for activity in the presence of yerba mate extract ($control_{no\ bacteria}$). Pure catalase (5 U) in buffer was compared to pure catalase (5 U) with incubated yerba mate extract ($control_{no\ bacteria}$). No significant difference was observed between catalase in buffer and catalase treated with incubated yerba mate extract sampled at different times.

A. Average standard catalase curve

Activity units	**Foam height**	
0	0 ± 0	
2.5	0.73 ± 0.04	
5	1.53 ± 0.04	←→
7.5	2.35 ± 0.07	
10	3.1 ± 0.14	

B. Average catalase activity with $control_{no\ bacteria}$

Time (minutes)	**Foam height**
0	1.54 ± 0.18
40	1.58 ± 0.11
100	1.58 ± 0.09
120	1.58 ± 0.09
240	1.53 ± 0.08
480	1.54 ± 0.05

Foam height (cm) ± standard deviation
n=4 for average catalase activity with $control_{no\ bacteria}$
n=2 for standard curves since experiments were run in parallel in sets of 2
5 activity units of pure catalase (boxed in standard curve table) were tested for catalase activity after the addition of 50 µl of $control_{no\ bacteria}$ treatment from 0 to 8 hours
There was no significant difference (P=0.97) in foam height between pure catalase treated with the $control_{no\ bacteria}$ treatment (5 activity units) and pure catalase under standard testing conditions (5 activity units) with the non-parametric Kruskal-Wallis test (R function 'kruskal.test' used with the 'interaction' function to expand model to a one-way design) that was used to account for unequal variance from unbalanced data.

Table S 10. Complete list of all metabolites found with LC-MS. (attachment)

Table S 11. List of all identified metabolites found with LC-MS. (attachment)

CHAPTER VI
CONCLUSION

The increasing prevalence of multi-drug resistant bacterial pathogens threatens to return us to a pre-antibacterial era if we fail to find new antibacterial compounds or alternative treatments. Nevertheless, we are lucky to have an immense, diverse pool of phytochemicals to draw from in our search for antibacterials. Many plant extracts are already known to have some degree of antibacterial activity, but information on the constituents contributing to antibacterial activity and their mechanisms of action are needed to push the field forward. This dissertation makes a small step in this direction by seeking the major chemical components with antibacterial activity and assaying yerba mate extract for a series of potential antibacterial mechanisms of action. A preliminary review of the literature for antibacterial mechanisms of action of phenolic compounds discussed a role for systems biology as a means of screening for novel mechanisms of action. Then, using a unique search method, GC-MS metabolite data from forty-two fractions of yerba mate extract were each characterized for antibacterial activity against MRSA and *S. aureus* and compounds were ranked by their contribution to the discrimination of antibacterial from non-antibacterial activities. Based on this assessment, 5-hydroxy-pipecolic acid and quinic acid were found to be candidates for involvement in antibacterial activity against MRSA, although pure 3, 4-dihydroxybenzaldehyde showed the best antibacterial activity of the pure compounds assayed. Moving to a different system, this work next surveyed the accumulated metabolic products of *L. casei* and *S.* Typhimurium when grown with yerba mate extract in a milk system. While few notable changes were observed in the significantly accumulated metabolic products of either *L. casei* or *S.* Typhimurium, the presence of increased oxalomalate in *S. Typhimurium* suggested inhibition of aconitase. The hypothesis of phenolic chelation as a possible mechanism of action based on knowledge of phenolic chelation tendencies revealed that

the presence of exogenous iron sulfate prompted the partial recovery of *S.* Typhimurium. Next, after shifting from *S*. Typhimurium in a milk system to a common growth media for further mechanistic assessments, bioassays revealed that cell membrane integrity was not definitively changed but catalase activity was reduced in the presence of yerba mate extract. Furthermore, altered abundances of metabolites were observed in central carbon metabolism, a cell wall precursor, two metabolic regulators, an energy molecule, and a hit to the known antibacterial compound yohimbine. We anticipate that the continuing work in the areas of antibacterial discovery and mechanisms will lead to a better understanding of how antibacterial compounds function and how resistance mechanisms can be dealt with.

VITA

Caroline Rempe graduated from the University of New Mexico (magna cum laude) with a B.S. in Biology and a B.A. in English. During her undergraduate time, she worked on summer research projects at Sandia Livermore and the Joint BioEnergy Institute in California and received second place in the Life Science category for a bioenergy-related poster presentation at the 2009 Science and Energy Research Challenge. She also had the UNM Presidential Scholarship for academic achievement and was a member of the Phi Beta Kappa honors society. After graduating, she interned at Oak Ridge National Lab, where work with a cellobiohydrolase contributed to a publication in *The Journal of Biological Chemistry*. Her interests in learning computational and informatics techniques brought her to the interdisciplinary programs at the University of Tennessee (UT), where she was awarded a fellowship through the NSF-IGERT program Scalable Leading Edge Technologies (SCALE-IT), which encourages collaboration between life science and computer science, and joined the interdisciplinary graduate school of Genome Science and Technology (GST). At UT, Caroline has gained expertise in Perl and Python scripting and basic data mining methods through courses and collaborative projects. She has also contributed curriculum to and taught a lab course designed to introduce biologists to computer programming with Perl, co-designed and co-taught "Virtual Biology: Using Computers to Discover New Medicines," a KIDSU summer camp for high school students, and lead undergraduate genetics students through discussion sessions as a teaching assistant. Caroline additionally had the unique opportunity to give a student perspective in the GST student recruitment process. She has been able to present work at several conferences, including the UT-ORNL-KBRIN Bioinfomatics Summit, the Institute of Food Technologist Annual Meeting, and the Southeast Women in Computing Conference. She was additionally able to gain grant-writing

experience with an interdisciplinary student group for a competitive internal funding opportunity (SCALE-IT IRE grant), which was funded and resulted in the first chapter of this dissertation. Caroline received her Doctorate in Philosophy from the Graduate School of Genome Science and Technology in August of 2016 and continued in her pursuit of an education career.